THE UNIVERSITY OF NAPLES "FEDERICO II"

DEPARTMENT OF NAVAL ARCHITECTURE AND
MARINE ENGINEERING

Ph.D. Course in

Aerospace, Naval and Quality Engineering

XXII cycle

Analysis of warping and shear stresses for ship structures

Theoretical developments and numerical applications

Tutor: Examinee:

Prof. Ing. Antonio Campanile   Ing. Vincenzo Piscopo

Supervisors:

Prof. Ing. Antonio Campanile

Prof. Ing. Masino Mandarino

Doctorate Coordinator:

Prof. Ing. Antonio Moccia

October, 2009

Quello che vide era molto bello.

Nessun limite, eh, Jonathan? pensò, e sorrideva.

Era come l'inizio di una gara: aveva cominciato a imparare.

R. Bach

To Willy, with love

Acknowledgements

At the end of my doctoral research, I'd like to thank my supervisors Prof. Antonio Campanile and Prof. Masino Mandarino for their care of guiding me during these years, as well as for the helpful comments and suggestions about all the critical aspects of the thesis.

I thank Prof. Renato Fiorenza for his courses of functional analysis and his enthusiasm in teaching.

I'd like to thank my parents, because they were during these years a certain support for all my problems and doubts and lovely inspired me to learn and to go on learning.

My final thank you is for Raffaela, not only for her lovely patience during the last months of working on the thesis, but also because she represents a fixed reference point in my life.

Contents

List of Figures

List of Tables

Introduction

In structural engineering the elastic equilibrium problem of any loaded
body can be properly solved assigning it to one of the following classes, ac-
cording to its spatial character: massive bodies, plates and shells, beams.
The first class includes all those bodies whose three dimensions are compa-
rable, so that the relative problems and solution methods, concerning the
stress and strain fields determination, are dealt with in the general theory of
elasticity. The second class, instead, is made up of all those elements hav-
ing one dimension, namely the thickness, small if compared with the other
two, namely the length and the breadth, which are of the same order of
magnitude. Finally, the third class, including all those bodies characterized
in that two of their dimensions, namely the cross-sectional ones, are small
if compared with the third one, namely the beam length, can be further
subdivided into solid and thin-walled beams. Solid beams, loaded only in
correspondence of the two extremities by a generic equilibrated system of
forces, are generally analyzed by the engineering theory based on the ap-
plication of the Saint-Venant's principle, according to which all the internal
forces acting on the cross-section can be reduced, sufficiently far away from
the beam ends, to a 6-dimensional space vector, made up of 3 force and 3
moment components, obtained thanks to the uncoupling and superposition
of four basic responses: stretching; major-axis bending, coupled with major
shear; minor-axis bending, coupled with minor shear and pure torsion.

On the other hand, the theory of thin-walled beams, having a wall thick-
ness small respect to the dimensions of the cross-section, takes its name from
the work of V.Z. Vlasov [1] who, in 1940, published a quite comprehensive
book on the argument, collecting the results of an entire lifetime of scien-

tific activity devoted to the analysis of thin structures. Its second edition, published posthumously in 1959, in a revised and enlarged form, was translated from Russian into English and introduced in the western scientific community by the Israel Program for Scientific Translations in 1961. Since the 1970s, thanks to the growing efficieny in terms of cost of thin-walled structures, significant advances have been made through experimental testings and theoretical works. From this point of view, either complete beam theories, essentially originated by the Vlasov's method, or restrained warping theories, mainly based on the Saint-Venant's theory, have been developed, the first ones by Capurso [2] and Pittaluga [3], the second ones by Kármán and Christensen [4]; Kollbrunner and Hajdin [5]; Burgoyne and Brown [6],[7]; Mandarino [8], [21].

The Vlasov's theory is based on the observation that thin-walled beams with open cross-section, subjected to a torque load and restrained at one or both ends, develop considerable axial warping stresses and deform without substantial shear deformations in the shell middle surface. The fundamental hypotheses of this theory are:

- further to Navier rigid body motions, the cross-section may develop warping out of its plane as a result of torsion;

- the separation of cross-sectional and along-the-axis variables is assumed, so that any displacement of a structural point may be expressed as the product of two functions: the first one, namely the warping function, independent of the position along the axis, the other one, namely the twist function, assumed equal to the unit twist angle and independent of the position on the section;

- the tangential stress field, produced by the applied twist moment, is divided into two parts: the primary and the secondary one; the primary stress, typical of Saint-Venant's theory, is associated to the so called pure torsion; the secondary one, instead, is connected with the normal stress field caused by the non-uniform warping of the beam cross-section.

The theory, developed for thin-walled beams with open (monoconnected) cross-section, was extended by Kármán and Christensen (1944) to beams with closed (pluriconnected) cross-section subjected to non-uniform torsion, as in this case the middle surface undergoes large shear strains, assumed equal to the Bredt's ones, as well as for the pure torsion problem. In the years, further theorical developments have been achieved. Kollbrunner and Hajdin (1972) modified the Vlasov's theory assuming that the twist function is not more proportional to the unit twist angle, but it is a function obtained thanks to a global congruence condition based on the principle of virtual work. Pittaluga (1978) applied the Vlasov's generalized method introducing new cross-sectional functions, called shear potentials, which allow for shear deformation and are related to the first derivative of the bending and warping curvature. Burgoyne and Browne (1994) treated the non-uniform torsion problem, as a mixed flexure/torque one, obtaining a solution non restricted to thin-walled beams and based on appropriate Fourier developments of the displacement field, in order to define a warping function which could fully respect the indefinite equilibrium equation along the beam axis. Finally, Mandarino proposed two new theories, the first one (1997) in which the influence of the cross-section distortions on the transversal shear stress (i.e. the non conservative character of the relative field) and the relevant influence on the restrained warping one, can be taken into due consideration, the second one (2007) for the bending-shear stress determination, in which the effect of the longitudinal variability of the vertical shear force is taken into due consideration.

As Vlasov's simplified model, particularly useful in the global analysis of longitudinally developed structures, offers some advantages such as a good feasibility in the structure's schematization and a great conciseness in the results' analysis, it was adopted from 1960s, by Abrahamsen [9]; De Wilde [10]; Haslum and Tonnensen [11] for the analysis of ships with large hatch openings, subjected to a torque load, for which considerable warping stresses arise, regarding a single hatch length as a thin-walled beam restrained in correspondence of two adjacent transverse bulkheads. As years went by, the feasibility of this theory was so proved that still today, despite the large use of three dimensional finite element programs, it is accepted by the major

3

classification registers, not only for the evaluation of tangential and warping stresses due to shear and torque, but also for determining the ship flexural and torsional vibration modes.

So, as this theory represents an important model to analyze ship structures, in this thesis the problem of the elastic equilibrium of a ship hull subjected to a combined bending/shear/torque load is discussed from the beginning, to highlight, and in some cases eliminate, the assumptions and approximations of the classical theories.

Chapter 1 deals with the Mandarino's bending-shear theory, whose numerical code was developed by the present writer. In this theory, in which it is assumed that the shear force can generate both warping displacements and rigid body translations of the structural section, new relations, based on the Vlasov's structural hypotheses and developed in orthogonal curvilinear coordinates, that allow to account for the influence of the branches curvature, are obtained for the normal and tangential stress fields. A numerical procedure, which differs from the one proposed by Hughes [12] is also proposed, assuming a cubic law for the warping function distribution along the branches and substituting the condition of absence of rigid body warping components for the one of zero value of the warping function on the section neutral axis, what allows to translate the classical Neumann boundary problem into a mixed Dirichlet-Neumann one. Besides, it is verified that warping shear stresses, not considered either by Rules or by the classical theories, depend directly on the unit vertical load $c(x)$, and can assume appreciable values, if compared with the bending ones, for all those loading conditions that include quasi-concentrated loads and, consequently, great values of $c(x)$, so significantly influencing the scantling procedures.

In Chapter 2 a new bending-shear theory for thin-walled beams, substantially based on the Saint-Venant's displacement field and suggested by the present writer, is developed, eliminating the fundamental Vlasov's structural hypothesis of maintenance of the cross-section contour. New relations are obtained for tangential and normal stresses; a numerical method, based on a Ritz variational technique, is developed and a procedure to determine the shear center vertical position, taking into account the cross-section's deformability, is presented. The fundamental differences between the Vlasov's

and Saint-Venant's theories are also pointed out, verifying that the Vlasov's theory may be regarded as the limit of the Saint-Venant's one, when the Poisson modulus $\nu \to 0$.

In Chapter 3 the problem of a ship with large hatch openings subjected to a variable torque is analyzed, starting from the displacement field proposed by Kollbrunner and Hajdin and analitically developed in a new original form by the present writer. Despite the classical theories, the longitudinal distribution of the applied torque proposed by RINA Rules [13] is taken into due consideration, so influencing the solution of the warping equation and the bimoment longitudinal distribution. Besides, as a still unsolved problem is the role of transverse bulkheads, generally assumed as rigid in the solution of the warping equation, a method based on the global energy procedure proposed by Senjanović *et al.* [14], but varied for the different bulkhead's deformed shape law, is presented, schematizing the bulkhead as a stiffened clamped orthotropic plate.

In Chapter 4 the mixed flexure/torque theory developed by Burgoyne and Brown (1994) for beams with axial-symmetric and asymmetric cross-section is discussed from the beginning and extended to beams with multiconnected cross-section, such as ship structures, imposing, by the present writer, boundary conditions different from the ones proposed by the authors and better adaptable to ships. The theory, based on the Fourier development of the displacement field, despite the classical ones, permits to fully respect the indefinite equilibrium equation along the beam axis, solving by a FE technique, for each harmonic three Neumann boundary problems associated to the Helmholtz equation.

In Chapter 5, as bulkheads have been schematized in Chapter 3 as clamped orthotropic plates, the Huber's differential equation for orthotropic plates with all edges clamped is solved by the Rayleigh-Ritz method, expressing the displacement field by a double cosine trigonometric series. Numerical results are presented as design charts similar to the ones given by Schade, [19] for all the non-dimensional coefficients identifying the plate response. Some comparisons with the well known data published by Timoshenko and Woinowsky-Krieger [20] for the isotropic plate case are also presented in order to verify the goodness of the applied numerical technique. In Chap-

ter 6 some comparisons with the results presented by Hughes and the ones obtained by a FEM analysis carried out by ANSYS, are presented for a simplified ship section; the open profile analyzed by Burgoyne and Brown is analyzed in order to verify the reliability of the developed numerical techniques proposed in Chapter 4. Finally, in order to apply and compare the proposed theories, two numerical applications, in which the normal and tangential stress fields due to vertical shear and torsion are determined, are carried out, the first one for a bulk-carrier, the second one for a containership. Suitable numerical codes have been developed by MATLAB MathWorks 7.0, applying both the Euler Lagrange functional technique, both a FEM analysis. For the second case the Partial Differential Equation Toolbox has been utilzed and integrated in a suitable code developed, for beams with axial-symmetric cross-section by the present writer and Ing. A. Pranzitelli, and for beams with asymmetric cross-section by the present writer only.

Chapter 1

The refined bending-shear theory

This chapter deals with the Mandarino's bending-shear theory, whose numerical code was developed by the present writer, in which it is admitted the longitudinal variability of the vertical shear force. It is well known, in fact, that in the traditional shear theory, bending and shear are assumed each other as independent, and the shear effect reduces only to warping; the invariability of the shear force is also admitted and, as a consequence, no warping effects are considered on the normal stresses. The stress field is reduced to the only σ and τ components, the first one evaluated by a the Saint-Venant's procedure, the second one by the Vlasov's procedure. The shear influence on the vertical displacement and the bending/shear interaction induces to a re-examination of the theory, devoted to a careful individuation of the stress and strain fields.

1.1 The displacement field

Let us regard the hull girder cylindrical body as a thin-walled beam, made up of homogeneous and isotropic material, and let us suppose that the external loads are neglegible respect to the internal stress characteristics. Let us define the global Cartesian frame, sketched in Fig. 1.1, with origin G in correspondence of the amidships structural centre and y, z axes defined in the
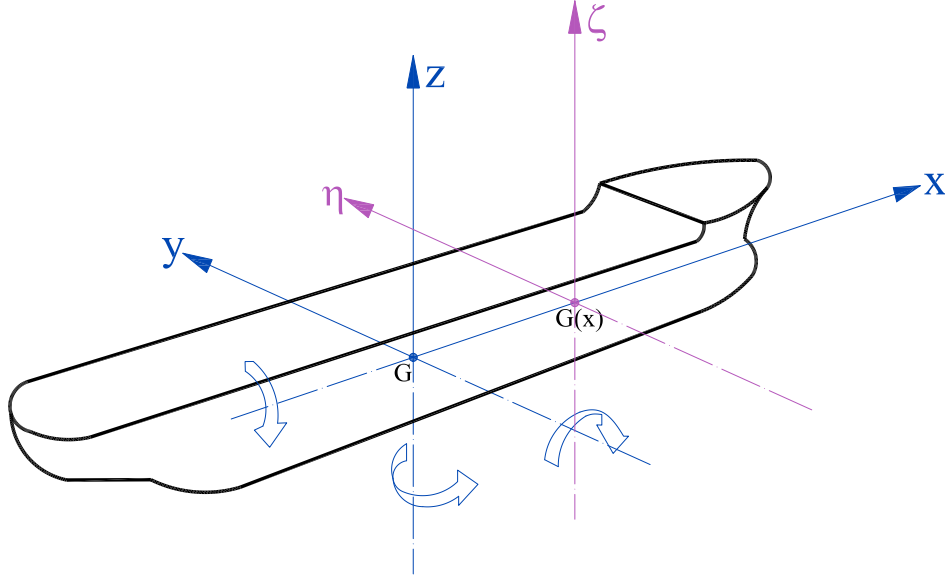
Figure 1.1: Global and local reference system

section plane and coinciding with the section principal axes of inertia. Let us also define the local Cartesian frame with origin $G(x)$ in correspondence of the section at x-abscissa, x-axis coinciding with the global one and η, ζ axes defined in the section plane and coinciding with the principal axes of inertia of the section at x-abscissa. Adopting a mixed $P(x, \eta, \zeta)$ representation and assuming the fundamental Vlasov's structural hypothesis - maintenance of the cross section contour - it is possible to reduce the displacement function $\boldsymbol{u}(x, \eta, \zeta)$ to the following one:

$$\boldsymbol{u}(x, \eta, \zeta) = \Big(\vartheta(x)\zeta + u_v(x, \eta, \zeta)\Big)\boldsymbol{i} + w(x)\boldsymbol{k} \tag{1.1}$$

where $\vartheta(x)$ is the rotation of the section about the η-axis, positive if counterclockwise, $w(x)$ is its ζ rigid translation and $u_v(x, \eta, \zeta)$ is the warping displacement, for which the following representation:

$$u_v(x, \eta, \zeta) = \frac{Q(x)}{GI(x)}\varphi(x, \eta, \zeta) \tag{1.2}$$

can be assumed, having denoted by $Q(x)$ the applied vertical shear force at x-abscissa, G the Coulomb modulus, $I(x)$ the section moment of inertia about η-axis at x-abscissa and $\varphi(x, \eta, \zeta)$ the warping function. The eq.(1.2)

8

can be simplified by the following one:

$$u_v(x, \eta, \zeta) = \frac{Q(x)}{GI} \varphi(\eta, \zeta) \tag{1.3}$$

where the I moment and the warping function have been assumed constant with x, according to the hypothesis of cylindrical hull, approximately valid in the neighbourhood of the section. With these assumptions and notations the displacement field can be rewritten as follows:

$$\begin{cases} u = \vartheta(x)\zeta + \dfrac{Q(x)}{GI}\varphi(\eta, \zeta) \\ v = 0 \\ w = w(x) \end{cases} \tag{1.4}$$

1.2   The strain and stress fields

The strain field (for small deformation) is given by:

$$\begin{cases} \varepsilon_y = \varepsilon_z = \gamma_{yz} = 0 \\[2mm] \varepsilon_x = \dfrac{d\vartheta}{dx}\zeta + \dfrac{c(x)}{GI}\varphi(\eta, \zeta) \\[2mm] \boldsymbol{\gamma} = \dfrac{Q(x)}{GI}\nabla\varphi + \lambda(x)\boldsymbol{k} \end{cases} \tag{1.5}$$

where the positions:

$$c(x) = \frac{dQ(x)}{dx} \; ; \; \boldsymbol{\gamma} = \gamma_{xy}\boldsymbol{j} + \gamma_{xz}\boldsymbol{k} \tag{1.6}$$

have been made and the function:

$$\lambda(x) = \vartheta(x) + \frac{dw}{dx} \tag{1.7}$$

has been introduced, which vanishes when it is admitted - as in the practical procedure - that the vertical displacement $w(x)$ of the beam section is connected with the rotation $\vartheta(x)$ by the geometrical condition of orthogonality between the section and the elastic surface $z = 0$.

The substitution of whatever sections with the equivalent angle profiles (with the thickness of the web equal to that one of the section, and the other three dimensions obtained imposing equal values of area, inertia moments

and equal center position) allows to consider the structural section constituted by branches of constant t thickness, whose smallness has three main consequences:

- the indefinite equilibrium equation assumes a simplified form, which directly involves the unit surface load $\boldsymbol{p}$;

- it can be admitted the anisotropic behaviour characteristic of a thin plate: rigid through the thickness, elastic along the orthogonal directions; what implies that the elastic stresses reduce to the only normal and tangential ones, $\sigma_x \boldsymbol{i}$ and $\boldsymbol{\tau}$;

- it is possible to reduce the bidimensional problem of the $\varphi(\eta, \zeta)$ determination to a monodimensional one, assuming all the geometrical and mechanical quantities constant on the thickness branch, with their integral mean values.

As regards the anisotropic behaviour, it can be satisfactory studied referring each branch to an appropriate local system of orthogonal curvilinear coordinates. Concerning this, let ℓ_1, ℓ_2 and ℓ be three parallel curves (see Fig.1.2) of a given branch, the first two lying on the structure boundary, the third one coinciding with the median line. The orthogonal curvilinear coordinates (ξ, s, n) can be so introduced:

- s is the curvilinear abscissa on the median line, with the O origin in one of the two extremities (nodes) of the line;

- n is the linear abscissa on the thickness line through the considered point P, with origin on ℓ;

- $\xi = x - \overline{x}$ (with: $\overline{x} =$ global coordinate of the considered cross-section) is the linear abscissa with origin in O, on the parallel through O, to the x-axis of the global frame.

Denoting by $\boldsymbol{r}$ the position vector relative to O, for the orthogonal coordinate curves through the point $P(\overline{s}, \overline{n})$, the following vectorial equations are given:

$$\begin{cases} \boldsymbol{r} = (P(\overline{s}, \overline{n}) - O) + \xi \boldsymbol{i} \\ \boldsymbol{r} = \boldsymbol{r}(s, \overline{n}) \\ \boldsymbol{r} = \boldsymbol{r}(\overline{s}, n) \end{cases} \qquad (1.8)$$
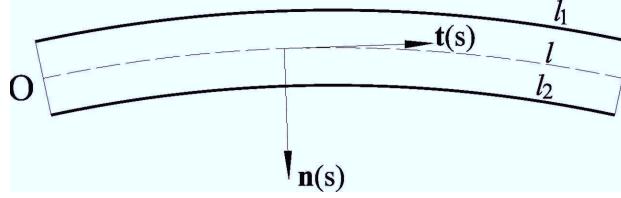
Figure 1.2: Local curvilinear reference system

The first curve coincides with the parallel to the x-axis, the second one with the line parallel to ℓ while the last one with the P thickness line. Denoting by S the curvilinear abscissa, the natural basis, variable with P, will be the system of the three orthogonal unit vectors:

$$\left\{ \frac{\partial \boldsymbol{r}}{\partial \xi}; \frac{\partial \boldsymbol{r}}{\partial n}; \frac{\partial \boldsymbol{r}}{\partial S} \right\} \; ; \; \frac{\partial \boldsymbol{r}}{\partial S} = \frac{\partial \boldsymbol{r}}{\partial s} \frac{\partial s}{\partial S} \tag{1.9}$$

Both the last two basis vectors are constant on any thickness line; their values coincide with the ones assumed in the ℓ intersection, and can be expressed by the functions of the only s variable:

$$\boldsymbol{t}(s) = \frac{d\boldsymbol{r}}{ds} \; ; \; \boldsymbol{n}(s) = \boldsymbol{t}(s) \times \boldsymbol{i} \tag{1.10}$$

when the conventional position has been assumed for the ℓ equation: $\boldsymbol{r}(s, 0) = \boldsymbol{r}(s)$ and the n coordinate has been assigned, according to the vector product (1.10); finally, the first vector is, in turn, constant on the entire cross section, because equal to $\boldsymbol{i}$.

The reference to the natural basis allows to analytically express the (approximate) anisotropic behaviour of the branch: denoting by $\sigma_x, \sigma_s, \sigma_n, \tau_{xs}, \tau_{xn}, \tau_{ns}$ the relative stress components, the only elastic ones will be, according to Vlasov's hypothesis:

$$\sigma_x, \sigma_s, \tau_{xs}$$

and, consequently, the same ones will be the only involved both in the Navier relations and in the expression of the Beltrami-von Mises sigma. Their expressions can be obtained starting from those ones of the strain components, referred to the curvilinear coordinates (ξ, s, n), that, in turn,

are obtained by the development of the general expressions (see [15]):

$$
\begin{cases}
\varepsilon_p = h_p \dfrac{\partial u_p}{\partial \alpha_p} + \sum_{i \neq p} \dfrac{\partial (\frac{1}{h_p})}{\partial \alpha_i} h_p h_i u_i \\[4mm]
\gamma_{pq} = \dfrac{h_p}{h_q} \dfrac{\partial (h_q u_q)}{\partial \alpha_p} + \dfrac{h_q}{h_p} \dfrac{\partial (h_p u_p)}{\partial \alpha_q}
\end{cases}
\;;\;
\begin{cases}
\alpha_p = \xi, s, n \\[2mm]
u_p = \boldsymbol{u} \cdot \boldsymbol{e}_p \\[2mm]
\boldsymbol{e}_p = \boldsymbol{i}, \boldsymbol{n}, \boldsymbol{t}
\end{cases}
\tag{1.11}
$$

where the Love's functions $h_p(\xi, s, n)$ have been introduced, connected with the Lamé parameters $\ell_p(\xi, s, n)$ by the relations:

$$
\ell_p(\xi, s, n) = \frac{1}{h_p^2(\xi, s, n)}
\tag{1.12}
$$

and so given by:

$$
h_x(\xi, s, n) = \frac{1}{\left| \dfrac{\partial \boldsymbol{r}}{\partial \xi} \right|} = 1 \;,\; h_n(\xi, s, n) = \frac{1}{\left| \dfrac{\partial \boldsymbol{r}}{\partial n} \right|} \;,\; h_s(\xi, s, n) = \frac{1}{\left| \dfrac{\partial \boldsymbol{r}}{\partial s} \right|}
\tag{1.13}
$$

As far as the (1.13) development is concerned, denoting by: $\rho = \rho(s, n)$ and $\rho(s) = \rho(s, 0)$ the algebraic curvature radii of the $\boldsymbol{r} = \boldsymbol{r}(s, n)$ and $\boldsymbol{r} = \boldsymbol{r}(s, 0)$ lines; by $C(s)$ the curvature center of the parallel lines through the s thickness line gives:

$$
\begin{cases}
\rho(s) = (C(s) - P(s)) \cdot \boldsymbol{n}(s) \\[2mm]
\rho(s, n) = (C(s) - P(s, n)) \cdot \boldsymbol{n}(s) = \rho(s) - n
\end{cases}
\tag{1.14}
$$

Then the second Frénet formula implies:

$$
\begin{cases}
\dfrac{\partial \boldsymbol{r}}{\partial s} = \dfrac{\partial P}{\partial s} = \dfrac{\rho(s) - n}{\rho(s)} \boldsymbol{t}(s) \\[4mm]
\dfrac{\partial \boldsymbol{r}}{\partial n} = \dfrac{\partial P}{\partial n} = \boldsymbol{n}(s)
\end{cases}
\tag{1.15}
$$

and the condition $\dfrac{\rho(s) - n}{\rho(s)} > 0$, verified on straight or quasi-straight branches for which $\left| \dfrac{n}{\rho(s)} \right| << 1$, gives:

$$
\begin{cases}
h_s(s, n) = \dfrac{\rho(s)}{\rho(s) - n} \\[4mm]
h_n(s, n) = 1
\end{cases}
\tag{1.16}
$$

Finally, denoting by $\varphi(s,n)$ the function composed of the three ones: $\varphi(\eta,\zeta)$, $\eta(s,n)$, $\zeta(s,n)$ and utilizing the relations (1.11), (1.16) and the first Frénet formula according to which:

$$\frac{d^2\zeta}{ds^2} = -\frac{1}{\rho(s)}\frac{d\eta}{ds} \; ; \; \frac{d^2\eta}{ds^2} = \frac{1}{\rho(s)}\frac{d\zeta}{ds} \tag{1.17}$$

the strain field in local curvilinear coordinates can be rewritten for straight branches, for which $\dfrac{\rho(s)-n}{\rho(s)} \to 1$, as follows:

$$\begin{cases} \varepsilon_x = \dfrac{d\vartheta}{dx}\zeta(s,n) + \dfrac{c(x)}{GI}\varphi(s,n) \\[2mm] \varepsilon_s = 0 \\[2mm] \varepsilon_n = 0 \end{cases} ; \begin{cases} \gamma_{xs} = \dfrac{Q(x)}{GI}\dfrac{\partial\varphi}{\partial s} + \lambda(x)\alpha_{sz} \\[2mm] \gamma_{xn} = \dfrac{Q(x)}{GI}\dfrac{\partial\varphi}{\partial n} + \lambda(x)\alpha_{nz} \\[2mm] \gamma_{sn} = 0 \end{cases} \tag{1.18}$$

where α_{sz} and α_{nz} are the director cosines of the unit vectors $\boldsymbol{s}$ and $\boldsymbol{n}$ respect to the ζ axis. Concerning the Navier relations, their general expressions in local curvilinear coordinates for linear elastic materials can be rewritten as follows:

$$\begin{cases} \varepsilon_x = \dfrac{1}{E}[\sigma_x - \nu(\sigma_s + \sigma_n)] \\[2mm] \varepsilon_s = \dfrac{1}{E}[\sigma_s - \nu(\sigma_x + \sigma_n)] \\[2mm] \varepsilon_n = \dfrac{1}{E}[\sigma_n - \nu(\sigma_x + \sigma_s)] \end{cases} ; \begin{cases} \gamma_{xs} = \dfrac{\tau_{xs}}{G} \\[2mm] \gamma_{xn} = \dfrac{\tau_{xn}}{G} \\[2mm] \gamma_{sn} = \dfrac{\tau_{sn}}{G} \end{cases} \tag{1.19}$$

Assuming the fundamental Vlasov's hypothesis of maintenance of the cross-section contour, according to which the beam section may be regarded as rigid along the thickness, the stress-strain relations can be rewritten as follows:

$$\begin{cases} \varepsilon_x = \dfrac{1}{E}[\sigma_x - \nu\sigma_s] \\[2mm] \varepsilon_s = \dfrac{1}{E}[\sigma_s - \nu\sigma_x] \\[2mm] \gamma_{xs} = \dfrac{\tau_{xs}}{G} \end{cases} \tag{1.20}$$

finally becoming, thanks to the fundamental result $\varepsilon_s = 0$ from which it follows $\sigma_s = \nu \sigma_x$:

$$\begin{cases} \sigma_x = \dfrac{E}{1-\nu^2}\varepsilon_x \\[2ex] \sigma_s = \nu \sigma_x \\[2ex] \tau_{xs} = G\gamma_{xs} \end{cases} \tag{1.21}$$

Now, according to the Beltrami-Von Mises criterion, the ideal stress is:

$$\sigma_{id} = \sqrt{\frac{1+\nu^2-\nu}{(1-\nu^2)^2}E^2\varepsilon_x^2 + 3\tau_{xs}^2} \tag{1.22}$$

that reduces for steel ($\nu = 0.3$) to:

$$\sigma_{id} = \sqrt{0.954 E^2\varepsilon_x^2 + 3\tau_{xs}^2} \tag{1.23}$$

This value is lightly lower than the one obtained taking $\sigma_x = E\varepsilon_x$ and $\sigma_s = 0$, as it is currently made in the scantling procedures, in favour of safety.

1.3 The warping function: local and global development

The indefinite equilibrium equations, which naturally involve all the stress components, can be written by applying a direct differential procedure to an infinitesimal volume element, of which one elementary dimension is t, so involving the unit surface load $\boldsymbol{p}$; on the contrary the boundary equation doesn't change, because applied to an elementary surface that doesn't include the thickness. Denoting by $\boldsymbol{\sigma}$ the stress tensor, defined in orthogonal curvilinear coordinates as follows:

$$\boldsymbol{\Sigma} = \begin{bmatrix} \sigma_x & \tau_{xs} & \tau_{xn} \\ \tau_{xs} & \sigma_s & \tau_{sn} \\ \tau_{xn} & \tau_{sn} & \sigma_n \end{bmatrix} \tag{1.24}$$

the indefinite and boundary equilibrium equations can be so expressed:

$$\begin{cases} \nabla \cdot \boldsymbol{\Sigma} + \dfrac{\boldsymbol{p}}{t} = \boldsymbol{0} \\[2ex] \boldsymbol{\Sigma}\boldsymbol{n} = \boldsymbol{p} \end{cases} \tag{1.25}$$

The only relevant scalar equations, in the study of the hull girder strength, are the x-projections of the vectorial (1.25), as the other ones include the components of $\boldsymbol{p}$ tangential and normal to the plating and so coinciding with the transverse stiffeners' reactions, that can be by them determined. Thanks to the hypothesis of cylindrical hull, that allows to assume $p_x = 0$ and denoting by A the cross-section domain and by ∂A its frontier, the warping function must be solution of the following differential problem:

$$\begin{cases} \dfrac{\partial \tau_{xs}}{\partial s} + \dfrac{\partial \tau_{xn}}{\partial n} = -\dfrac{\partial \sigma_x}{\partial x} \; \forall P \in A \\[3mm] \tau_{xn} = 0 \; \forall P \in \partial A \end{cases} \tag{1.26}$$

whence:

$$\begin{cases} \dfrac{Q(x)}{I} \nabla^2 \varphi = -\dfrac{E}{1-\nu^2}\left[\dfrac{d^2\vartheta}{dx^2}\zeta(s,n) + \dfrac{1}{GI}\dfrac{dc}{dx}\varphi(s,n)\right] \; \forall P \in A \\[4mm] \dfrac{\partial \varphi}{\partial n} = -\dfrac{G\lambda(x)}{Q(x)}I\alpha_{nz} \; \forall P \in \partial A \end{cases} \tag{1.27}$$

From the first of (1.27) it is possible to remarke a noticeable property of the warping function. It must be firstly considered that the symmetry of the structural section A as regards the ζ axis allows to introduce the parity notion, respect to η for functions defined on A. Particularly, as the function $\dfrac{d^2\vartheta}{dx^2}\zeta(s,n)$ is even on A, then $\dfrac{Q(x)}{I}\nabla^2\varphi + \dfrac{2}{I(1-\nu)}\dfrac{dc}{dx}\varphi(s,n)$ must be even on A too, what is verified if φ is, in turn, even respect to η, as it will be from now on admitted.

Denoting by $M(x)$ the applied bending moment in correspondence of the section at x-abscissa, the second order derivative of $\vartheta(x)$ may be obtained by the following global equilibrium equation:

$$M(x) = \int_A \sigma_x \zeta dA = \frac{EI}{1-\nu^2}\frac{d\vartheta}{dx} + \frac{2}{1-\nu}\frac{c(x)}{I}\int_A \varphi\zeta dA \tag{1.28}$$

from which it follows that:

$$\frac{d^2\vartheta}{dx^2} = (1-\nu^2)\frac{Q(x)}{EI} - \frac{1}{GI^2}\frac{dc}{dx}\int_A \varphi\zeta dA \tag{1.29}$$

Assuming from now on that the shear force longitudinal distribution is linear at intervals, what implies $\dfrac{dc}{dx} = 0$, and substituting the equation (1.29)

into the first of (1.27), the problem of the φ determination reduces to the following one:

$$\begin{cases} \nabla^2 \varphi = -\zeta \ \ \forall P \in A \\ \\ \dfrac{\partial \varphi}{\partial n} = -\dfrac{G\lambda(x)}{Q(x)} I \alpha_{nz} \ \forall P \in \partial A \end{cases} \tag{1.30}$$

according to which the warping function φ is solution of the Neumann boundary problem associated to the Poisson equation. Concerning $\lambda(x)$, this function can be obtained by the global equilibrium equation involving the vertical shear force, according to which:

$$Q(x) = G \int_A \boldsymbol{\gamma} \cdot \boldsymbol{k} dA = \int_A \Big[\tau_{xs} \alpha_{sz} + \tau_{xn} \alpha_{nz} \Big] dA \tag{1.31}$$

whence:

$$Q(x) = \frac{Q(x)}{I} \int_A \Big[\frac{\partial \varphi}{\partial s} \alpha_{sz} + \frac{\partial \varphi}{\partial n} \alpha_{nz} \Big] dA + G\lambda(x)A \tag{1.32}$$

from which it is possible to obtain $\lambda(x)$:

$$\lambda(x) = \frac{Q(x)}{GI} \frac{I - \displaystyle\int_A \Big[\frac{\partial \varphi}{\partial s} \alpha_{sz} + \frac{\partial \varphi}{\partial n} \alpha_{nz} \Big] dA}{A} \tag{1.33}$$

Applying, now, the first Green identity (see [17]), the following equality holds:

$$\int_A \nabla^2 \varphi \zeta dA = \int_{\partial A} \frac{\partial \varphi}{\partial n} \zeta d\Gamma - \int_A \Big[\frac{\partial \varphi}{\partial s} \alpha_{sz} + \frac{\partial \varphi}{\partial n} \alpha_{nz} \Big] dA = -I \tag{1.34}$$

from which it follows, by the first of (1.30), that:

$$\lambda(x) = -\frac{Q(x)}{GI} \frac{\displaystyle\int_{\partial A} \frac{\partial \varphi}{\partial n} \zeta d\Gamma}{A} \tag{1.35}$$

By (1.35) the problem (1.30) becomes:

$$\begin{cases} \nabla^2 \varphi = -\zeta \ \ \forall P \in A \\ \\ \dfrac{\partial \varphi}{\partial n} = \dfrac{\alpha_{nz}}{A} \displaystyle\int_{\partial A} \frac{\partial \varphi}{\partial n} \zeta d\Gamma \ \forall P \in \partial A \end{cases} \tag{1.36}$$

This problem shows that the geometrical quantities of the cross-section are the only ones involved, and so it is proved that φ is related to the only

16

geometry of the structural cross-section, what allows to assume the warping function constant with x, as it has been made according to the hypothesis of cylindrical hull. To determine the solution of this differential problem, let us rewrite the warping function as the sum of two unknown functions $\varphi_1(\eta, \zeta)$ and $\varphi_2(\eta, \zeta)$, so obtaining:

$$\begin{cases} \nabla^2(\varphi_1 + \varphi_2) = -\zeta \ \forall P \in A \\ \\ \dfrac{\partial}{\partial n}\Big(\varphi_1 + \varphi_2\Big) = \dfrac{\alpha_{nz}}{A} \displaystyle\int_{\partial A} \dfrac{\partial}{\partial n}\Big(\varphi_1 + \varphi_2\Big)\zeta d\Gamma \ \forall P \in \partial A \end{cases} \tag{1.37}$$

The problem (1.37) can be uncoupled as follows:

$$\begin{cases} \nabla^2 \varphi_1 = -\zeta \ \forall P \in A \\ \\ \dfrac{\partial \varphi_1}{\partial n} = 0 \, \forall P \in \partial A \end{cases} \tag{1.38}$$

and:

$$\begin{cases} \nabla^2 \varphi_2 = 0 \ \forall P \in A \\ \\ \dfrac{\partial \varphi_2}{\partial n} = \dfrac{\alpha_{nz}}{A} \displaystyle\int_{\partial A} \dfrac{\partial}{\partial n}\Big(\varphi_1 + \varphi_2\Big)\zeta d\Gamma \ \forall P \in \partial A \end{cases} \tag{1.39}$$

Thanks to the boundary condition of (1.38) the problem (1.39) can be rewritten as follows:

$$\begin{cases} \nabla^2 \varphi_2 = 0 \ \forall P \in A \\ \\ \dfrac{\partial \varphi_2}{\partial n} = \dfrac{\alpha_{nz}}{A} \displaystyle\int_{\partial A} \dfrac{\partial \varphi_2}{\partial n}\zeta d\Gamma \ \forall P \in \partial A \end{cases} \tag{1.40}$$

The problem (1.40) admits, for thin-walled beams, the solution $\varphi_2(\eta, \zeta) = 0$, formally obtaining the equality: $\varphi(\eta, \zeta) = \varphi_1(\eta, \zeta)$. From this result, by (1.35) it also follows $\lambda(x) = 0$, so verifying the orthogonality condition between the section and the elastic surface $z = 0$, what implies that the

stress field and the differential problem (1.36) can be so rewritten:

$$\begin{cases} \sigma_x = E\Big[\dfrac{d\vartheta}{dx}\zeta(s,n) + \dfrac{c(x)}{GI}\varphi(s,n)\Big] \\\\ \tau_{xs} = \dfrac{Q(x)}{I}\dfrac{\partial\varphi}{\partial s} \\\\ \tau_{xn} = \dfrac{Q(x)}{I}\dfrac{\partial\varphi}{\partial n} \end{cases} \tag{1.41}$$

and:

$$\begin{cases} \nabla^2\varphi = -\zeta \ \ \forall P \in A \\\\ \dfrac{\partial\varphi}{\partial n} = 0 \ \forall P \in \partial A \end{cases} \tag{1.42}$$

Concerning the necessary solvability condition of the problem (1.42), it can be so expressed (see [16]):

$$\int_A \nabla^2\varphi dA = \int_{\partial A} \frac{\partial\varphi}{\partial n}d\Gamma \tag{1.43}$$

By the second of (1.42) the right side integral is certainly null; concerning the left side integral, by the first of (1.42), it is also null, because the reference system has the origin in correspondence of the structural center of mass: so the condition (1.43) is always verified. From (1.42) it also follows that φ is solution of a Neumann problem, defined except an arbitrary constant: this indeterminacy is generall removed for beams with monoconnected cross-section assigning the φ value in the section center; for multiconnected cross-section whose center doesn't normally belong to the φ domain, a method useful for the numerical applications may consist of a separate calculation of the two φ restrictions to the parts A_1 and A_2 of A, the first one above the neutral axis, the second one under it; each one uniquely determined as solution of a mixed Dirichlet-Neumann boundary problem, given by the assumption $\varphi = const.$ on the section neutral axis:

$$\begin{cases} \nabla^2\varphi = -\zeta \ \ \forall P \in A_i \\\\ \dfrac{\partial\varphi}{\partial n} = 0 \ \forall P \in \partial(A)\cap\partial(A_i) \ for \ i = 1,2 \\\\ \varphi = const. \ \forall P \ \in \partial(A_i) - \Big(\partial(A)\cap\partial(A_i)\Big) \end{cases} \tag{1.44}$$

Concerning the global equilibrium conditions, with $\lambda(x) = 0$, by (1.32) and (1.34) it is immediately possible to verify that the tangential stress field automatically balances the vertical shear. Besides, the other following global equilibrium conditions are implicitly satisfied:

$$\int_A \sigma_x \eta \, dA = 0 \tag{1.45}$$

$$\int_A \tau_{xy} \, dA = 0 \tag{1.46}$$

$$\int_A \left[\tau_{xy} \zeta - \tau_{xz} \eta \right] dA = 0 \tag{1.47}$$

Particularly, the (1.45) is verified as the following integrals are null:

$$\int_A \eta \zeta \, dA = 0 \; ; \; \int_A \varphi \eta \, dA = 0 \tag{1.48}$$

The (1.46) is null as the partial derivative as regards η of the warping function is an odd function, respect to η, on A so obtaining:

$$\int_A \frac{\partial \varphi}{\partial \eta} \, dA = 0 \tag{1.49}$$

Finally, the (1.47) is verified as, respect to η, $\dfrac{\partial \varphi}{\partial \zeta}$ and ζ are even functions, while $\dfrac{\partial \varphi}{\partial \eta}$ and η are odd functions on A, so that the products under the following integrals are odd functions, too:

$$\int_A \frac{\partial \varphi}{\partial \eta} \zeta \, dA = 0 \; ; \; \int_A \frac{\partial \varphi}{\partial \zeta} \eta \, dA = 0 \tag{1.50}$$

Concerning the stretching condition, the warping function must verify the following global equation:

$$\int_A \sigma_x \, dA = 0 \Rightarrow \int_A \varphi \, dA = 0 \tag{1.51}$$

1.4 Minimum of the Euler-Lagrange functional

To solve the problem (1.44) with the global equilibrium condition (1.51), it is preferable to preliminarily assume all the geometrical and mechanical quantities constant on the branch thickness with their integral mean values, what is rigorously verified by the unit vectors of the "natural" basis and can

be accepted for the other ones, because of the thickness smallness. Furthermore all branches are assumed straight, so approximating a curvilinear one by a sufficient number of straight branches with nodes on its center line. The first hypothesis allows to substitute the bidimensional parameter (s, n) with the monodimensional one s in all the equations and relations till now considered; the second one, instead, allows to express all the vector operators in the same way they are for the Cartesian basis ($h_x = h_n = h_s = 1$). Denoting by l_i and t_i the length and the thickness of the $i - th$ branch and starting from the equation:

$$\zeta_i(s, n) = \zeta_i(s, 0) + \frac{\zeta_i\left(s, \frac{t_i}{2}\right) - \zeta_i\left(s, -\frac{t_i}{2}\right)}{t_i} n \tag{1.52}$$

it is immediately possible to verify that the $\overline{\zeta}_i(s)$ mean value coincides with the one on the median line $\zeta_i(s, 0)$, as it follows from the following relation:

$$\overline{\zeta}_i(s) = \zeta_i(s, 0) = \frac{1}{t_i} \int_{-\frac{t_i}{2}}^{\frac{t_i}{2}} \zeta_i(s, n) dn \tag{1.53}$$

Denoting by the suffixes m and n, with $m < n$, the initial and final nodes of each branch, the function $\overline{\zeta}_i(s)$ can be so expressed:

$$\overline{\zeta}_i(s) = \overline{\zeta}_{m,i} + \frac{\overline{\zeta}_{n,i} - \overline{\zeta}_{m,i}}{l_i} s \tag{1.54}$$

Similarly, for the $i - th$ branch, it is possible to introduce the mean value $\overline{\varphi}_i(s)$ of the warping function:

$$\overline{\varphi}_i(s) = \frac{1}{t_i} \int_{-\frac{t_i}{2}}^{\frac{t_i}{2}} \varphi_i(s, n) dn \tag{1.55}$$

so that, denoting by $\overline{\varphi}_{m,i}$ and $\overline{\varphi}_{n,i}$ the mean warping function nodal values in correspondence of the initial and final nodes of each branch, the problem (1.44) can be rewritten in a local form as follows:

$$\begin{cases} \dfrac{d^2\overline{\varphi}_i}{ds^2} = -\overline{\zeta}_i(s) \ \forall s \in [0, \ell_i] \\ \\ \overline{\varphi}_i(0) = \overline{\varphi}_{m,i} \, ; \ \overline{\varphi}_i(\ell_i) = \overline{\varphi}_{n,i} \end{cases} \tag{1.56}$$

as the Neumann boundary condition is in this case implicitly satisfied. Obviously, the condition $\overline{\varphi}_i = const.$ in correspondence of the nodes belonging

20

to the section neutral axis must be added. The (1.56) represents the local approximate form of the (1.44) and shows that the points belonging to the neutral axis are inflexion points for $\overline{\varphi}(s)$, whose expression and its first derivative are uniquely determined:

$$
\begin{cases}
\overline{\varphi}_i(s) = \overline{\varphi}_{m,i} + \left[\dfrac{\overline{\varphi}_{n,i} - \overline{\varphi}_{m,i}}{\ell_i} + \dfrac{\ell_i(\overline{\zeta}_{n,i} + 2\overline{\zeta}_{m,i})}{6} \right] s - \left[\overline{\zeta}_{m,i} + \dfrac{\overline{\zeta}_{n,i} - \overline{\zeta}_{m,i}}{3\ell_i} s \right] \dfrac{s^2}{2} \\[4mm]
\dfrac{d\overline{\varphi}_i}{ds} = \dfrac{\overline{\varphi}_{n,i} - \overline{\varphi}_{m,i}}{\ell_i} + \dfrac{\ell_i}{6}(\overline{\zeta}_{n,i} + 2\overline{\zeta}_{m,i}) - \left[\overline{\zeta}_{m,i} + \dfrac{\overline{\zeta}_{n,i} - \overline{\zeta}_{m,i}}{2\ell_i} s \right] s
\end{cases}
\tag{1.57}
$$

As far as the $\overline{\varphi}$ nodal values are concerned, their numerical determination can be carried out by the resolution of a variational problem, whose Euler's equation is the first of (1.56). It's well known (e.g.: [18]) that solving the Poisson equation with some boundary conditions is equivalent to finding the function that satisfies the same boundary conditions and minimizes the corresponding Euler-Lagrange functional, that can be written, according to the introduced notation, as follows:

$$
U = \int_A \left[\left(\frac{d\overline{\varphi}}{ds} \right)^2 - 2\overline{\varphi}\,\overline{\zeta} \right] dA
\tag{1.58}
$$

So, denoting by N the number of branches of the half-section, thanks to the ship symmetry respect to the xz plane, the functional can be so rewritten:

$$
U = 2 \sum_{i=1}^{N} t_i \int_0^{\ell_i} \left[\left(\frac{d\overline{\varphi}_i}{ds} \right)^2 - 2\overline{\varphi}_i \overline{\zeta}_i \right] ds
\tag{1.59}
$$

To determine the warping function nodal values, it is necessary to search for the extremals of the functional U. The stationarity condition permits to write P linear equations, if P is the nodes number on the half-section:

$$
\frac{\partial}{\partial \overline{\varphi}_k} \sum_{i=1}^{N} t_i \int_0^{\ell_i} \left[\left(\frac{d\overline{\varphi}_i}{ds} \right)^2 - 2\overline{\varphi}_i \overline{\zeta}_i \right] ds = 0 \; for \, k = 1...P
\tag{1.60}
$$

The uniform continuity of the under integral functions allows the derivation under the integral sign, so obtaining:

$$
\sum_{i=1}^{n(k)} t_i \int_0^{\ell_i} \frac{\partial}{\partial \overline{\varphi}_k} \left[\left(\frac{d\overline{\varphi}_i}{ds} \right)^2 - 2\overline{\varphi}_i \overline{\zeta}_i \right] ds = 0
\tag{1.61}
$$

having denoted by $n(k)$ the number of branches concurrent in the k-th-node. The eq. (1.61) can be rewritten as follows:

$$\sum_{i=1}^{n(k)} t_i \int_0^{\ell_i} \left[\frac{d\overline{\varphi}_i}{ds} \frac{\partial}{\partial \overline{\varphi}_k} \left(\frac{d\overline{\varphi}_i}{ds} \right) - \overline{\zeta}_i \frac{\partial}{\partial \overline{\varphi}_k} \overline{\varphi}_i \right] ds = 0 \qquad (1.62)$$

finally becoming:

$$\sum_{i=1}^{n(k)} \frac{t_i}{\ell_i} \left(\overline{\varphi}_k - \overline{\varphi}_{r,i} \right) = \frac{1}{6} \sum_{i=1}^{n(k)} t_i \ell_i \left(2\overline{\zeta}_k + \overline{\zeta}_{r,i} \right) \qquad (1.63)$$

having denoted, for each branch concurrent in the k-th-node, by r the node different from the k-th one. Obviously, as this equation system is indetermined, to obtain a solution, it's necessary to impose the condition $\overline{\varphi}_i = const.$ in correspondence of the nodes belonging to the section neutral axis. Finally, as the global condition (1.51) has to be verified, too, the following constant $c_{\overline{\varphi}}$ must be added to the obtained nodal values:

$$c_{\overline{\varphi}} = -\frac{\int_A \overline{\varphi} dA}{A} \qquad (1.64)$$

whence:

$$c_{\overline{\varphi}} = -\frac{\sum_{i=1}^{N} t_i \ell_i \left[\overline{\varphi}_{m,i} + \overline{\varphi}_{n,i} + \frac{l_i^2}{12} \left(\overline{\zeta}_{m,i} + \overline{\zeta}_{n,i} \right) \right]}{2 \sum_{i=1}^{N} t_i \ell_i} \qquad (1.65)$$

1.5 Analysis of the stress field

Obviously, as well as for the warping function, it is possible to introduce the mean values of the stress components. The $\overline{\sigma}_x$ mean value may be expressed in a local form for the $i - th$ branch as follows:

$$\overline{\sigma}_{x,i} = \frac{1}{t_i} \int_{-\frac{t_i}{2}}^{\frac{t_i}{2}} \sigma_{x,i}(s,n) dn \qquad (1.66)$$

from which it follows:

$$\overline{\sigma}_{x,i} = \frac{E}{1-\nu^2} \frac{d\theta}{dx} \overline{\zeta}_i(s) + \frac{2}{1-\nu} \frac{c(x)}{I} \overline{\varphi}_i(s) \qquad (1.67)$$

The mean value of the tangential stress component can be similarly introduced:

$$\overline{\tau}_{xs,i} = \frac{1}{t_i} \int_{-\frac{t_i}{2}}^{\frac{t_i}{2}} \tau_{xs,i}(s,n)dn \tag{1.68}$$

finally becoming, thanks to the uniform continuity of the under integral function:

$$\overline{\tau}_{xs,i} = \frac{Q(x)}{I} \frac{d\overline{\varphi}_i}{ds} \tag{1.69}$$

Then the stress field becomes:

$$\begin{cases} \overline{\sigma}_{x,i} = \overline{\sigma}_{B,i} + \overline{\sigma}_{W,i} \\[2mm] \overline{\tau}_{xs,i} = \dfrac{Q(x)}{I} \dfrac{d\overline{\varphi}_i}{ds} \end{cases} \tag{1.70}$$

with:

$$\begin{cases} \overline{\sigma}_{B,i} = \dfrac{M(x)}{I}\overline{\zeta}_i(s) \\[4mm] \overline{\sigma}_{W,i} = \dfrac{2c(x)}{(1-\nu)I}\Big[\overline{\varphi}_i(s) - 2\dfrac{\overline{\zeta}_i(s)}{I}\sum_{i=1}^{N} t_i \int_0^{\ell_i} \overline{\varphi}_i(s)\overline{\zeta}_i(s)ds\Big] \end{cases} \tag{1.71}$$

The warping part of the normal stress field can be rewritten as follows:

$$\overline{\sigma}_{W,i} = \frac{2c(x)}{(1-\nu)I}\overline{\psi}_i(s) \tag{1.72}$$

with:

$$\overline{\psi}_i(s) = \overline{\varphi}_i(s) - \frac{2}{I}\overline{\zeta}_i(s)\sum_{i=1}^{N} t_i \kappa_i \tag{1.73}$$

and:

$$\kappa_i = \frac{(\overline{\varphi}_{n,i} + 2\overline{\varphi}_{m,i})\overline{\zeta}_{m,i} + (\overline{\varphi}_{m,i} + 2\overline{\varphi}_{n,i})\overline{\zeta}_{n,i}}{6} + \frac{4\overline{\zeta}_{m,i}^2 + 4\overline{\zeta}_{n,i}^2 + 7\overline{\zeta}_{m,i}\overline{\zeta}_{n,i}}{180} \tag{1.74}$$

It seems quite clear that the variability of the shear force generates warping normal stresses and, consequently, a consistent redistribution of the σ stresses, strictly related to the $c(x)$ values, which can have an appreciable influence on the global and local scantling procedures, especially for all those loading conditions including quasi-concentrated loads, such as the alternate holds loading condtion for bulk-carriers.

1.6 The shear center vertical position

It is well known that in all beam theories the shear forces are assumed to be applied in correspondence of the section shear center, defined as the point that permits to avoid torsion. For ship structures, thanks to the symmetry respect to the xz plane, the shear center will lie on the ship symmetry plane, so that only its vertical position has to be determined. In the following paragraph a procedure to determine the shear center vertical position is proposed, starting from the horizontal bending-shear displacement field; all the assumptions made in the previous paragraphs will be considered valid and only the fundamental steps will be pointed out. The displacement field can be assumed as follows:

$$\begin{cases} u = -\vartheta_H(x)\eta + \dfrac{Q_H}{GI_\zeta}\chi(\eta,\zeta) \\ v = v(x) \\ w = 0 \end{cases} \tag{1.75}$$

having denoted by $\vartheta_H(x)$ the rotation of the section about the ζ-axis positive if counter-clockwise, $v(x)$ its η rigid translation, Q_H the applied horizontal shear force constant vs. x, I_ζ the section moment of inertia about the ζ axis and χ the horizontal warping function. Thanks to the orthogonality condition between the section and the elastic surface $y = 0$:

$$\vartheta_H(x) = \frac{dv}{dx} \tag{1.76}$$

the mean values of the stress field for the $i - th$ branch are:

$$\begin{cases} \overline{\sigma}_{x,i} = -E\dfrac{d\vartheta_H}{dx}\overline{\eta}_i(s) \\[4mm] \overline{\tau}_{xs,i} = \dfrac{Q_H}{I_\zeta}\dfrac{d\overline{\chi}_i}{ds} \end{cases} \tag{1.77}$$

with:

$$\overline{\eta}_i(s) = \overline{\eta}_{m,i} + \frac{\overline{\eta}_{n,i} - \overline{\eta}_{m,i}}{\ell_i}s \tag{1.78}$$

and:

$$\begin{cases} \overline{\chi}_i(s) = \overline{\chi}_{m,i} + \left[\dfrac{\overline{\chi}_{n,i} - \overline{\chi}_{m,i}}{\ell_i} + \dfrac{\ell_i(\overline{\eta}_{n,i} + 2\overline{\eta}_{m,i})}{6}\right]s - \left[\overline{\eta}_{m,i} + \dfrac{\overline{\eta}_{n,i} - \overline{\eta}_{m,i}}{3\ell_i}s\right]\dfrac{s^2}{2} \\[4mm] \dfrac{d\overline{\chi}_i}{ds} = \dfrac{\overline{\chi}_{n,i} - \overline{\chi}_{m,i}}{\ell_i} + \dfrac{\ell_i}{6}(\overline{\eta}_{n,i} + 2\overline{\eta}_{m,i}) - \left[\overline{\eta}_{m,i} + \dfrac{\overline{\eta}_{n,i} - \overline{\eta}_{m,i}}{2\ell_i}s\right]s \end{cases}$$
(1.79)

The unknown warping function nodal values can be determined after solving the following equation system extended, in this case, to the nodes of the entire cross-section:

$$\sum_{i=1}^{n(k)} \frac{t_i}{\ell_i}\left(\overline{\chi}_k - \overline{\chi}_{r,i}\right) = \frac{1}{6}\sum_{i=1}^{n(k)} t_i\ell_i\left(2\overline{\eta}_k + \overline{\eta}_{r,i}\right)$$
(1.80)

having denoted, for each branch concurrent in the *k-th*-node, by r the node different from the *k-th* one. As regards the shear center vertical position, it can be easily determined taking into account that the horizontal shear, if applied in correspondence of the section barycenter, can determine a twist moment, so considering the equivalence of the following systems:

$$\left\{G(x), Q_H\boldsymbol{j}, M_t\boldsymbol{i}\right\} \Leftrightarrow \left\{P(0, \zeta_Q), Q_H\boldsymbol{j}\right\}$$
(1.81)

having denoted by ζ_Q the unknown vertical position of the shear center as regards the Cartesian frame sketched in Fig. 1.1. As the two systems must have the same resultant, the following equality holds:

$$Q_H\left[P(0, \zeta_Q) - G(x)\right] \times \boldsymbol{j} = M_t\boldsymbol{i}$$
(1.82)

from which it follows:

$$\zeta_Q\boldsymbol{k} \times \boldsymbol{j} = \frac{M_t}{Q_H}\boldsymbol{i}$$
(1.83)

finally obtaining:

$$\zeta_Q = -\frac{M_t}{Q_H}$$
(1.84)

The twist moment generated by the horizontal shear can be so expressed:

$$M_t = \int_A \boldsymbol{r} \times \tau_{xs}\boldsymbol{s} \cdot \boldsymbol{i}dA$$
(1.85)

with: $\boldsymbol{r} = P - G(x) = \eta\boldsymbol{j} + \zeta\boldsymbol{k}$. Denoting by M the number of branches of the entire cross-section and assuming for all the geometrical and mechanical

quantities their integral mean values, the eq. (1.85) becomes:

$$M_t = \sum_{i=1}^{M} t_i \int_0^{\ell_i} \left[\boldsymbol{r}_i \times \overline{\tau}_{xs,i} \boldsymbol{s}_i \cdot \boldsymbol{i} \right] ds \tag{1.86}$$

so obtaining:

$$M_t = \frac{Q_H}{I_\zeta} \sum_{i=1}^{M} t_i \overline{h}_i \int_0^{\ell_i} \frac{d\overline{\chi}_i}{ds} ds \tag{1.87}$$

with: $\overline{h}_i = \dfrac{\overline{\eta}_{m,i}\overline{\zeta}_{n,i} - \overline{\eta}_{n,i}\overline{\zeta}_{m,i}}{\ell_i}$. Finally the vertical position of the shear center can be easily determined:

$$\zeta_Q = - \frac{\displaystyle\sum_{i=1}^{M} t_i \overline{h}_i \left(\overline{\chi}_{n,i} - \overline{\chi}_{m,i} \right)}{I_\zeta} \tag{1.88}$$

Chapter 2

The SV-like bending-shear theory for thin-walled beams

This chapter focuses on the application of Saint-Venant's bending-shear theory to thin-walled beams, generally analyzed assuming the fundamental Vlasov's structural hypothesis of maintenance of the cross-section contour. New relations are obtained for tangential and normal stresses; a numerical method, based on a Ritz variational procedure, is developed and a procedure to determine the vertical position of the shear center is presented. Finally, the fundamental differences between Vlasov's and Saint-Venant's theories are pointed out, particularly for the tangential stress field evaluation, verifying that the Vlasov's tangential stress field may be regarded as the limit of the Saint-Venant's one, when the material Poisson modulus $\nu \to 0$.

2.1   The displacement field

Let us consider the hull girder cylindrical body as a Saint-Venant solid, composed of homogeneous and isotropic material, and loaded only on the two beam-ends, hypothesis certainly true if the external loads are negligible, if compared to the internal stress characteristics. With reference to the global and local Cartesian frames schetched in Fig. 1.1 and Fig. 1.2, let us define by u, v, w the three displacement components in the x, η, ζ directions respectively. Assuming the Saint-Venant's hypotheses: body forces' negleg-

ibility, lateral surface unloaded, $\sigma_y = \sigma_z = \tau_{yz}$ everywhere in the body, it is well known that a displacement field is a *Saint-Venant field* only if it satisfies the following conditions:

Navier relations

$$\begin{cases} \varepsilon_y = \varepsilon_z = -\nu\varepsilon_x \\ \\ \gamma_{yz} = 0 \end{cases} \tag{2.1}$$

Indefinite equilibrium equations

$$\begin{cases} \dfrac{\partial \tau_{xy}}{\partial x} = 0 \\ \\ \dfrac{\partial \tau_{xz}}{\partial x} = 0 \\ \\ \dfrac{\partial \tau_{xy}}{\partial \eta} + \dfrac{\partial \tau_{xz}}{\partial \zeta} = -\dfrac{\partial \sigma_x}{\partial x} \end{cases} \tag{2.2}$$

Boundary condition on the lateral unloaded surface

$$\tau_{xy}\alpha_{ny} + \tau_{xz}\alpha_{nz} = 0 \tag{2.3}$$

having defined by ν the Poisson modulus and by α_{ny} and α_{nz} the director cosines of the unit normal vector $\boldsymbol{n}$, positive outwards. The Saint-Venant's bending-shear displacement field can be introduced as follows:

$$\begin{cases} u = \vartheta(x)\zeta + \dfrac{Q}{GI}\varphi(\eta,\zeta) \\ \\ v = -\nu\dfrac{d\vartheta}{dx}\eta\zeta \\ \\ w = w_0(x) + \dfrac{\nu}{2}\dfrac{d\vartheta}{dx}\left(\eta^2 - \zeta^2\right) \end{cases} \tag{2.4}$$

having denoted by $\vartheta(x)$ the section's rotation about the η-axis, positive if counter-clockwise; Q the applied vertical shear force, constant vs. x; $\varphi(\eta,\zeta)$ the warping function and $w_0(x)$ the section rigid body motion along the ζ-axis, connected with the rotation by the geometrical condition of orthogonality between the section and the elastic surface $z = 0$:

$$\vartheta(x) = -\dfrac{dw_0}{dx} \tag{2.5}$$

As it will be subsequently verified, the condition $Q = const.$ permits to assume:

$$\frac{d^3\vartheta}{dx^3} = 0 \qquad (2.6)$$

so that the equations (2.3) define a Saint-Venant's displacement field.

2.2 The stress and strain fields

With the previous assumptions and notations, the strain field for small deformations becomes:

$$\begin{cases} \varepsilon_x = \dfrac{d\vartheta}{dx}\zeta \\[2em] \varepsilon_y = -\nu\varepsilon_x \\[2em] \varepsilon_z = -\nu\varepsilon_x \end{cases} \qquad (2.7)$$

and:

$$\begin{cases} \gamma_{xy} = \dfrac{Q}{GI}\dfrac{\partial\varphi}{\partial\eta} - \nu\dfrac{d^2\vartheta}{dx^2}\eta\zeta \\[2em] \gamma_{xz} = \dfrac{Q}{GI}\dfrac{\partial\varphi}{\partial\zeta} + \dfrac{\nu}{2}\dfrac{d^2\vartheta}{dx^2}\left(\eta^2 - \zeta^2\right) \\[2em] \gamma_{yz} = 0 \end{cases} \qquad (2.8)$$

Denoting by E the Young modulus, the inverse Navier relations can be written as follows:

$$\begin{cases} \sigma_x = \dfrac{E}{1+\nu}\left[\varepsilon_x + \dfrac{\nu}{1-2\nu}\left(\varepsilon_x + \varepsilon_y + \varepsilon_z\right)\right] \\[2em] \sigma_y = \dfrac{E}{1+\nu}\left[\varepsilon_y + \dfrac{\nu}{1-2\nu}\left(\varepsilon_x + \varepsilon_y + \varepsilon_z\right)\right] \\[2em] \sigma_z = \dfrac{E}{1+\nu}\left[\varepsilon_z + \dfrac{\nu}{1-2\nu}\left(\varepsilon_x + \varepsilon_y + \varepsilon_z\right)\right] \end{cases} \qquad (2.9)$$

and:

$$
\begin{cases}
\tau_{xy} = G\gamma_{xy} \\[2em]
\tau_{xz} = G\gamma_{xz} \\[2em]
\tau_{yz} = G\gamma_{yz}
\end{cases}
\tag{2.10}
$$

By (2.9) and (2.10), it is immediately possible to verify that the non-null stress components are:

$$
\begin{cases}
\sigma_x = E\dfrac{d\vartheta}{dx}\zeta \\[2em]
\tau_{xy} = \dfrac{Q}{I}\dfrac{\partial\varphi}{\partial\eta} - \nu G\dfrac{d^2\vartheta}{dx^2}\eta\zeta \\[2em]
\tau_{xz} = \dfrac{Q}{I}\dfrac{\partial\varphi}{\partial\zeta} + G\dfrac{\nu}{2}\dfrac{d^2\vartheta}{dx^2}\left(\eta^2 - \zeta^2\right)
\end{cases}
\tag{2.11}
$$

Introducing from now on for each branch of the cross-section the curvilinear reference system defined in Chapter 1 and denoting by α_{sy} and α_{sz} the components of the unit tangential vector respect to the η and ζ axes, the stress field can be rewritten in local curvilinear coordinates as follows:

$$
\begin{cases}
\sigma_x = E\dfrac{d\vartheta}{dx}\zeta(s,n) \\[2em]
\tau_{xs} = \dfrac{Q}{I}\dfrac{\partial\varphi}{\partial s} + G\dfrac{\nu}{2}\dfrac{d^2\vartheta}{dx^2}\left[\left(\eta^2 - \zeta^2\right)\alpha_{sz} - 2\eta\zeta\alpha_{sy}\right] \\[2em]
\tau_{xn} = \dfrac{Q}{I}\dfrac{\partial\varphi}{\partial n} + G\dfrac{\nu}{2}\dfrac{d^2\vartheta}{dx^2}\left[\left(\eta^2 - \zeta^2\right)\alpha_{nz} - 2\eta\zeta\alpha_{ny}\right]
\end{cases}
\tag{2.12}
$$

2.3 The warping function: local and global development

First of all, it is convenient to determine the function $\dfrac{d^2\vartheta}{dx^2}$, connected to the applied vertical shear Q by the global condition:

$$
M(x) = \int_A \sigma_x \zeta \, dA
\tag{2.13}
$$

from which it follows:

$$\frac{d\vartheta}{dx} = \frac{M(x)}{EI} \tag{2.14}$$

and:

$$\frac{d^2\vartheta}{dx^2} = \frac{Q}{EI} \tag{2.15}$$

having denoted by A the cross-section domain. The indefinite equilibrium equation along the beam axis and the relevant boundary condition are:

$$\begin{cases} \dfrac{\partial \tau_{xy}}{\partial \eta} + \dfrac{\partial \tau_{xz}}{\partial \zeta} = -\dfrac{\partial \sigma_x}{\partial x} \, \forall P \in A \\[2ex] \tau_{xn} = 0 \, \forall P \in \partial A \end{cases} \tag{2.16}$$

By (2.12) and (2.15) the differential problem (2.16) becomes:

$$\begin{cases} \nabla^2 \varphi = -\dfrac{1}{1+\nu} \zeta \, \forall P \in A \\[2ex] \dfrac{\partial \varphi}{\partial n} = \dfrac{\nu}{2(1+\nu)} \Big[\eta \zeta \alpha_{ny} - \dfrac{\alpha_{nz}}{2} \big(\eta^2 - \zeta^2 \big) \Big] \, \forall P \in \partial A \end{cases} \tag{2.17}$$

From (2.17) it follows that the warping function must be solution of a Neumann boundary problem associated to the Poisson equation and depends, by means of the Poisson modulus, on the material, supposed homogeneous and isotropic and on the cross-section's geometry. It is well known that the necessary solvability condition for a Neumann boundary problem associated to the Poisson equation is the following one:

$$\int_{\partial A} \frac{\partial \varphi}{\partial n} ds = \int_A \nabla^2 \varphi \, dA \tag{2.18}$$

Thanks to the second of (2.17) the first member of (2.18) can be rewritten as follows:

$$\int_{\partial A} \frac{\partial \varphi}{\partial n} ds = \frac{\nu}{2(1+\nu)} \int_A \Big[\eta \zeta \alpha_{ny} - \frac{\alpha_{nz}}{2} \big(\eta^2 - \zeta^2 \big) \Big] dA \tag{2.19}$$

and then, thanks to the Gauss theoreme, it becomes:

$$\int_{\partial A} \frac{\partial \varphi}{\partial n} ds = \frac{\nu}{2(1+\nu)} \int_A \Big[\frac{\partial}{\partial \eta} \big(\eta \zeta \big) - \frac{1}{2} \frac{\partial}{\partial \zeta} \big(\eta^2 - \zeta^2 \big) \Big] dA \tag{2.20}$$

so obtaining:

$$\int_{\partial A} \frac{\partial \varphi}{\partial n} ds = \frac{\nu}{(1+\nu)} \int_A \zeta \, dA = 0 \tag{2.21}$$

as the ζ axis passes through the section's centroid. Finally, the necessary solvability condition (2.18) can be rewritten as follows:

$$\int_A \nabla^2 \varphi dA = 0 \qquad (2.22)$$

so that, thanks to the first of (2.17), it is always verified. It is also possible to verify immediately that the tangential stress field obtained after solving the problem (2.17) automatically balances the vertical shear; in other terms the following global condition must be verified:

$$\int_A \tau_{xz} dA = Q \qquad (2.23)$$

Starting from the third of (2.11), by (2.15), the left hand side of (2.23) can be so rewritten:

$$\frac{Q}{I} \Big[\int_A \frac{\partial \varphi}{\partial \zeta} dA + \frac{\nu}{4(1+\nu)} \Big(I_\zeta - I \Big) \Big] = Q \qquad (2.24)$$

having denoted by I_ζ the section moment of inertia as regards the ζ axis. Applying now the generalized integration by parts formula and then the Gauss theoreme, the following equality holds:

$$\int_A \frac{\partial \varphi}{\partial \zeta} dA = \int_{\partial A} \frac{\partial \varphi}{\partial n} \zeta ds - \int_A \nabla^2 \varphi \zeta dA = \frac{\nu}{4(1+\nu)} \Big[\Big(5 + \frac{4}{\nu} \Big) I - I_\zeta \Big] \quad (2.25)$$

Finally, substituting the eq. (2.25) into the (2.24) it is simply possible to verify that the equation (2.23) becomes an identity. Now, the negligibility of the thickness branch as regards its length permits, without great errors, to neglect the dependence of the function $\eta(s, n)$ and $\zeta(s, n)$ on the variable n, regarding them as functions of the only curvilinear abscissa s, evaluated on the branch center line. Denoting, from now on, by ℓ_i and t_i the length and the thickness of the i-th branch and by m, i and n, i, with $m, i < n, i$ the initial and final nodes of each branch, these functions can be expressed as follows:

$$\overline{\eta}_i(s) = \overline{\eta}_{m,i} + \frac{\overline{\eta}_{n,i} - \overline{\eta}_{m,i}}{\ell_i} s \; ; \; \overline{\zeta}_i(s) = \overline{\zeta}_{m,i} + \frac{\overline{\zeta}_{n,i} - \overline{\zeta}_{m,i}}{\ell_i} s \qquad (2.26)$$

Furthermore, the warping function $\varphi(s, n)$ can be expressed as the sum of two terms: the first one $\overline{\varphi}(s)$ constant through the thickness and defined on the branch center line, the second one $\psi(s, n)$ determined assuming that the

tangential stress component τ_{xn}, null on the beam boundary surface, is null along the thickness too, thanks to its smallness:

$$\varphi(s,n) = \overline{\varphi}(s) + \psi(s,n) \tag{2.27}$$

Thanks to the condition $\tau_{xn} = 0$, the restriction of the function $\psi(s,n)$ to the i-th branch remains uniquely determined:

$$\psi_i(s.n) = -\frac{\nu}{4(1+\nu)}\left[\left(\overline{\eta}_i^2 - \overline{\zeta}_i^2\right)\alpha_{nz} - 2\overline{\eta}_i\overline{\zeta}_i\alpha_{ny}\right]n \tag{2.28}$$

Now, denoting by $\overline{\varphi}_{m,i}$ and $\overline{\varphi}_{n,i}$ the unknown values of the warping function in correspondence of the initial and final nodes of each branch, the other component can be obtained as a solution of the following differential problem, whose local form relative to the i-th branch, is:

$$\begin{cases} \dfrac{d^2\overline{\varphi}_i}{ds^2} = -k_\nu\overline{\zeta}_i(s) \\[2mm] \overline{\varphi}_i(0) = \overline{\varphi}_{m,i} \,;\, \overline{\varphi}_i(l_i) = \overline{\varphi}_{n,i} \end{cases} \tag{2.29}$$

with $k_\nu = \dfrac{2+\nu}{2+2\nu}$. The assumption $\tau_{xn} = 0 \;\; \forall(s,n) = \left[0, l_i\right] \times \left[-\dfrac{t_i}{2}, \dfrac{t_i}{2}\right]$ implies that the tangential stress field τ_{xs} doesn't necessary balance the vertical shear, so that it is necessary to modify the differential problem, adding an unknown constant k:

$$\begin{cases} \dfrac{d^2\overline{\varphi}_i}{ds^2} = -\dfrac{k_\nu}{k}\overline{\zeta}_i(s) \\[2mm] \overline{\varphi}_i(0) = \overline{\varphi}_{m,i} \,;\, \overline{\varphi}_i(l_i) = \overline{\varphi}_{n,i} \end{cases} \tag{2.30}$$

The constant k can be determined from the following global condition:

$$Q = \int_A \tau_{xs}\alpha_{sz}dA = \frac{Q}{I}\int_A \frac{\partial\varphi}{\partial s}\alpha_{sz}dA + \frac{\nu}{4(1+\nu)}\int_A \left[\left(\overline{\eta}^2 - \overline{\zeta}^2\right)\alpha_{sz}^2 - 2\overline{\eta}\overline{\zeta}\alpha_{sy}\alpha_{sz}\right]dA \tag{2.31}$$

Applying the generalized integration by parts formula, the following equality holds:

$$\int_A \frac{\partial^2\varphi}{\partial s^2}\zeta dA = \int_{\partial A} \frac{\partial\varphi}{\partial s}\zeta\left(\boldsymbol{s}\cdot\boldsymbol{n}\right)ds - \int_A \frac{\partial\varphi}{\partial s}\alpha_{sz}dA = \frac{k_\nu}{k}I \tag{2.32}$$

Taking into account that $\boldsymbol{s} \cdot \boldsymbol{n} = 0$ and substituting the eq. (2.32) into the (2.31) the unknown constant k can be immediately obtained:

$$k = \frac{k_\nu}{1 - \dfrac{\nu}{4(1+\nu)I} \displaystyle\int_A \left[\left(\overline{\eta}^2 - \overline{\zeta}^2\right)\alpha_{sz}^2 - 2\overline{\eta}\,\overline{\zeta}\alpha_{sy}\alpha_{sz}\right]dA} \tag{2.33}$$

Finally, the differential problem to be solved can be rewritten as follows:

$$\begin{cases} \dfrac{d^2\overline{\varphi}_i}{ds^2} = -\rho\overline{\zeta}_i(s) \\[2ex] \overline{\varphi}_i(0) = \overline{\varphi}_{m,i} \,;\, \overline{\varphi}_i(l_i) = \overline{\varphi}_{n,i} \end{cases} \tag{2.34}$$

with:

$$\rho = 1 - \frac{\nu}{4(1+\nu)I} \int_A \left[\left(\overline{\eta}^2 - \overline{\zeta}^2\right)\alpha_{sz}^2 - 2\overline{\eta}\,\overline{\zeta}\alpha_{sy}\alpha_{sz}\right]dA \tag{2.35}$$

It is noticed that this corrective constant ρ for ship structures generally assumes values comprised between 0.92 and 0.94, so that it is very near to the unity. Furthermore it appears clear that when the Poisson modulus $\nu \to 0$, then $\rho \to 1$, so that the problem (2.34) coincides with the one obtained applying the Vlasov's theory. In other terms, this constant permits to approximately take into account the effect of the section lateral contraction for thin-walled beams, assumed null in the classical theories of thin-walled beams, where the shape of the section is totally preserved after the application of the external loads.

2.4   Minimum of the Euler-Lagrange functional

Starting from the problem (2.30), that represents the local approximate form of (2.17), the warping function and its first derivative are uniquely determined:

$$\begin{cases} \overline{\varphi}_i(s) = \overline{\varphi}_{m,i} + \left[\dfrac{\overline{\varphi}_{n,i} - \overline{\varphi}_{m,i}}{\ell_i} + \rho\dfrac{\ell_i(\overline{\zeta}_{n,i} + 2\overline{\zeta}_{m,i})}{6}\right]s - \rho\left[\overline{\zeta}_{m,i} + \dfrac{\overline{\zeta}_{n,i} - \overline{\zeta}_{m,i}}{3\ell_i}s\right]\dfrac{s^2}{2} \\[3ex] \dfrac{d\overline{\varphi}_i}{ds} = \dfrac{\overline{\varphi}_{n,i} - \overline{\varphi}_{m,i}}{\ell_i} + \rho\dfrac{\ell_i}{6}(\overline{\zeta}_{n,i} + 2\overline{\zeta}_{m,i}) - \rho\left[\overline{\zeta}_{m,i} + \dfrac{\overline{\zeta}_{n,i} - \overline{\zeta}_{m,i}}{2\ell_i}s\right]s \end{cases} \tag{2.36}$$

As far as the $\overline{\varphi}$ nodal values are concerned, their numerical determination can be carried out by the resolution of a variational problem, whose Euler's equation is the first of (2.34). It's well known (e.g.: [18]) that solving the Poisson equation with some boundary conditions is equivalent to finding the function that satisfies the same boundary conditions and minimizes the corresponding Euler-Lagrange functional, that can be written, according to the introduced notation, as follows:

$$U = \int_A \left[\left(\frac{d\overline{\varphi}}{ds} \right)^2 - 2\rho\overline{\varphi}\overline{\zeta} \right] dA \qquad (2.37)$$

So, denoting by N the number of branches of the half-section, thanks to the ship symmetry respect to the xz plane, the functional can be so rewritten:

$$U = 2 \sum_{i=1}^{N} t_i \int_0^{\ell_i} \left[\left(\frac{d\overline{\varphi}_i}{ds} \right)^2 - 2\rho\overline{\varphi}_i\overline{\zeta}_i \right] ds \qquad (2.38)$$

To determine the warping function nodal values, it is necessary to search for the extremals of the functional U. The stationarity condition permits to write P linear equations, if P is the nodes number on the half-section:

$$\frac{\partial}{\partial\overline{\varphi}_k} \sum_{i=1}^{N} t_i \int_0^{\ell_i} \left[\left(\frac{d\overline{\varphi}_i}{ds} \right)^2 - 2\rho\overline{\varphi}_i\overline{\zeta}_i \right] ds = 0 \; for \, k = 1...P \qquad (2.39)$$

The uniform continuity of the under integral functions allows the derivation under the integral sign, so obtaining:

$$\sum_{i=1}^{n(k)} t_i \int_0^{\ell_i} \frac{\partial}{\partial\overline{\varphi}_k} \left[\left(\frac{d\overline{\varphi}_i}{ds} \right)^2 - 2\rho\overline{\varphi}_i\overline{\zeta}_i \right] ds = 0 \qquad (2.40)$$

having denoted by $n(k)$ the number of branches concurrent in the k-th-node. The eq. (2.40) can be rewritten as follows:

$$\sum_{i=1}^{n(k)} t_i \int_0^{\ell_i} \left[\frac{d\overline{\varphi}_i}{ds} \frac{\partial}{\partial\overline{\varphi}_k} \left(\frac{d\overline{\varphi}_i}{ds} \right) - \rho\overline{\zeta}_i \frac{\partial}{\partial\overline{\varphi}_k} \overline{\varphi}_i \right] ds = 0 \qquad (2.41)$$

finally becoming:

$$\sum_{i=1}^{n(k)} \frac{t_i}{\ell_i} \left(\overline{\varphi}_k - \overline{\varphi}_{r,i} \right) = \frac{1}{6}\rho \sum_{i=1}^{n(k)} t_i \ell_i \left(2\overline{\zeta}_k + \overline{\zeta}_{r,i} \right) \qquad (2.42)$$

having denoted, for each branch concurrent in the k-th-node, by r the node different from the k-th one. Obviously, as the solution of a Neumann boundary problem is always indetermined, to make the solution determined, it is necessary to impose the condition $\overline{\varphi}_i = const.$ in correspondence of whatever node. Also in this case it is immediately possible to verify that if $\rho \to 1$ the equation system coincides with the one obtained applying the Vlasov's theory.

2.5 Analysis of the stress field

Considering the restriction to the i-th branch of the stress field, the axial stress component reduces to the Navier one:

$$\overline{\sigma}_{x,i} = \frac{M(x)}{I}\overline{\zeta}_i(s) \tag{2.43}$$

while the tangential component can be expressed as the sum of two terms, the first one depending on the first derivative of the warping function, the second one instead depending on the branch position over the cross-section:

$$\overline{\tau}_{xs,i} = \overline{\tau}_{\varphi,i}(s) + \overline{\tau}_{g,i}(s) = \frac{Q}{I}\frac{d\overline{\varphi}_i}{ds} + \frac{Q}{I}\frac{\nu}{4(1+\nu)}\left[\left(\overline{\eta}_i^2 - \overline{\zeta}_i^2\right)\frac{d\overline{\zeta}_i}{ds} - 2\overline{\eta}_i\overline{\zeta}_i\frac{d\overline{\eta}_i}{ds}\right] \tag{2.44}$$

In order to determine the warping function nodal values it is preliminarily necessary to evaluate the corrective factor ρ that can be easily obtained as follows:

$$\rho = 1 - \frac{\nu}{6(1+\nu)I}\left(A_1 - A_2 - A_3\right) \tag{2.45}$$

with:

$$\begin{cases} A_1 = \sum_{i=1}^{N}\frac{t_i}{\ell_i}\left(\overline{\eta}_{n,i} - \overline{\eta}_{m,i}\right)\left(\overline{\zeta}_{n,i} - \overline{\zeta}_{m,i}\right)\left(2\overline{\eta}_{m,i}\overline{\zeta}_{m,i} + 2\overline{\eta}_{n,i}\overline{\zeta}_{n,i} + \overline{\eta}_{m,i}\overline{\zeta}_{n,i} + \overline{\eta}_{n,i}\overline{\zeta}_{m,i}\right) \\ \\ A_2 = \sum_{i=1}^{N}\frac{t_i}{\ell_i}\left(\overline{\zeta}_{m,i} - \overline{\zeta}_{n,i}\right)^2\left(\overline{\eta}_{m,i}^2 + \overline{\eta}_{n,i}^2 + \overline{\eta}_{m,i}\overline{\eta}_{n,i}\right) \\ \\ A_3 = \sum_{i=1}^{N}\frac{t_i}{\ell_i}\left(\overline{\zeta}_{m,i} - \overline{\zeta}_{n,i}\right)^2\left(\overline{\zeta}_{m,i}^2 + \overline{\zeta}_{n,i}^2 + \overline{\zeta}_{m,i}\overline{\zeta}_{n,i}\right) \end{cases} \tag{2.46}$$

Also in this case the Vlasov tangetial stress field can be obtained imposing the condition $\nu \to 0$.

2.6 The shear center vertical position

Similarly to Chapter 1, in order to determine the shear center vertical position (the only interesting coordinate for ship structures, symmetric respect to the xz plane), it is necessary to start from the Saint-Venant horizontal bending-shear stress field. According to the introduced symbols and notations the Saint-Venant displacement field can be so expressed:

$$
\begin{cases}
u = \vartheta_H(x)\zeta + \dfrac{Q_H}{GI}\chi(\eta,\zeta) \\[3mm]
v = v_0(x) + \dfrac{\nu}{2}\dfrac{d\vartheta_H}{dx}\left(\eta^2 - \zeta^2\right) \\[3mm]
w = \nu\dfrac{d\vartheta_H}{dx}\eta\zeta
\end{cases}
\tag{2.47}
$$

having defined by Q_H the horizontal shear, $\chi(\eta,\zeta)$ the horizontal warping function, v_0 the rigid body motion of the section along the η axis and $\vartheta_H(x)$ its rigid rotation around the ζ axis, connected to $v_0(x)$ by the geometrical condition of orthogonality between the section and the elastic surface:

$$
\vartheta_H(x) = \frac{dv_0}{dx}
\tag{2.48}
$$

Assuming all the hypotheses relative to the vertical bending-shear stress case, the restrictions to the i-th branch of the mean stress components can be easily obtained:

$$
\begin{cases}
\overline{\sigma}_{x,i} = -\dfrac{M_H}{I_\zeta}\overline{\eta}_i(s) \\[5mm]
\overline{\tau}_{xs,i} = \overline{\tau}_{\chi,i}(s) + \overline{\tau}_{g,i}(s) = \dfrac{Q_H}{I_\zeta}\dfrac{d\overline{\chi}_i}{ds} + \dfrac{\nu}{4(1+\nu)}\dfrac{Q_H}{I_\zeta}\left[\left(\overline{\zeta}_i^2 - \overline{\eta}_i^2\right)\dfrac{d\overline{\eta}_i}{ds} - 2\overline{\eta}_i\overline{\zeta}_i\dfrac{d\overline{\zeta}_i}{ds}\right]
\end{cases}
\tag{2.49}
$$

The mean value of the warping function can be obtained as solution of the following equation system, extended in this case to the nodes of the entire

cross-section:

$$\sum_{i=1}^{n(k)} \frac{t_i}{\ell_i} \left(\overline{\chi}_k - \overline{\chi}_{r,i} \right) = \frac{1}{6} \rho_H \sum_{i=1}^{n(k)} t_i \ell_i \left(2\overline{\eta}_k + \overline{\eta}_{r,i} \right) \tag{2.50}$$

The corrective constant ρ_H can be expressed similarly to the previously described case:

$$\rho_H = 1 - \frac{\nu}{12(1+\nu)I_\zeta} \left(H_1 - H_2 - H_3 \right) \tag{2.51}$$

with:

$$\begin{cases} H_1 = \sum_{i=1}^{M} \frac{t_i}{\ell_i} \left(\overline{\eta}_{m,i} - \overline{\eta}_{n,i} \right)^2 \left(\overline{\zeta}_{m,i}^2 + \overline{\zeta}_{n,i}^2 + \overline{\zeta}_{m,i} \overline{\zeta}_{n,i} \right) \\ H_2 = \sum_{i=1}^{M} \frac{t_i}{\ell_i} \left(\overline{\eta}_{n,i} - \overline{\eta}_{m,i} \right) \left(\overline{\zeta}_{n,i} - \overline{\zeta}_{m,i} \right) \left(2\overline{\eta}_{m,i} \overline{\zeta}_{m,i} + 2\overline{\eta}_{n,i} \overline{\zeta}_{n,i} + \overline{\eta}_{m,i} \overline{\zeta}_{n,i} + \overline{\eta}_{n,i} \overline{\zeta}_{m,i} \right) \\ H_3 = \sum_{i=1}^{M} \frac{t_i}{\ell_i} \left(\overline{\eta}_{m,i} - \overline{\eta}_{n,i} \right)^2 \left(\overline{\eta}_{m,i}^2 + \overline{\eta}_{n,i}^2 + \overline{\eta}_{m,i} \overline{\eta}_{n,i} \right) \end{cases} \tag{2.52}$$

having denoted by M the branches of the entire cross-section. Concerning the shear center vertical position, similarly to Chapter 1, it can be determined starting from (1.84) and (1.85), from which it follows:

$$\zeta_Q = - \frac{\sum_{i=1}^{M} t_i \overline{h}_i \int_0^{\ell_i} \frac{d\overline{\chi}_i}{ds} ds - \frac{\nu}{4(1+\nu)} \sum_{i=1}^{M} t_i \overline{h}_i \int_0^{\ell_i} \left[\left(\overline{\eta}_i^2 - \overline{\zeta}_i^2 \right) \frac{d\overline{\eta}_i}{ds} + 2\overline{\eta}_i \overline{\zeta}_i \frac{d\overline{\zeta}_i}{ds} \right] ds}{I_\zeta} \tag{2.53}$$

whence:

$$\zeta_Q = - \frac{\sum_{i=1}^{M} t_i \overline{h}_i \left(\overline{\chi}_{n,i} - \overline{\chi}_{m,i} \right) - \frac{\nu}{4(1+\nu)} \sum_{i=1}^{M} t_i \overline{h}_i \left(Z_i^I + Z_i^{II} \right)}{I_\zeta} \tag{2.54}$$

with:

$$\begin{cases} Z_i^I = \frac{\overline{\zeta}_{n,i} - \overline{\zeta}_{m,i}}{3} \left(2\overline{\eta}_{m,i} \overline{\zeta}_{m,i} + 2\overline{\eta}_{n,i} \overline{\zeta}_{n,i} + \overline{\eta}_{m,i} \overline{\zeta}_{n,i} + \overline{\eta}_{n,i} \overline{\zeta}_{m,i} \right) \\ \\ Z_i^{II} = \frac{\overline{\eta}_{n,i} - \overline{\eta}_{m,i}}{3} \left(\overline{\eta}_{m,i}^2 + \overline{\eta}_{n,i}^2 + \overline{\eta}_{m,i} \overline{\eta}_{n,i} - \overline{\zeta}_{m,i}^2 - \overline{\zeta}_{n,i}^2 - \overline{\zeta}_{m,i} \overline{\zeta}_{n,i} \right) \end{cases} \tag{2.55}$$

38

Comparing the expression (1.88) with this last one, a corrective term appears. Particularly, also in this case when $\nu \to 0$ the corrective term becomes null and the horizontal warping function coincides with the Vlasov's one. So it is possible to adfirm that, starting from the bending-shear Saint-Venant displacement field applied to thin-walled beams, the Vlasov's theory can be easily obtained as a particular case when the Poisson modulus is fixed equal to zero.

Chapter 3

The refined theory of non-uniform torsion

In this chapter the problem of the elastic equilibrium of a thin-walled beam subjected to a variable torque and restrained at both ends is discussed from the beginning, assuming the fundamental hypothesis of Kollbrunner and Hajdin, based on the assumption that the longitudinal distribution of the warping deformations is an arbitrary function independent of the unit twist angle. Despite the classical theories, the effective longitudinal distribution of the applied torque, given by RINA Rules 2009, is taken into due consideration to determine the longitudinal distribution of the warping function and the unit twist angle, imposing that the unit twist angle is null in correspondence of the extremities of a single hull module. Furthermore, as a still unsolved problem is the role of transverse bulkheads, generally assumed as perfectly rigid in the evaluation of the bimoment longitudinal distribution, a method, based on a global energy approach, is presented to take into account the deformability of transverse bulkheads, schematized as orthotropic plates.

3.1   The displacement field

The classical theory of non-uniform torsion in thin-walled beams, normally known as theory of sectorial areas, was initially developed by Vlasov,

1941 and Timoshenko, 1945, for beams with monoconnected cross-section, and generalized by Kármán and Christensen, 1944, for beams with a generic cross-section. The theory is based on the subdivision of the tangential stress flow, produced by the applied twist moment, into two parts: the primary and the secondary one. The primary flow, typical of the Saint-Venant's theory, is associated to the so-called pure torsion; the secondary one, instead, is associated to the tangential stress field connected, for the equilibrium, to the normal one caused by a non-uniform warping of the beam cross-section, due to the primary flow. This theory, however, neglects the warping produced by the secondary stress flow that, in some cases, can be as considerable as the primary one.

The fundamental hypothesis that, from now on, will be done, is the transverse indeformability of the beam cross-section. This hypothesis, typical of the theory of sectorial areas, can be considered sufficiently true, thanks to the presence of transverse frames that prevent shape variations of the beam cross-section. Furthermore, thanks to their neglegible bending stiffness around the in-plane axes, these frames gain no resistance to any longitudinal deformation of the cross-section. Let us regard the hull girder cylindrical body as a thin-walled beam, composed of homogeneous and isotropic material, and let us suppose that the external loads are negligible respect to the ones of the internal stress characteristics. Let us define the global Cartesian frame, sketched in Fig. 1.1, with origin G in correspondence of the amidships structural section centre, and y, z axes defined in the section plane and coinciding with the section principal axes of inertia. Let us also define the local Cartesian frame, with origin $G(x)$ in correspondence of the cross-structural section at the x-abscissa, x-axis coinciding with the global one and η, ζ axes defined in the section plane and coinciding with the principal axes of inertia of the section at x-abscissa.

In the hypothesis of pure torsion, assuming that the cross-sections rotation occurs around the shear centre, denoting by u, v, w the three displacement components in the x, η,ζ directions respectively, with a mixed $P(x, \eta, \zeta)$ representation, and applying to the first function a by parts decomposition,

the displacement field can be expressed as follows:

$$\begin{cases} u = -\theta(x)\omega(\eta,\zeta) \\ v = -\vartheta_t(x)\big(\zeta - \zeta_Q\big) \\ w = \vartheta_t(x)\eta \end{cases} \tag{3.1}$$

where $\theta(x)$ is the axial displacement function, $\omega(\eta,\zeta)$ is the warping function, $\vartheta_t(x)$ is the section's rotation about an axis parallel to the x-axis and passing through the shear center, positive counter-clockwise , ζ_Q is the vertical position of the shear center; the transverse component of the shear center η_Q was assumed directly null, because of the symmetry of ship structures as regards the xz plane. It is noticed that the displacement field (3.1) differs from the Vlasov's one for the axial component, which is assumed directly equal to $u = -\vartheta_1(x)\omega(\eta,\zeta)$ having defined the unit twist angle as the first derivative of the section's rotation:

$$\vartheta_1(x) = \frac{d\vartheta_t}{dx} \tag{3.2}$$

3.2 The strain and stress fields

With the previous assumptions and notations, the strain components (for small deformation) are then given by:

$$\begin{cases} \varepsilon_x = -\dfrac{d\theta}{dx}\omega(\eta,\zeta) \\[4mm] \gamma_{xy} = -\theta(x)\dfrac{\partial\omega}{\partial\eta} - \vartheta_1(\zeta - \zeta_Q) \\[4mm] \gamma_{xz} = -\theta(x)\dfrac{\partial\omega}{\partial\zeta} + \vartheta_1\eta \\[4mm] \varepsilon_y = \varepsilon_z = \gamma_{yz} = 0 \end{cases} \tag{3.3}$$

Introducing the orthogonal curvelinear coordinate system defined in Figure 1.2 with:

- s the curvilinear abscissa on the median line, with the O origin in one of the two extremities (nodes) of the line;

- n the linear abscissa on the thickness line through the considered point P, with origin on ℓ;

- $\xi = x - \overline{x}$ (with: $\overline{x}$ = global coordinate of the considered cross-section) the linear abscissa with origin in O, on the parallel through O, to the x-axis of the global frame.

and applying the relations $\gamma_{pq} = 2\left(\boldsymbol{E}\boldsymbol{e_p}\right) \cdot \boldsymbol{e_q}$ for $p \neq q$ and $\varepsilon_p = \left(\boldsymbol{E}\boldsymbol{e_p}\right) \cdot \boldsymbol{e_p}$ for $p = q$, it is possible to rewrite the strain components respect to the local curvlinear coordinate system, having denoted by $\boldsymbol{E}$ the strain tensor, written with regard to the orthonormal basis $\{\boldsymbol{i}, \boldsymbol{j}, \boldsymbol{k}\}$, and by $\boldsymbol{e_p}$ the unit vector of the local coordinate system relative to the orthonormal basis. Denoting by $\omega(s, n)$ the function composed of the three ones: $\omega(\eta, \zeta)$, $\eta(s, n)$ and $\zeta(s, n)$, by α_{ij} the director cosine of the unit vector $\boldsymbol{i}$ of the local coordinate system as regards the unit vector $\boldsymbol{j}$ of the orthonormal basis, the strain field written with regard to the local curvilinear coordinate system, becomes:

$$
\begin{cases}
\varepsilon_x = -\dfrac{d\theta}{dx}\omega(s, n) \\[2mm]
\gamma_{xs} = -\theta(x)\dfrac{\partial \omega}{\partial s} + \vartheta_1\left[\eta\alpha_{sz} - \left(\zeta - \zeta_Q\right)\alpha_{sy}\right] \\[2mm]
\gamma_{xn} = -\theta(x)\dfrac{\partial \omega}{\partial n} + \vartheta_1\left[\eta\alpha_{nz} - \left(\zeta - \zeta_Q\right)\alpha_{ny}\right] \\[2mm]
\varepsilon_s = \varepsilon_n = \gamma_{sn} = 0
\end{cases}
\tag{3.4}
$$

Denoting by E, G and ν the Young, Coulomb, and Poisson modulus respectively and taking into account that only σ_x, σ_s and τ_{xs} are elastic stresses, the Navier equations can be specialized as follows:

$$
\begin{cases}
\sigma_x = \dfrac{E}{1 - \nu^2}\varepsilon_x \\[3mm]
\sigma_s = \nu\sigma_x \\[3mm]
\tau_{xs} = G\gamma_{xs}
\end{cases}
\tag{3.5}
$$

Now, according to the Hencky-Von Mises criterion, the ideal stress reduces for steel ($\nu = 0.3$) to $\sigma_{id.} = \sqrt{0.954E^2\varepsilon_x^2 + 3\tau_{xs}^2}$ which is slightly lower than

the values obtained taking $\sigma_x = E\varepsilon_x$ and $\sigma_s = 0$, as it is currently made in favour of safety, so that the stress field can be so simplified:

$$\begin{cases} \sigma_x = E\varepsilon_x \\ \\ \tau_{xs} = G\gamma_{xs} \end{cases} \tag{3.6}$$

3.3 The warping function: local and global development

Concerning the indefinite and boundary equations, the only ones, relevant in the study of the hull girder strength, are the x-projections. In the further hypothesis of cylindrical body, assuming $\boldsymbol{n} \cdot \boldsymbol{i} = 0$, the equilibrium conditions inside the body and on the boundary become:

$$\begin{cases} \dfrac{\partial \tau_{xs}}{\partial s} + \dfrac{\partial \tau_{xn}}{\partial n} = -\dfrac{\partial \sigma_x}{\partial x} \, \forall P \in A \\ \\ \tau_{xn} = 0 \, \forall P \in \partial A \end{cases} \tag{3.7}$$

having denoted by A the cross-section domain and by ∂A its frontier. It is easy to verify that the full respect of (3.7) implies the warping function variability vs. x and, consequently, the rigorous unacceptability of the hypothesis about the u function. The normally applied method assumes for the ω differential condition the same solution of the uniform torsion problem:

$$\begin{cases} \nabla^2 \omega = 0 \, \forall P \in A \\ \\ \dfrac{\partial \omega}{\partial n} = \eta \alpha_{nz} - \left(\zeta - \zeta_Q\right) \alpha_{ny} \, \forall P \in \partial A \end{cases} \tag{3.8}$$

having denoted by α_{ny} and α_{nz} the director cosines of the unit normal vector, positive outwards. Concerning the necessary solvability condition of a Neumann boundary problem associated to the Laplace equation, it is well known that this problem admits a solution if the following global condition is verified:

$$\int_{\partial A} \frac{\partial \omega}{\partial n} ds = 0 \tag{3.9}$$

Substituting the second of (3.8) in the (3.9) and applying the Gauss theoreme, it is possible to verify that the previously defined condition is always verified:

$$\int_A \left[\frac{\partial}{\partial \zeta} \eta \right] dA - \int_A \left[\frac{\partial}{\partial \eta} \left(\zeta - \zeta_Q \right) \right] dA = 0 \tag{3.10}$$

The negligibility of the thickness branch allows to assume all the geometrical and mechanical quantities uniformly distributed along the thickness with their mean values, what implies for straight branches that:

$$\overline{\eta}_i(s) = \eta_i(s) = \overline{\eta}_{m,i} + \frac{\overline{\eta}_{n,i} - \overline{\eta}_{m,i}}{\ell_i} s \; ; \; \overline{\zeta}_i(s) = \zeta_i(s) = \overline{\zeta}_{m,i} + \frac{\overline{\zeta}_{n,i} - \overline{\zeta}_{m,i}}{\ell_i} s \tag{3.11}$$

having denoted, for the i-th branch, by $\overline{\eta}_i(s)$ and $\overline{\zeta}_i(s)$ the mean values, $\eta_i(s)$ and $\zeta_i(s)$ the values on the mean line, by ℓ_i and t_i the lenght and the thickness of the branch and by the suffixes m and n the initial and final nodes. Consequently it is also possible to assume the restriction to the $i-th$ branch $\frac{\partial \omega_i}{\partial n}$ uniformly distributed on the thickness with its mean value $\frac{\partial \omega_i}{\partial n} = \eta_i \alpha_{nz,i} - \left(\zeta_i - \zeta_Q \right) \alpha_{ny,i}$ where the following equalities hold:

$$\alpha_{sy,i} = -\alpha_{nz,i} = \frac{d\eta_i}{ds} = \frac{\overline{\eta}_{n,i} - \overline{\eta}_{m,i}}{\ell_i} \tag{3.12}$$

$$\alpha_{sz,i} = \alpha_{ny,i} = \frac{d\zeta_i}{ds} = \frac{\overline{\zeta}_{n,i} - \overline{\zeta}_{m,i}}{\ell_i} \tag{3.13}$$

The restriction of the warping function to the $i - th$ branch can be seen as the sum of terms: the first one $\overline{\omega}_i(s)$ variable with the curvilinear abscissa s, the second one $\chi_i(s,n)$ variable along the thickness and the branch and null in correspondence of the median line:

$$\omega_i(s,n) = \overline{\omega}_i(s) + \chi_i(s,n) \; with \; \chi_i(s,0) = 0 \tag{3.14}$$

and $\chi_i(s,n) = \left[\eta_i \alpha_{nz,i} - \left(\zeta_i - \zeta_Q \right) \alpha_{ny,i} \right] n$. It is noticed that the expression (3.14) implicitly satisfies the Laplace equation $\nabla^2 \chi_i = 0$ with the relevant Neumann boundary condition. On the other hand, the mean values of the warping function may be obtained as solution of the following differential problem:

$$\begin{cases} \dfrac{d^2 \overline{\omega}_i}{ds^2} = 0 \; \forall s \in \left[0, \ell_i \right] \\ \\ \overline{\omega}_i(0) = \overline{\omega}_{m,i} \; ; \; \overline{\omega}_i(\ell_i) = \overline{\omega}_{n,i} \end{cases} \tag{3.15}$$

having denoted by $\overline{\omega}_{m,i}$ and $\overline{\omega}_{n,i}$ the unknown values of the warping function in correspondence of the initial and final nodes. Obviously, to make the solution determined, it is sufficient to impose the condition $\overline{\omega}_i = 0$ in correspondence of wathever node. From the problem (3.15) it also follows that the mean value of the warping function varies linearly along each branch according to the following law:

$$\overline{\omega}_i(s) = \overline{\omega}_{m,i} + \frac{\overline{\omega}_{n,i} - \overline{\omega}_{m,i}}{\ell_i} s \qquad (3.16)$$

Similarly, it is possible to introduce the mean value of the tangential stress component:

$$\overline{\tau}_{xs,i} = \frac{1}{t_i} \int_{-\frac{t_i}{2}}^{\frac{t_i}{2}} \tau_{xs,i} dn = G\Big[\vartheta_1(x) h_i(s) - \theta(x) \frac{d\overline{\omega}_i}{ds}\Big] \boldsymbol{s} \qquad (3.17)$$

with $h_i(s) = h_i = \eta_i(s)\alpha_{sz,i} - \big(\zeta_i(s) - \zeta_Q\big)\alpha_{sy,i} = \overline{\eta}_{m,i}\alpha_{sz,i} - \big(\overline{\zeta}_{m,i} - \zeta_Q\big)\alpha_{sy,i}$. Thanks to these assumptions for multiconnected cross-sections, denoting by M the number of branches of the entire cross-section, the tangetial stress field must also verify the following global condition in which the applied external torque appears:

$$M_t(x) = \sum_{i=1}^{M} t_i \int_o^{\ell_i} \overline{\tau}_{xs,i} h_i ds = G\Big[\vartheta_1(x) I_{hh} - \theta(x) I_{h\partial\omega}\Big] \qquad (3.18)$$

having done the following positions:

$$I_{hh} = \sum_{i=1}^{M} t_i \int_0^{\ell_i} h_i^2 ds \ , \ I_{h\partial\omega} = \sum_{i=1}^{M} t_i \int_0^{\ell_i} h_i \frac{\partial\omega_i}{\partial s} ds \qquad (3.19)$$

The compatibility condition between the functions $\vartheta_1(x)$ and $\theta(x)$ can be established by the principle of virtual works. The external work is the sum of the one done by the applied torque and the one done by the increment of the normal stresses σ_x over dx. This external work must be equal to the internal work absorbed by the shear stresses, so obtaining:

$$M_t(x)\vartheta_1(x) + \int_A \frac{\partial\sigma_x}{\partial x} u dA = G \int_A \gamma_{xs}^2 dA \qquad (3.20)$$

The second member of (3.20) can be rewritten as follows:

$$\vartheta_1 \int_A \tau_{xs} h(s) dA - \theta(x) \int_A \tau_{xs} \frac{\partial\omega}{\partial s} dA \qquad (3.21)$$

so that, by (3.18), and taking into account that $\dfrac{\partial u}{\partial s} = -\theta(x)\dfrac{\partial \omega}{\partial s}$ the compatibility condition (3.19) becomes:

$$\int_A \frac{\partial \sigma_x}{\partial x} u \, dA = \int_A \tau_{xs} \frac{\partial u}{\partial s} \, dA \tag{3.22}$$

whence:

$$2\left(1 + \nu\right)\frac{d^2\theta}{dx^2} I_{\omega\omega} = \theta(x) I_{\partial\omega\partial\omega} - \vartheta_1 I_{h\partial\omega} \tag{3.23}$$

having done the following positions:

$$I_{\omega\omega} = \sum_{i=1}^{M} t_i \int_0^{\ell_i} \overline{\omega}_i^2 \, ds \; ; \; I_{\partial\omega\partial\omega} = \sum_{i=1}^{M} t_i \int_0^{\ell_i} \left(\frac{d\overline{\omega}_i}{ds}\right)^2 ds \tag{3.24}$$

The term $\dfrac{d^2\theta}{dx^2}$ can be easily obtained considering the second order derivative of (3.20), whence:

$$\frac{d^2\theta}{dx^2} = \rho\frac{d^2\vartheta_1}{dx^2} - \frac{1}{GI_{h\partial\omega}}\frac{dm_t}{dx} \tag{3.25}$$

having done the positions $m_t(x) = \dfrac{dM_t}{dx}$ and $\rho = \dfrac{I_{hh}}{I_{h\partial\omega}}$. By (3.23) and (3.25) the function $\theta(x)$ can be expressed as follows:

$$\theta(x) = \vartheta_1 + 2\left(1 + \nu\right)\frac{I_{\omega\omega}}{I_{h\partial\omega}}\left[\rho\frac{d^2\vartheta_1}{dx^2} - \frac{1}{GI_{h\partial\omega}}\frac{dm_t}{dx}\right] \tag{3.26}$$

Finally, substituting the eq. (3.26) into the (3.20), it is possible to obtain the warping equation:

$$G\vartheta_1\left(I_{hh} - I_{h\partial\omega}\right) - \rho EI_{\omega\omega}\frac{d^2\vartheta_1}{dx^2} = M_t(x) - k_t\frac{dm_t}{dx} \tag{3.27}$$

having done the position:

$$k_t = 2\left(1 + \nu\right)\frac{I_{\omega\omega}}{I_{h\partial\omega}} \tag{3.28}$$

According to the classical theory of warping restrained torsion, it is possible to introduce the beam torsional modulus $I_t = I_{hh} - I_{h\partial\omega}$ and the beam warping modulus $I_w = \rho I_{\omega\omega}$, so that the left hand side of the warping equation can be considered as the sum of two terms: the first one $T_t = GI_t\vartheta_1$ relative to the pure torsional part, the second one $T_w = -EI_w\frac{d^2\vartheta_1}{dx^2}$ relative to the warping contribution:

$$GI_t\vartheta_1 - EI_w\frac{d^2\vartheta_1}{dx^2} = M_t(x) - k_t\frac{dm_t}{dx} \tag{3.29}$$

3.4 The classical solution of the warping equation

In the classical warping restrained theory, it is assumed that the beam, of length $2L$, is warping restrained at both ends and is loaded at the two extremities by a torque M_t. Considering the first order derivative of (3.29) the warping equation can be rewritten as follows:

$$GI_t \frac{d^2\vartheta_t}{dx^2} - EI_w \frac{d^4\vartheta_t}{dx^4} = 0 \qquad (3.30)$$

Its general solution reads: $\vartheta_t(x) = A_0 + A_1 x + A_2 cosh\left(\sqrt{\beta}x\right) + A_3 sinh\left(\sqrt{\beta}x\right)$, having done the position $\beta = \dfrac{GI_t}{EI_w}$. First of all, thanks to the symmetry of the beam and the antysymmetry of the loading, the following two boundary conditions can be written:

$$\begin{cases} \vartheta_t(x = 0) = 0 \\[2ex] \vartheta_t(x = x^+) = -\vartheta_t(x = x^-) = -\vartheta_t(x = -x^+) \end{cases} \qquad (3.31)$$

from which it follows that $A_0 = A_2 = 0$. The other two coefficients can be determined by the following two other boundary conditions:

$$\begin{cases} \dfrac{d\vartheta_t}{dx}\left(x = L\right) = 0 \\[3ex] \dfrac{d^3\vartheta_t}{dx^3}\left(x = L\right) = 0 \end{cases} \qquad (3.32)$$

from which it follows that $\vartheta_t(x) = \dfrac{M_t L}{GI_t}\left[\dfrac{x}{L} - \dfrac{sinh\left(\sqrt{\beta}L\right)}{\sqrt{\beta}L cosh\left(\sqrt{\beta}L\right)}\right]$. The two parts of the section forces, i.e. the pure twisting and the warping ones can be expressed as follows:

$$T_t = M_t\left[1 - \dfrac{cosh\left(\sqrt{\beta}x\right)}{cosh\left(\sqrt{\beta}L\right)}\right] ; \; T_w = \dfrac{cosh\left(\sqrt{\beta}x\right)}{cosh\left(\sqrt{\beta}L\right)} \qquad (3.33)$$

In the following figure the $\dfrac{T_w}{M_t}$ distribution is shown for different values of $\sqrt{\beta}L$: it is possible to verify that close to the support the warping torque alone counteracts the external torque M_t, while close to the mid span this term may be of little significance. Furthermore, larger is the value $\sqrt{\beta}L$, smaller is the region where the warping torque is dominant. According to
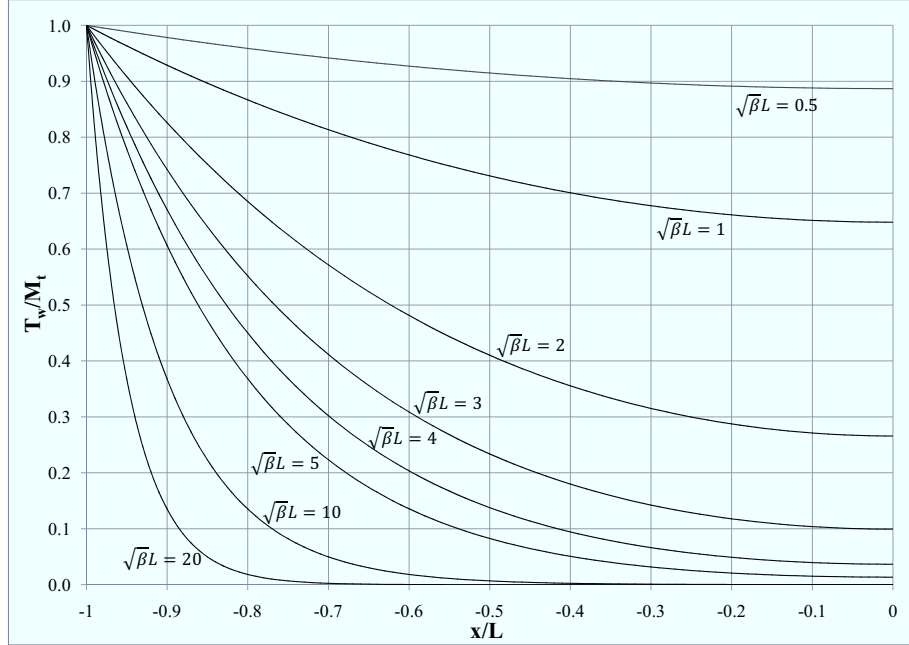
Figure 3.1: Warping torque distribution

the classical theories of warping restrained torsion, it is possible to introduce the bimoment sectional force, defined as follows:

$$B = -EI_w \frac{d^2\vartheta_t}{dx^2} = M_t \frac{sinh\left(\sqrt{\beta}x\right)}{\sqrt{\beta}cosh\left(\sqrt{\beta}L\right)} \qquad (3.34)$$

From (3.34), it is possible to verify that the largest value of the bimoment occurs near the supports. It is of interest to know how far from the support this generalized sectional force has any significant influence. Particularly, when $\sqrt{\beta}L = 0$ the bimoment decays at least at a linear rate between the support and the middle span.

3.5 The still water and wave torque

For ship structures the total torque is, as usual, the sum of a a still water term and a wave one. According to RINA Rules 2009, the still water torque must be considered only for containerships: in this case (see Part E Ch2,Sec2) the still water torque $M_{t,SW}$ induced by the non-uniform distribution of cargo, consumable liquids and ballast, may be obtained in kNm
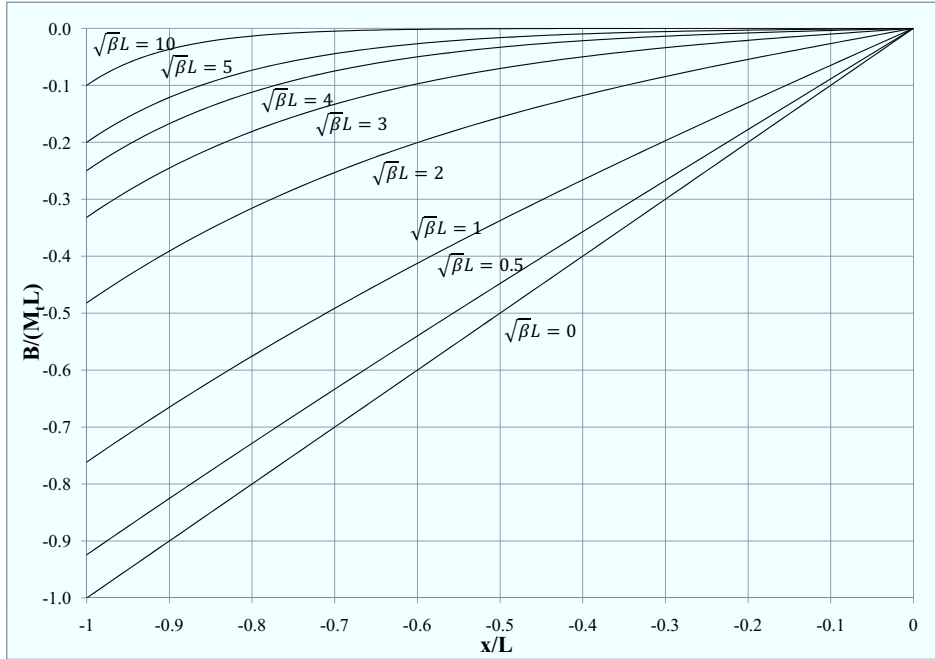
Figure 3.2: Bimoment distribution

at any hull transverse section, by the following formula:

$$M_{t,SW} = 31.4 S T_c B F_T(x) \tag{3.35}$$

where:

- B is the ship breadth in m;

- S is the number of container stacks over the breadth B;

- T_c is the number of container tiers in cargo hold amidships (excluding containers on deck or on hatch covers);

- $F_T(x)$ is the longitudinal distribution factor as function of the x-coordinate of the hull transverse section (it is noticed that the expression suggested by RINA Rules doesn't coincide with the one adopted from now on, as the RINA reference co-ordinate system has the origin in correspondence of the ship aft extremity).

The distribution factor $F_T(x)$ is linear with a maximum in correspondence of the amidships (see figure 3.3) ; denoting by L the ship scantling length it
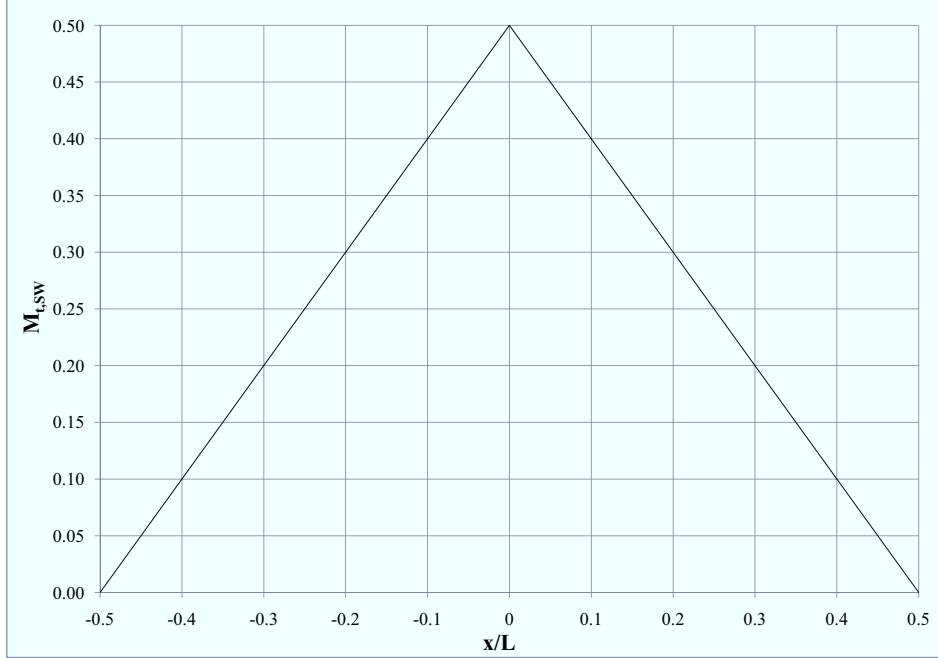
Figure 3.3: Static torque distribution

can be expressed as follows:

$$
\begin{cases}
F_T(x) = 0.5 - \dfrac{x}{L} \quad \forall x \in \left[0, \dfrac{L}{2}\right] \\[4mm]
F_T(x) = 0.5 + \dfrac{x}{L} \quad \forall x \in \left[-\dfrac{L}{2}, 0\right[
\end{cases}
\tag{3.36}
$$

The wave torque, instead, can be expressed according to PartB, Ch5, Sec2, considering the ship in two different conditions:

- *condition 1*: ship direction forming an angle of 60 deg with the prevailing sea direction;

- *condition 2*: ship direction forming an angle of 120 deg with the prevailing sea direction.

The wave torque, calculated as regards the section center of torsion, can be expressed for the first and second condition respectively, as follows:

$$
M_{t,WT-1} = a_1\left\{1 - cos\left[\pi\left(\frac{2x}{L} + 1\right)\right]\right\} + a_2 sin\left[\pi\left(\frac{2x}{L} + 1\right)\right]
\tag{3.37}
$$
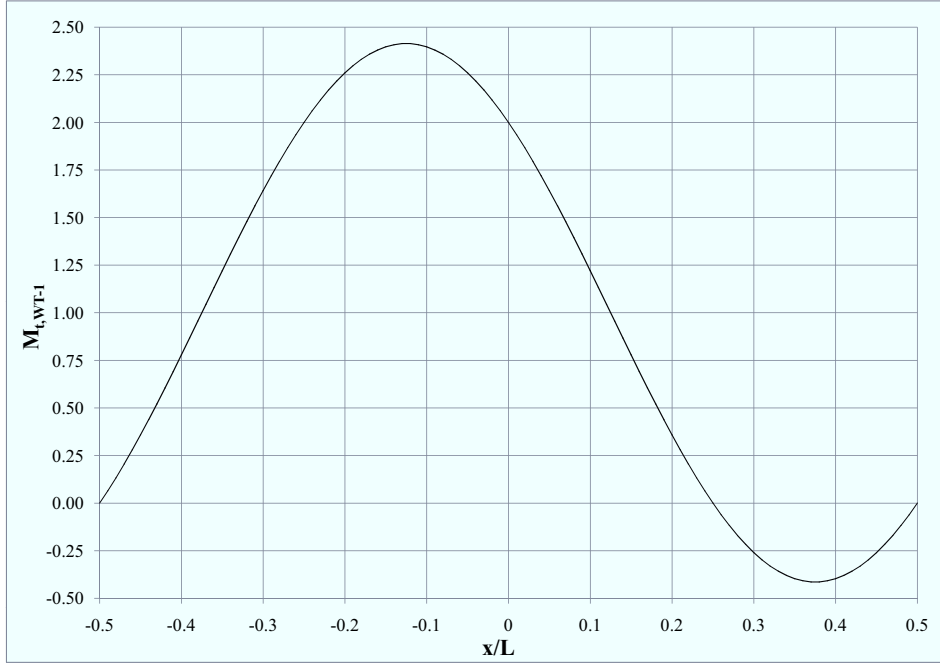
Figure 3.4: Wave torque distribution - condition 1

and:

$$M_{t,WT-2} = a_1\Big\{1 - cos\Big[\pi\Big(1 - \frac{2x}{L}\Big)\Big]\Big\} + a_2 sin\Big[\pi\Big(1 - \frac{2x}{L}\Big)\Big] \qquad (3.38)$$

with:

$$\begin{cases} a_1 = \dfrac{HL}{4}nC_M \\[3mm] a_2 = \dfrac{HL}{4}nC_Qd \end{cases} \qquad (3.39)$$

having done the following positions:

- H is the wave parameter so defined: $H = 8.13 - \Big(\dfrac{250 - 0.7L}{125}\Big)^2$;

- n is the navigation coefficient, equal to one for unrestricted navigation;

- C_M is the wave torque coefficient so defined: $C_M = 0.38B^2C_W^2$;

- C_W is the waterplane coefficient, to be taken not greater than the value obtained from the following formula: $C_W = 0.165 + 0.95C_B$ with C_B block coefficient, to be taken not less than 0.6;

52
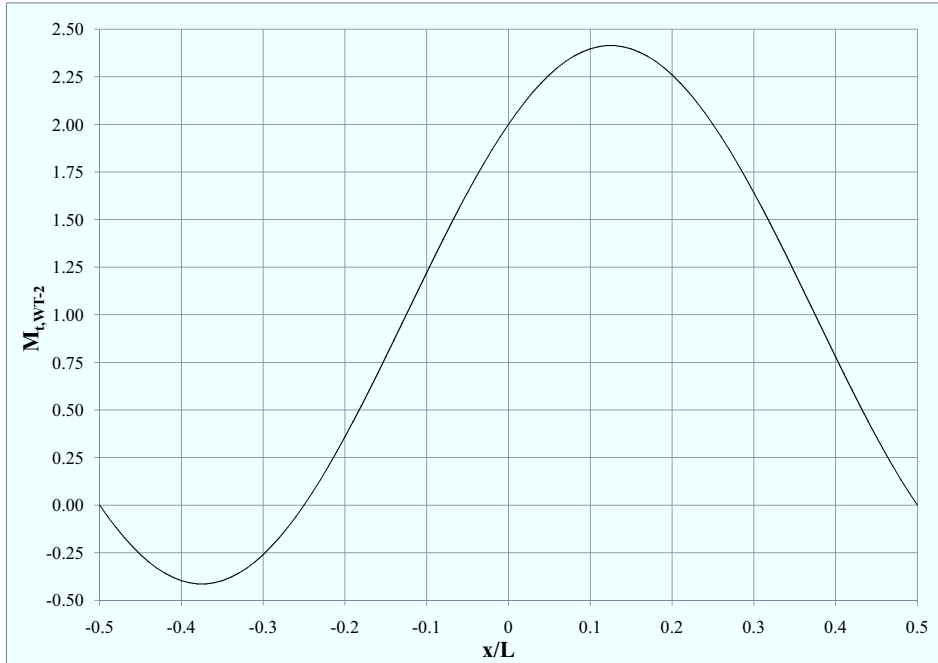
Figure 3.5: Wave torque distribution - condition 2

- C_Q is the horizontal wave shear coefficient so defined: $C_Q = 2.8 T C_B$ with T scantling draught in m;

- d is the vertical distance, in m, from the center of torsion to a point located at $0.6T$ above the baseline.

In the following figures the wave torque distribution for the loading conditions 1 and 2 respectively is shown.

3.6 Solution of the warping equation for ship structures

In this section the solution of the warping equation (3.29) is obtained, assuming as external torque the static and wave components obtained by (3.35), (3.37) and (3.38). The solution may be obtained in the following form:

$$\vartheta_1(x) = A_1 sinh\left(\sqrt{\beta}x\right) + A_2 cosh\left(\sqrt{\beta}x\right) + \vartheta_P(x) \qquad (3.40)$$

53

where $\vartheta_P(x)$ represents its particular solution. Considering the sum of the static term and the wave component of the applied torque, for the loading conditions 1 and 2 respectively, it can be expressed as follows:

$$\vartheta_{P-I} = \frac{M_{t,SW} + a_1}{\beta_1} - \left(1 + \frac{4\pi^2}{L^2}k_t\right)\frac{a_1 cos\left[\pi\left(\frac{2x}{L} + 1\right)\right] - a_2 sin\left[\pi\left(\frac{2x}{L} + 1\right)\right]}{\beta_1 + \frac{4\pi^2}{L^2}\beta_2}$$

(3.41)

and:

$$\vartheta_{P-II} = \frac{M_{t,SW} + a_1}{\beta_1} - \left(1 + \frac{4\pi^2}{L^2}k_t\right)\frac{a_1 cos\left[\pi\left(1 - \frac{2x}{L}\right)\right] - a_2 sin\left[\pi\left(1 - \frac{2x}{L}\right)\right]}{\beta_1 + \frac{4\pi^2}{L^2}\beta_2}$$

(3.42)

having done the positions: $\beta_1 = GI_t$ and $\beta_2 = EI_w$. Concerning the two boundary conditions, as the warping of a ship hull subjected to torsion is restrained in correspondence of two adjacent bulkheads, considering a single hold between the abscissa x_1 and x_2, it is possible to assume:

$$\vartheta_1(x_1) = \vartheta_1(x_2) = 0$$

(3.43)

So, denoting by $\beta = \dfrac{\beta_1}{\beta_2}$, the two constants A_1 and A_2 are solution of the following equation system:

$$\begin{cases} cosh\left(\sqrt{\beta}x_1\right)A_1 + sinh\left(\sqrt{\beta}x_1\right)A_2 = -\vartheta_P(x_1) \\ \\ cosh\left(\sqrt{\beta}x_2\right)A_2 + sinh\left(\sqrt{\beta}x_2\right)A_2 = -\vartheta_P(x_2) \end{cases}$$

(3.44)

3.7 Minimum of the Euler-Lagrange functional

It is well known that solving the Laplace equation with some boundary conditions is equivalent to find the function satisfying the same boundary conditions that minimizes the functional:

$$U = \int_A |\nabla\omega|^2 dA$$

(3.45)

which is equal to the Euler-Lagrange functional of the equation $\nabla^2\omega = 0$. Thanks to the eq. (3.14) the eq. (3.45) can be rewritten as follows:

$$U = \sum_{i=1}^N t_i \int_0^{\ell_i} \left(\frac{d\overline{\omega}_i}{ds}\right)^2 ds$$

(3.46)

The stationarity condition permits to write P linear equation, if P is the node's number of the entire cross-section:

$$\frac{\partial}{\partial \overline{\omega}_k} \sum_{i=1}^{N} t_i \int_0^{\ell_i} \left(\frac{d\overline{\omega}_i}{ds}\right)^2 ds = 0 \ \ for \ k = 1...P \tag{3.47}$$

so that, denoting on each branch concurrent in the $k-th$ node by r,i the node different from the $k-th$ one, the following system is obtained:

$$\sum_{i=1}^{n(k)} \frac{t_i}{\ell_i} \left(\overline{\omega}_k - \overline{\omega}_{r,i}\right) = \sum_{i=1}^{n(k)} \pm h_i \tag{3.48}$$

where, with reference to the second member, it is necessary to introduce the plus sign when the index $k > r,i$ and the minus sign when $k < r,i$. As the equation system is obviously indetermined, to make it determined it is sufficient to impose the condition $\overline{\omega}_i = 0$ in whatever node of the section. Furthermore, as the axial stress field must be equivalent to zero, the following sectional conditions must be always satisfied:

$$\int_A \omega dA = \int_A \omega \eta dA = \int_A \omega \zeta dA = 0 \tag{3.49}$$

For ships structures, whose transverse section is symmetric as regards the ζ axis, the first and the third conditions are implicitly satisfied, if the equation system is solved imposing the condition $\overline{\omega}_i = 0$ in correspondence of a node belonging to the ζ axis. The second condition, instead, is verified only if the rotation occurs around the shear center: so if the vertical position of the shear center is preliminary known, the second integral is null; otherwise assuming preliminarily $\zeta_Q = 0$, it is possible to obtain another distribution of the warping function $\widetilde{\omega}$, solution of the equation system (3.48) and connected to $\overline{\omega}$ by the following relation, according to Vlasov's theory:

$$\overline{\omega} = \widetilde{\omega} + \eta \zeta_Q \tag{3.50}$$

Finally, by the second of (3.49) it is possible to determine the vertical position of the shear center:

$$\zeta_Q = -\frac{\int_A \widetilde{\omega} \eta dA}{I_\zeta} \tag{3.51}$$

3.8 The stress field

As it is well known the warping stresses define a new balanced generalized force system, namely the bimoment, so defined:

$$B = \int_A \sigma_x \omega dA = -EI_{\omega\omega}\frac{d\theta}{dx} \tag{3.52}$$

from which it is possible to express the mean values of the stress field for the $i - th$ as follows:

$$\begin{cases} \overline{\sigma}_{x,i} = \dfrac{B}{I_{\omega\omega}}\left(\overline{\omega}_{m,i} + \dfrac{\overline{\omega}_{n,i} - \overline{\omega}_{m,i}}{\ell_i}s\right) \\[3mm] \overline{\tau}_{xs,i} = G\left(\vartheta_1(x)h_i - \theta(x)\dfrac{\overline{\omega}_{n,i} - \overline{\omega}_{m,i}}{\ell_i}\right) \end{cases} \tag{3.53}$$

3.9 Effect of transverse bulkheads

As a dry cargo hull consists of both open and closed cross-sections, according to Senjanović t al., it is possible to take into account the effect of transverse bulkheads substituting the section torsional modulus I_t by an equivalent torsional modulus I_t^* defined as follows:

$$I_t^* = I_t + I_b \tag{3.54}$$

where I_b is the bulkhead contribution, sum of two terms: one due to the high torsional rigidity of the closed cross-section at the extremities of the hull module, the second due to the bulkhead deformation as an orthotropic plate. These two terms can be obtained by a global energetic approach. Let us denote by l_0 the bulkhead spacing, by a the longitudinal extension of the closed cell at the two extremities of the hull module, by $l_1 = l_0 - a$ the net hatch length and by I_t^0 the torsional modulus of the closed section. Starting from the position: $\vartheta_1 = \dfrac{M_t}{GI_t}$ and assuming M_t constant vs. x, the torsional strain energy of a hull module can be so expressed:

$$U_m = \frac{1}{2}\int_0^l M_t\vartheta_1 dx = \frac{M_t^2 l}{2GI_t} = \frac{1}{2}GI_t l\vartheta_1^2 \tag{3.55}$$

The contribution due to the high torsional rigidity of the closed cross-section can be obtained from the following energy equivalence:

$$\frac{M_t^2 l_0}{2GI_{t1}^*} = \frac{M_t^2 l_1}{GI_t} + \frac{M_t^2 a}{2GI_t^0} \tag{3.56}$$
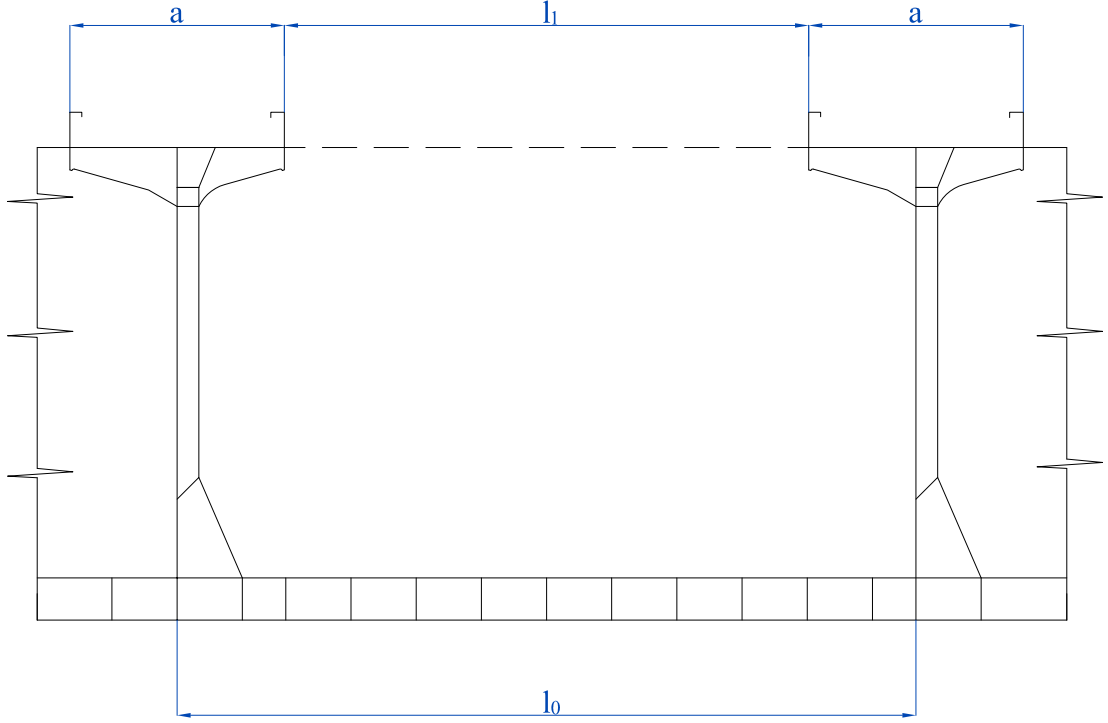
Figure 3.6: Hull module scheme

from which, taking into account that $a << l_0$ and $I_t << I_t^0$, it follows that:

$$I_{t1}^* = \left(1 + \frac{a}{l_1}\right)I_t \tag{3.57}$$

The energy absorbed by the bulkhead as an orthotropic plate can be expressed as follows:

$$U_b = 2(1 + \nu)GC\vartheta_1^2 \tag{3.58}$$

with:

$$C = \frac{U_b}{E\vartheta_1^2} \tag{3.59}$$

The energy balance in this case becomes:

$$\frac{1}{2}I_{t2}^* l_0 \vartheta_1^2 = \frac{1}{2}I_t^* l_0 \vartheta_1^2 + 2(1 + \nu)GC\vartheta_1^2 \tag{3.60}$$

from which it follows:

$$I_{t2}^* = \left[1 + \frac{4(1 + \nu)C}{I_t l_0}\right]I_t \tag{3.61}$$

57

So the final expression of the hull torsional modulus will be:

$$I_t^* = \left[1 + \frac{a}{l_1} + \frac{4(1 + \nu)C}{I_t l_0}\right] I_t \qquad (3.62)$$

Obviously, to obtain the equivalent torsional modulus it is necessary to evaluate the bulkhead energy coefficient C, preliminarily determining its deformed shape. First of all, it is possible to assume that the bulkhead reduces only the intensity of the axial displacements, while the warping function $\omega(\eta, \zeta)$ remains the same one of the open section. This hypothesis implies that the bulkhead will be subjected to the following three types of deformation:

1. screwing;

2. horizontal bending;

3. vertical bending.

so that, to determine C it is sufficient to express three displacement functions, each one relative to one of the previously defined deformation fields. The bulkhead screwing substantially coincides with the axial displacement of the open hull section; it can be approximated by the following deflection distribution, linear vs. η and ζ, having denoted by ζ_B and ζ_D the vertical coordinates of bottom and deck, the first one negative the second one positive, as regards the assumed reference system:

$$u^{(s)}(\eta, \zeta) = -\eta\Big(\zeta - \zeta_B - \zeta_D\Big)\vartheta_1 \qquad (3.63)$$

As the side boundaries of the bulkhead have to be orthogonal to the deformed hull double shell, the bulkhead is also exposed to bending in horizontal plane with respect to screwing. The rotation of the hull side shells can be expressed by the following relation:

$$\vartheta_z = -\frac{\partial v}{\partial x} = \vartheta_1\Big(\zeta - \zeta_Q\Big) \qquad (3.64)$$

The total bulkhead rotation β_z, instead, is the sum of two terms: the first one $\chi_z = \dfrac{\partial u^{(s)}}{\partial \eta}$ is the screwing rotation at the shell boundary, the second one φ_z is the rotation due to the horizontal bending:

$$\beta_z = \chi_z + \varphi_z \qquad (3.65)$$

Imposing the orthogonality condition $\vartheta_z = \beta_z$, the rotation due to the horizontal bending can be expressed as follows:

$$\varphi_z = 2\Big[\zeta - \frac{\zeta_Q + \zeta_B + \zeta_D}{2}\Big]\vartheta_1 \qquad (3.66)$$

The bulkhead horizontal bending deformation field will be an antisymmetric function represented by the odd terms of a third order polinomial with zero boundary displacement and rotation:

$$u^{(h)}(\eta, \zeta) = -\eta\Big[1 - \Big(\frac{\eta}{b}\Big)^2\Big]\Big[\zeta - \frac{\zeta_Q + \zeta_B + \zeta_D}{2}\Big]\vartheta_1 \qquad (3.67)$$

Similarly, the lower boundary of the transverse bulkhead has to be orthogonal to the deformed hull double bottom. The longitudinal variation of the vertical displacement w will generate a rotation of the hull bottom, so expressed:

$$\vartheta_y = -\frac{\partial w}{\partial x} = -\eta\vartheta_1 \qquad (3.68)$$

The bulkhead rotation β_y will be the sum of three terms: the first one $\chi_y = \dfrac{\partial u^{(s)}}{\partial \zeta}$ is the bulkhead screwing rotation at the bottom, the second one $\varphi_y = \dfrac{\partial u^{(h)}}{\partial \zeta}$ is the rotation due to the horizontal bending, the third one δ_y is the rotation due to the vertical bending. The total bulkhead rotation will be:

$$\beta_y = \chi_y + \varphi_y + \delta_y \qquad (3.69)$$

Imposing the orthogonality condition $\beta_y = \vartheta_y$, the rotation due to the vertical bending becomes:

$$\delta_y = \eta\Big[1 - \Big(\frac{\eta}{b}\Big)^2\Big]\vartheta_1 \qquad (3.70)$$

This rotation can be obtained by a displacement field with null bottom and deck deflections and zero deck rotation; such function, recognized in the second type of Hermitian polinomials can be so expressed:

$$u^{(v)}(\eta, \zeta) = \eta\Big[1 - \Big(\frac{\eta}{b}\Big)^2\Big]\Big[1 - \frac{\zeta - \zeta_B}{\zeta_D - \zeta_B}\Big]^2\Big(\zeta - \zeta_B\Big)\vartheta_1 \qquad (3.71)$$

The total bulkhead deformed shape will be a screwed antisymmetric function with a more pronounced horizontal deflection than the vertical one:

$$u^{(b)}(\eta, \zeta) = u^{(s)}(\eta, \zeta) + u^{(h)}(\eta, \zeta) + u^{(v)}(\eta, \zeta) \qquad (3.72)$$

To evaluate the bulkhead energy coefficient C, it is preliminary necessary to evaluate the total absorbed strain energy. Regarding the bulkhead as an orthotropic plate and denoting by D_Y, D_Z and H its two flexural and torsional rigidities, the strain energy can be so expressed:

$$U_b = \frac{1}{2} \int_{\zeta_B}^{\zeta_D} \int_{-b}^{b} \left[D_Y \left(\frac{\partial^2 u^{(b)}}{\partial \eta^2} \right)^2 + D_Z \left(\frac{\partial^2 u^{(b)}}{\partial \zeta^2} \right)^2 + H \frac{\partial u^{(b)}}{\partial \eta} \frac{\partial u^{(b)}}{\partial \zeta} \right] d\eta d\zeta \quad (3.73)$$

So, denoting by $h_B = \zeta_D - \zeta_B$ the bulkhead height, the total strain energy becomes:

$$U_b = \left[\frac{116 h_B^3}{35b} D_Y \alpha_Y + \frac{32 b^3}{105 h_B} D_Z \frac{16 b h_B}{75} H \alpha_T \right] \vartheta_1^2 \quad (3.74)$$

with:

$$\begin{cases} \alpha_Y = 1 - \frac{175}{116} \left(1 + \frac{\zeta_Q}{h_B} \right) + \frac{105}{116} \left(1 + \frac{\zeta_Q}{h_B} \right)^2 \\ \\ \alpha_T = 1 + \frac{195}{4} \left(1 + \frac{\zeta_Q}{h_B} \right) \end{cases} \quad (3.75)$$

According to Shade's work, the flexural and torsional rigidities can be so expressed:

$$\begin{cases} D_Y = E \dfrac{I_{eY}}{s_Y} \\ \\ D_Z = E \dfrac{I_{eZ}}{s_Z} \\ \\ H = E \sqrt{\dfrac{I_{pY}}{s_Y} \dfrac{I_{pZ}}{s_Z}} \end{cases} \quad (3.76)$$

where $s_Y (s_Z)$ is the distance betwenn horizontal (vertical) bulkhead girders, $I_{eY} (I_{eZ})$ is the moment of inertia, including effective width $b_{eY} (b_{eZ})$ of plating, of horizontal (vertical) girders respect to the section neutral axis, $I_{pY} (I_{pZ})$ is the moment of inertia of effective breath of plating working with horizontal (vertical) girders. Finally, the bulkhead energy coefficient becomes:

$$C = \frac{116 h_B^3}{35b} \frac{I_{eY}}{s_Y} \alpha_Y + \frac{32 b^3}{105 h_B} \frac{I_{eZ}}{s_Z} + \frac{16 b h_B}{75} \sqrt{\frac{I_{pY}}{s_Y} \frac{I_{pZ}}{s_Z}} \alpha_T \quad (3.77)$$

A similar procedure can be adopted to determine the contribution of an upper stool exposed to bending, shear and torsion. Assuming for the vertical position of the upper stool the equality $\zeta_{stool} = \zeta_D$, the three energy

components can be expressed as follows:

Horizontal bending

$$U_{s-h} = \frac{1}{2} \int_{-b}^{b} EI_s \left[\frac{\partial^2 u^{(b)}}{\partial \eta^2}(\eta, \zeta_D) \right]^2 d\eta = \frac{3I_s \left(h_B - \zeta_Q \right)^2}{b} E\vartheta_1^2 \qquad (3.78)$$

Horizontal shear

$$U_{s-s} = \frac{1}{2} \frac{(EI_s)^2}{GA_s} \int_{-b}^{b} \left[\frac{\partial^3 u^{(b)}}{\partial \eta^3}(\eta, \zeta_D) \right]^2 d\eta = 18(1+\nu) \frac{\left(h_B - \zeta_Q \right)^2}{b^3} \frac{I_s^2}{A_s} E\vartheta_1^2 \qquad (3.79)$$

Torsion

$$U_{s-t} = \frac{1}{2} GI_{s-t} \int_{-b}^{b} \left[\frac{\partial^2 u^{(b)}}{\partial \eta \partial \zeta}(\eta, \zeta_D) \right]^2 d\eta = \frac{9bI_{s-t}}{10(1+\nu)} E\vartheta_1^2 \qquad (3.80)$$

having denoted by I_s the upper stool moment of inertia as regards an axis parallel to ζ and passing through its center of mass, by I_{s-t} its torsional moment of inertia and by A_s the effective shear area.

Chapter 4

The exact theory of non-uniform torsion

This chapter deals with the problem of non-uniform torsion in thin-walled elastic beams, removing the basic concept of a fixed center of twist, necessary in the Vlasov's and Benscoter's theories to obtain a warping stress field equivalent to zero. In this new torsion/flexure theory, despite the classical ones, the warping function will punctually satisfy the first indefinite equilibrium equation along the beam axis and it won't be necessary to introduce the classical compatibility condition, to take into account the effect of the beam restraints. The solution, based on the Fourier development of the displacement field, is obtained assuming that the applied external torque is constant along the beam axis and the unit twist angle and the warping axial displacement functions are totally restrained at both beam ends. The theory is developed for beams with asymmetric cross-section and the special case of a beam with a section having two symmetry axes is analyzed as well.

4.1 The displacement field

It is well known that the classical Saint Venant's theory is based on the uncoupling and superposition of four basic responses: stretching; major-axis bending, coupled with major shear; minor-axis bending, coupled with minor shear and pure torsion. Anyway, when the beam is subjected to a varying
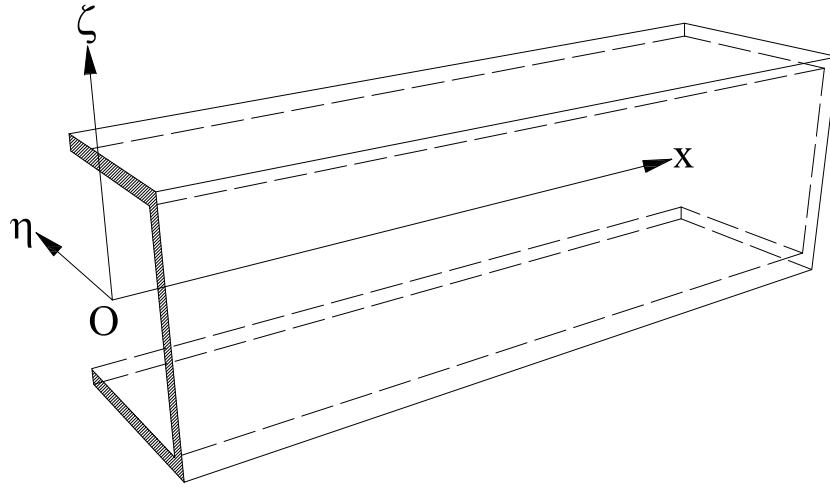
Figure 4.1: Global reference system

torque or the axial warping displacements are partially or totally restrained at one or both member ends, the torsion becomes non-uniform, the twist rate varies along the beam and the displaced centroids describe a curve. In this case two great problems arise: first of all, it is not possible to uncouple a pure torque loading from the bending one caused by the curvature of the centroidal axis; then, the centre of twist is not constant along the beam axis. So, in the following, the traditional concept of a fixed centre of twist is abandoned and a more general theory is developed.

Let us assume that the beam cross-section rotates undeformed through a small angle $\vartheta_t(x)$about the centroidal axis x, warps out of its plane and is subjected to rigid body motions along the section principal axes of inertia. Let us define the global Cartesian frames sketched in the following figure, with origin O in correspondence of the left beam end, x axis defined along the beam length and passing through the section centroid and η, ζ axes defined in the section plane and coinciding with the section principal axes of inertia. In this hypothesis, denoting by u,v, and w the three displacement components in the x, η and ζ directions respectively, the displacement field

can be assumed as follows:

$$
\begin{cases}
u = \tilde{u}(x, \eta, \zeta) - \eta \dfrac{dv_0}{dx} - \zeta \dfrac{dw_0}{dx} \\[3mm]
v = v_0(x) - \vartheta_t(x)\zeta \\[3mm]
w = w_0(x) + \vartheta_t(x)\eta
\end{cases}
\tag{4.1}
$$

where $\tilde{u}(x, \eta, \zeta)$ is the axial displacement function, $\vartheta_t(x)$ is the rotation of the section about the x-axis, positive if counter-clockwise, $v_0(x)$ and $w_0(x)$ are the centroidal lateral rigid body motions along the η and ζ axes, respectively.

4.2 The strain and stress fields

With the previous assumptions and notations the strain field (for small deformation) is given by:

$$
\begin{cases}
\epsilon_x = \dfrac{\partial \tilde{u}}{\partial x} - \eta \dfrac{d^2 v_0}{dx^2} - \zeta \dfrac{d^2 w_0}{dx^2} \\[3mm]
\gamma_{xy} = \dfrac{\partial \tilde{u}}{\partial \eta} - \vartheta_1 \zeta \\[3mm]
\gamma_{xz} = \dfrac{\partial \tilde{u}}{\partial \zeta} + \vartheta_1 \eta \\[3mm]
\epsilon_y = \epsilon_z = \gamma_{yz} = 0
\end{cases}
\tag{4.2}
$$

Denoting by E the Young Modulus, G the Coulomb modulus and ν the Poisson modulus, the Navier equations can be so specialized:

$$
\begin{cases}
\sigma_x = E\left[\dfrac{\partial \tilde{u}}{\partial x} - \eta \dfrac{d^2 v_0}{dx^2} - \zeta \dfrac{d^2 w_0}{dx^2}\right] \\[3mm]
\tau_{xy} = G\left[\dfrac{\partial \tilde{u}}{\partial \eta} - \vartheta_1 \zeta\right] \\[3mm]
\tau_{xyz} = G\left[\dfrac{\partial \tilde{u}}{\partial \zeta} + \vartheta_1 \eta\right]
\end{cases}
\tag{4.3}
$$

As regards the first of (4.3), it is derived by assuming as inelastic tensions σ_y in the web, σ_z in the flanges, what allows to reduce the relevant coefficient to the ratio $\dfrac{E}{1+\nu^2} \simeq E$.

4.3 The FE solution: local and global formulations

The first indefinite equilibrium equation and the relevant boundary condition on the lateral surface can be expressed as follows:

$$\begin{cases} \dfrac{\partial \tau_{xy}}{\partial \eta} + \dfrac{\partial \tau_{xz}}{\partial \zeta} = -\dfrac{\partial \sigma_x}{\partial x} \,\forall P \in A \\[4mm] \tau_{xn} = 0 \,\forall P \in \partial A \end{cases} \tag{4.4}$$

having denoted by A the cross-section domain and by τ_{xn} the tangential stress component, normal to the boundary. In terms of displacements the problem (4.4) can be rewritten as follows:

$$\begin{cases} \dfrac{\partial^2 \tilde{u}}{\partial \eta^2} + \dfrac{\partial^2 \tilde{u}}{\partial \zeta^2} = -2\Big(1+\nu\Big)\Big[\dfrac{\partial^2 \tilde{u}}{\partial x^2} - \eta\dfrac{d^3 v_0}{dx^3} - \zeta\dfrac{d^3 w_0}{dx^3}\Big] \,\forall P \in A \\[4mm] \dfrac{\partial \tilde{u}}{\partial n} = -\vartheta_1\Big(\eta \alpha_{nz} - \zeta \alpha_{ny}\Big) \,\forall P \in \partial A \end{cases} \tag{4.5}$$

having denoted by α_{ny} and α_{nz} the director cosine of the unit normal vector, positive if outside. The axial stress field must also verify the following global conditions:

$$\begin{cases} \displaystyle\int_A \sigma_x dA = 0 \\[4mm] \displaystyle\int_A \sigma_x \eta dA = 0 \\[4mm] \displaystyle\int_A \sigma_x \zeta dA = 0 \end{cases} \tag{4.6}$$

The tangential stress field, instead, is connected to the external torque M_t, assumed constant vs. x, by the global condition:

$$M_t = GI_p\vartheta_1 + G\int_A \Big[\dfrac{\partial \tilde{u}}{\partial \zeta} - \dfrac{\partial \tilde{u}}{\partial \eta}\Big]dA \tag{4.7}$$

having denoted by I_p the polar inertia moment, defined as follows:

$$I_p = \int_A \left[\eta^2 + \zeta^2 \right] dA = I_\zeta + I_\eta \tag{4.8}$$

Concerning the support end conditions, denoting by L the beam length, let us suppose that the beam is "warping clamped" in correspondence of two adjacent bulkheads where the two lateral dispacements and the torsional rotation are free and the following constraints can be addded, so obtaining:

$$u(0, \eta, \zeta) = u(L, \eta, \zeta) = 0 \; ; \; \vartheta_1(0) = \vartheta_1(L) = 0 \tag{4.9}$$

and:

$$\frac{dv_0}{dx}(0) = \frac{dv_0}{dx}(L) = 0 \; ; \; \frac{dw_0}{dx}(0) = \frac{dw_0}{dx}(L) = 0 \tag{4.10}$$

from which it results that $\tilde{u}(0, \eta, \zeta) = \tilde{u}(L, \eta, \zeta) = 0$. In order to solve the problem, it is possible to preliminarily expand the axial displacement function, the unit twist angle and the two rigid body motion functions into appropriate trigonometric series, verifying the previous boundary conditions at both beam ends, and reduced to the partial M-sums:

$$
\begin{cases}
\tilde{u}(x, \eta, \zeta) = \displaystyle\sum_{m=1}^{M} W_m(\eta, \zeta) sin\frac{m\pi x}{L} \\[2em]
\vartheta_1(x) = \displaystyle\sum_{m=1}^{M} \Omega_m sin\frac{m\pi x}{L} \\[2em]
v_0(x) = \displaystyle\sum_{m=1}^{M} B_m cos\frac{m\pi x}{L} \\[2em]
w_0(x) = \displaystyle\sum_{m=1}^{M} C_m cos\frac{m\pi x}{L}
\end{cases}
\tag{4.11}
$$

The indefinite and boundary equations (4.5), thanks to the orthogonality of the trigonometric functions, can be rewritten $\forall m = 1...M$ as follows:

$$
\begin{cases}
\nabla^2 W_m = 2\left(1+\nu\right)\dfrac{m^2\pi^2}{L^2}W_m + 2\left(1+\nu\right)\dfrac{m^3\pi^3}{L^3}\left[\eta B_m + \zeta C_m\right] \\[2em]
\dfrac{\partial W_m}{\partial n} = \Omega_m\left(\zeta\alpha_{ny} - \eta\alpha_{nz}\right)
\end{cases}
\tag{4.12}
$$

Expressing the unknown *m-th* term $W_m(\eta, \zeta)$ in the form:

$$W_m(\eta, \zeta) = \alpha_m(\eta, \zeta)\Omega_m + \beta_m(\eta, \zeta)B_m + \gamma_m(\eta, \zeta)C_m \tag{4.13}$$

the problem (4.12) can be decomposed into three Neumann boundary problems associated to the Helmholtz equation:

$$\begin{cases} \nabla^2 \alpha_m = 2\left(1 + \nu\right)\dfrac{m^2\pi^2}{L^2}\alpha_m \\[3mm] \dfrac{\partial \alpha_m}{\partial n} = \zeta\alpha_{ny} - \eta\alpha_{nz} \end{cases} \tag{4.14}$$

$$\begin{cases} \nabla^2 \beta_m = 2\left(1 + \nu\right)\dfrac{m^2\pi^2}{L^2}\beta_m + 2\left(1 + \nu\right)\dfrac{m^3\pi^3}{L^3}\eta \\[3mm] \dfrac{\partial \beta_m}{\partial n} = 0 \end{cases} \tag{4.15}$$

$$\begin{cases} \nabla^2 \gamma_m = 2\left(1 + \nu\right)\dfrac{m^2\pi^2}{L^2}\gamma_m + 2\left(1 + \nu\right)\dfrac{m^3\pi^3}{L^3}\zeta \\[3mm] \dfrac{\partial \gamma_m}{\partial n} = 0 \end{cases} \tag{4.16}$$

The first of (4.6) implies that the three unknown functions $\alpha_{(\eta, \zeta)}$, $\beta_m(\eta, \zeta)$ and $\gamma_m(\eta, \zeta)$ must also respect the following global conditions:

$$\begin{cases} \displaystyle\int_A \alpha_m dA = 0 \\[5mm] \displaystyle\int_A \beta_m dA = 0 \\[5mm] \displaystyle\int_A \gamma_m dA = 0 \end{cases} \tag{4.17}$$

The unknown amplitudes Ω_m, B_m and C_m can be determined thanks to the second and third of (4.6) and the eq. (4.7), obtaining the following equation system:

$$\left[S\right] \cdot \begin{bmatrix} \Omega_m \\ B_m \\ C_m \end{bmatrix} = \begin{bmatrix} \dfrac{2}{GL}\displaystyle\int_0^L M_t sin\dfrac{m\pi x}{L}dx \\ 0 \\ 0 \end{bmatrix} \tag{4.18}$$

specialized as follows, if M_T constant vs. x is assumed:

$$\left[S\right] \cdot \begin{bmatrix} \Omega_m \\ B_m \\ C_m \end{bmatrix} = \begin{bmatrix} \dfrac{2M_t}{G}\dfrac{1 - cosm\pi}{m\pi} \\ 0 \\ 0 \end{bmatrix} \qquad (4.19)$$

The matrix $\left[S\right]$ is the following one:

$$\left[S\right] = \begin{bmatrix} \alpha_{m1} + I_p & \beta_{m1} & \gamma_{m1} \\ \\ \alpha_{m2} & \beta_{m2} - \dfrac{m\pi}{L}I_\zeta & \gamma_{m2} - \dfrac{m\pi}{L}I_{\eta\zeta} \\ \\ \alpha_{m3} & \beta_{m3} - \dfrac{m\pi}{L}I_{\eta\zeta} & \gamma_{m3} - \dfrac{m\pi}{L}I_\eta \end{bmatrix} \qquad (4.20)$$

having denoted by $I_{\eta\zeta}$ the section product of inertia and by α_{m1}, α_{m2}, α_{m3} the following coefficients (similarly for β_m and γ_m):

$$\begin{cases} \alpha_{m1} = \displaystyle\int_A \left[\eta\frac{\partial\alpha_m}{\partial\zeta} - \zeta\frac{\partial\alpha_m}{\partial\eta}\right]dA \\ \\ \alpha_{m2} = -\displaystyle\int_A \eta\alpha_m dA \\ \\ \alpha_{m3} = -\displaystyle\int_A \zeta\alpha_m dA \end{cases} \qquad (4.21)$$

4.4 Analysis of the stress field

The stress field can be finally expressed as follows:

$$\begin{cases} \sigma_x = E\displaystyle\sum_{i=1}^{M} F_m(\eta,\zeta)\frac{m\pi}{L}cos\frac{m\pi x}{L} \\ \\ \tau_{xy} = G\displaystyle\sum_{i=1}^{M} \left[\left(\frac{\partial\alpha_m}{\partial\eta} - \zeta\right)\Omega_m + \frac{\partial\beta}{\partial\eta}B_m + \frac{\partial\gamma}{\partial\eta}C_m\right]sin\frac{m\pi x}{L} \\ \\ \tau_{xz} = G\displaystyle\sum_{i=1}^{M} \left[\left(\frac{\partial\alpha_m}{\partial\zeta} + \eta\right)\Omega_m + \frac{\partial\beta}{\partial\zeta}B_m + \frac{\partial\gamma}{\partial\zeta}C_m\right]sin\frac{m\pi x}{L} \end{cases} \qquad (4.22)$$

having introduced the following function:

$$F_m(\eta, \zeta) = \alpha_m(\eta, \zeta)\Omega_m + \left[\beta_m + \eta\frac{m\pi}{L}\right]B_m + \left[\gamma_m + \zeta\frac{m\pi}{L}\right]C_m \qquad (4.23)$$

Similarly to the Vlasov's theory it is possible to introduce the bimoment as follows:

$$B = \frac{E}{L}\sum_{m=1}^{M}\frac{m\pi}{\Omega_m}\cos\frac{m\pi x}{L}\int_A F_m^2(\eta, \zeta)dA \qquad (4.24)$$

4.5   The simplified solution for beams with axial symmetric cross-section

A special case of the previously analyzed problem concerns a beam having an axialsymmetric cross-section. In this case, in fact, the bending components are directly null, so that the displacement field can be reduced to the following one:

$$\begin{cases} u = \tilde{u}(x, \eta, \zeta) \\\\ v = v_0(x) - \vartheta_t(x)\zeta \\\\ w = w_0(x) + \vartheta_t(x)\eta \end{cases} \qquad (4.25)$$

With all the previous notations the strain field becomes:

$$\begin{cases} \epsilon_x = \dfrac{\partial\tilde{u}}{\partial x} \\\\ \gamma_{xy} = \dfrac{\partial\tilde{u}}{\partial\eta} - \vartheta_1\zeta \\\\ \gamma_{xz} = \dfrac{\partial\tilde{u}}{\partial\zeta} + \vartheta_1\eta \\\\ \epsilon_y = \epsilon_z = \gamma_{yz} = 0 \end{cases} \qquad (4.26)$$

while the stress field can be so expressed:

$$
\begin{cases}
\sigma_x = E\dfrac{\partial \tilde{u}}{\partial x} \\[4mm]
\tau_{xy} = G\Big[\dfrac{\partial \tilde{u}}{\partial \eta} - \vartheta_1 \zeta\Big] \\[4mm]
\tau_{xyz} = G\Big[\dfrac{\partial \tilde{u}}{\partial \zeta} + \vartheta_1 \eta\Big]
\end{cases}
\tag{4.27}
$$

The first indefinite equilibrium equation with the relevant boundary conditions on the beam lateral surface and at the two extremities can be written, in terms of displacements, as follows:

$$
\begin{cases}
\dfrac{\partial^2 \tilde{u}}{\partial \eta^2} + \dfrac{\partial^2 \tilde{u}}{\partial \zeta^2} = -2\Big(1+\nu\Big)\dfrac{\partial^2 \tilde{u}}{\partial x^2} \ \forall P \in A \\[4mm]
\dfrac{\partial \tilde{u}}{\partial n} = -\vartheta_1\Big(\eta\alpha_{nz} - \zeta\alpha_{ny}\Big) \ \forall P \in \partial A \\[4mm]
\tilde{u}(0,\eta,\zeta) = \tilde{u}(L,\eta,\zeta) = 0 \ ; \ \vartheta_1(0) = \vartheta_1(L) = 0
\end{cases}
\tag{4.28}
$$

Adopting for the warping function and the unit twist angle the same developments into trigonometric series of eq. (4.11), which already satisfy the boundary conditions at the two beam extremities, and taking into account that in this case for any Ω_m equal to zero also $W_m(\eta,\zeta)$ will be equivalent to zero, for non zero Ω_m it is possible to introduce another unknown function $f_m(\eta,\zeta)$ so defined:

$$
f_m(\eta,\zeta) = \frac{W_m(\eta,\zeta)}{\Omega_m}
\tag{4.29}
$$

Thanks to the orthogonality of the trigonometric functions, by (4.11) and (4.29), the differential problem (4.28) can be so rewritten:

$$
\begin{cases}
\nabla^2 f_m = 2\Big(1+\nu\Big)\dfrac{m^2\pi^2}{L^2}f_m \ \forall P \in A \\[4mm]
\dfrac{\partial f_m}{\partial n} = \zeta\alpha_{ny} - \eta\alpha_{nz} \ \forall P \in \partial A
\end{cases}
\tag{4.30}
$$

so that $\forall m = 1...M$, $f_m(\eta,\zeta)$ will be the solution of a Neumann boundary problem associated to the pure Helmholtz equation. It is noticed that the

previous developements into trigonometric series of the axial displacement function and the unit twist angle automatically satisfy the boundary conditions at the two beam extremities. Also in this case, since it is not possible to find an analytical solution of the problem (4.30), for a generic beam cross-section, it is necessary to resort to numerical methods to solve it. In the applications the Finite Element Method (FEM) is adopted, by means of the Mathworks Matlab software. To solve this problem for an assigned beam section and for the varying harmonics' index m, it was necessary to realize a suitable script file. In our case the computational domain is subdivided by a triangular mesh, made up of an enough large number of elements and the partial differential equation is discretized on it. The solution $f_m(\eta, \zeta)$ is calculated at the vertices of the triangles (i.e. the nodes of the mesh) and it is assumed to vary linearly on each triangle, obtaining a continuous piecewise linear function on the mesh. Its first derivatives, as regards the η and ζ axes, instead, are evaluated in correspondence of the centre of each triangle. Furthermore, as the axial stress σ_x must also verify the eq. (4.6), thanks to the double symmetry of the section as regards the η and ζ axis, it is sufficient that the function $f_m(\eta, \zeta)$ satisfies the following global condition:

$$\int_A f_m dA = 0 \qquad (4.31)$$

Finally, to determine uniquely the solution, it is necessary to find the unknown coefficient Ω_m. Starting from eq. (4.7), this global condition can be expressed as follows:

$$M_t(x) = GI_p \sum_{m=1}^{M} \Omega_m sin\frac{m\pi x}{L} + G \sum_{i=1}^{M} \Omega_m H_m sin\frac{m\pi x}{L} \qquad (4.32)$$

having done the position:

$$H_m = \int_A \left[\eta \frac{\partial f_m}{\partial \zeta} - \zeta \frac{\partial f_m}{\partial \eta}\right] dA \qquad (4.33)$$

Then, thanks to the orthogonality of the trigonometric functions. it is possible to determine the coefficient Ω_m as follows:

$$\Omega_m = \frac{2 \int_0^L M_t(x) sin\frac{m\pi x}{L} dx}{GL(I_p + H_m)} \qquad (4.34)$$

Particularly, assuming $M_t(x) = const.$ the eq. (4.34) can be so specialized:

$$\Omega_m = \frac{2M_t}{G(I_p + H_m)} \frac{1 - cosm\pi}{m\pi} \tag{4.35}$$

Similarly to the Vlasov's theory, denoting by σ_{x-m} the m-th component of σ_x, it is possible to introduce the bimoment as follows:

$$B = \sum_{m=1}^{M} B_m = \sum_{m=1}^{M} \int_A \sigma_{x-m} f_m dA \tag{4.36}$$

so that, defining the warping modulus relative to the m-th harmonic $I_{w-m} = \int_A f_m^2 dA$, the bimoment can be finally expressed as follows:

$$B = \frac{4(1+\nu)M_t}{L} \sum_{m=1}^{M} \frac{1 - cosm\pi}{I_p + H_m} cos\frac{m\pi x}{L} I_{w-m} \tag{4.37}$$

The stress field finally becomes:

$$\begin{cases} \sigma_x = \sum_{m=1}^{M} \frac{B_m}{I_{w-m}} f_m(\eta, \zeta) \\[3em] \tau_{xy} = 2M_t \sum_{m=1}^{M} \frac{1 - cosm\pi}{m\pi} \frac{\dfrac{\partial f_m}{\partial \eta} - \zeta}{I_p + H_m} sin\frac{m\pi x}{L} \\[3em] \tau_{xz} = 2M_t \sum_{m=1}^{M} \frac{1 - cosm\pi}{m\pi} \frac{\dfrac{\partial f_m}{\partial \zeta} + \eta}{I_p + H_m} sin\frac{m\pi x}{L} \end{cases} \tag{4.38}$$

Chapter 5

Solution of the clamped orthotropic plate equation

This chapter focuses on the application of orthotropic plate bending theory to stiffened platings. Schades design charts for rectangular plates are extended to the case where the boundary contour is clamped, which is almost totally incomplete in the afore mentioned charts. A numerical solution for the clamped orthotropic plate equation is obtained: the Rayleigh-Ritz method is adopted, expressing the vertical displacement field by a double cosine trigonometric series, whose coefficients are determined by solving a linear equation system. Numerical results are proposed as design charts similar to those ones by Schade. In particular, each chart is relative to one of the non-dimensional coefficients identifying the plate response; each curve of any chart is relative to a given value of the torsional parameter η_t, in a range comprised between 0 and 1, and is function of the virtual aspect ratio ρ, comprised between 1 and 8, so that the asymptotic behaviour of the orthotropic plate for $\rho \to \infty$ is clearly shown.

5.1   The Huber's differential equation

Schade, 1942, proposed some practical general design curves, based on the orthotropic plate theory, in order to obtain a rapid, but accurate, dimensioning of plating stiffeners. Schade considered four types of boundary
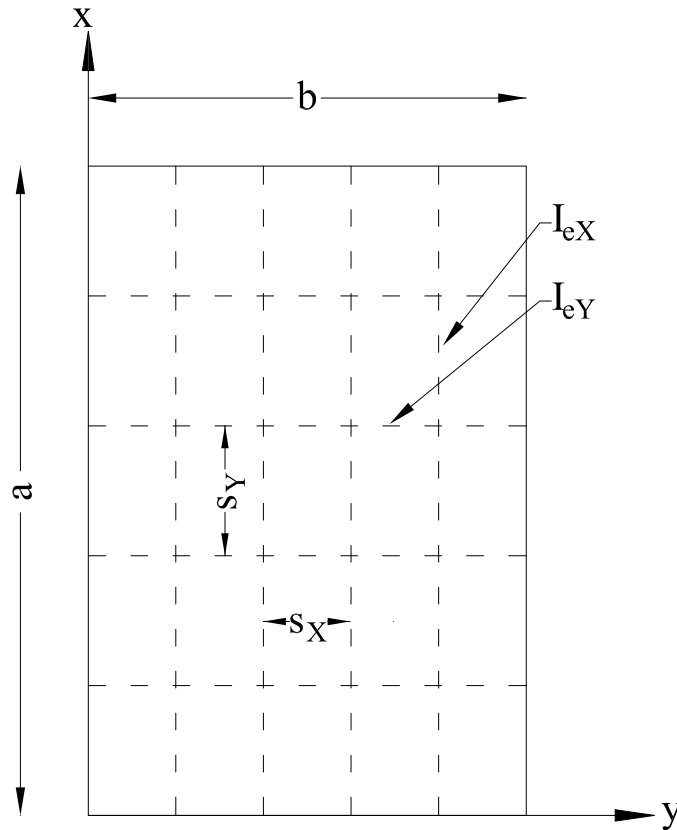
Figure 5.1: Orthotropic plate reference system

conditions for the orthotropic partial differential equation: all edges rigidly supported but not fixed; both short edges clamped, both long edges supported; both long edges clamped, both short edges supported; all edges clamped. The last case with all edges clamped was left almost totally incomplete. The few data useful for this boundary condition were taken from Timoshenko et al. [22], and Young [23], as given for the isotropic plate only for the torsional coefficient value $\eta_t = 1$ and for a range of the virtual aspect ratio ρ comprised between 1 and 2. In the following paragraph a numerical solution of the clamped orthotropic plate equation is obtained. Numerical results are presented in a series of charts similar to the ones given by Schade.

It is well known that orthotropic plate theory refers to materials which have different elastic properties along two orthogonal directions. In order to

apply this theory to panels having a finite number of stiffeners, it is neces-
sary to idealize the structure, assuming that the structural properties of the
stiffeners may be approximated by their average values, which are assumed
to be distributed uniformly over the width and the length of the plate. Re-
ferring to the coordinate system of Fig. 5.1, the deflection field in bending
is governed by the so called Hubers differential equation:

$$D_X \frac{\partial^4 w}{\partial x^4} + 2H \frac{\partial^4 w}{\partial x^2 \partial y^2} + D_Y \frac{\partial^4 w}{\partial y^4} = p(x, y) \tag{5.1}$$

having denoted by w the vertical displacement field, D_X the unit flexural
rigidity around the y axis, D_Y the unit flexural rigidity around the x axis,
$H = \eta_t \sqrt{D_X D_Y}$ the unit torsional rigidity according to Schade's works,
$p(x, y)$ the pressure load over the surface. It is noticed that the behaviour
of the isotropic plate with the same flexural rigidities in all directions is a
special case of the orthotropic plate problem. Indicating by n the normal
external to the plate contour, the following boundary conditions are added
to the differential equation along all edges:

$$w = 0 \, ; \, \frac{\partial w}{\partial n} = 0 \tag{5.2}$$

Now, as the plate domain is rectangular, the boundary conditions (5.2) can
be rewritten as follows:

$$w = 0 \, ; \, \frac{\partial w}{\partial x} = \frac{\partial w}{\partial y} = 0 \tag{5.3}$$

So, any displacement function $w(x, y)$, satisfying the boundary conditions
(5.3), must belong with the first order derivatives to the function space with
compact support in Ω, having denoted by Ω the function domain.

5.2 The numerical solution

In order to solve the eq. (5.1) with the boundary conditions (5.3) along
all edges, two solution methods are available: the double cosine series and the
Henky's method. It's well known the second one converges very quickly but
it gives some difficulties concerning the programming due to over/underlow
problems in the evaluation of hyperbolic trigonometric functions with large

arguments. The double cosine series method, instead, is devoid of the over/underflow issue but it is known to converge very slowly. Denoting by a an b the plate lengths in the x and y directions respectively, the vertical displacement field may be expressed by means of the following double cosine trigonometric series:

$$w(x,y) = \sum_{m=1}^{M} \sum_{n=1}^{N} \left(1 - cos2\pi m\frac{x}{a}\right) \cdot \left(1 - cos2\pi n\frac{y}{b}\right) w_{m,n} \qquad (5.4)$$

whose terms already satisfy the boundary condtions (5.3). The unknown coefficients $w_{m,n}$ may be determined using the Rayleigh-Ritz method, searching for the minimum of a variational functional. Now, denoting bu u the and f two classes of functions belonging to a Hilbert Space, for linear differential operators as:

$$\ell u = f \qquad (5.5)$$

that are auto-added and defined positive, it is possible to find a numerical solution of the eq. (5.5) searching for the stationary point of the functional:

$$\Pi(u) = \frac{1}{2} \int_{\Omega} \ell u \cdot u d\Omega - \int_{\Omega} f \cdot u d\Omega \qquad (5.6)$$

The linear operator ℓ of the eq. (5.5) is auto-added if, $\forall u(x,y) \in \mathbf{L}^2(\Omega)$ and $\forall v(x,y) \in \mathbf{L}^2(\Omega)$ satisfying the assigned boundary conditions, it is verified that:

$$\int_{\Omega} \ell u \cdot v d\Omega = \int_{\Omega} \ell v \cdot u d\Omega \qquad (5.7)$$

where Ω is an open set of $\mathbf{R}^k$. Now, let us consider the generalized integration by parts formula:

$$\int_{\Omega} \left(uD_i v\right) dt = \int_{\partial\Omega} uv\left(\boldsymbol{e}_i \cdot \boldsymbol{n}\right) d\sigma - \int_{\Omega} \left(vD_i u\right) dt \qquad (5.8)$$

where $\boldsymbol{n}$ is the versor of the normal external to $\partial\Omega$ and $\boldsymbol{e}_i$ is the versor of the t_i axis. First of all, in order to apply the eq. (5.8), it is necessary to suppose that $\Omega \subset \mathbf{R}^2$ is a regular domain, i.e. that it is a limited domain with one or more contours that have to be generally regular curves.In the case under examination, as Ω is a rectangular domain these conditions are certainly verified. Furthermore as $w \in \mathbf{C}_0^1(\Omega)$, it derives that:

$$\int_{\Omega} \left(uD_i v\right) dt = - \int_{\Omega} \left(vD_i u\right) dt \qquad (5.9)$$

but, thanks to the boundary conditions (5.3), it is also possible to verify that:

$$\int_\Omega \left(uD^\alpha v\right)dt = -(1)^{|\alpha|}\int_\Omega \left(vD^\alpha u\right)dt \tag{5.10}$$

whatever is the multi-index $\alpha = (\alpha_1, \alpha_2)$ with $|\alpha| < 4$, having denoted by $|\alpha| = \alpha_1 + \alpha_2$ the sum of the derivation number respect to the first variable and the second one, respectively. From eq. (5.10) it is immediately verified the condition (5.7), as the partial differential operators are of even order. Furthermore the linear operator ℓ is defined positive if it is verified that:

$$\int_\Omega \ell u \cdot u d\Omega > 0 \tag{5.11}$$

Applying the generalized integration by parts formula the integral (5.12) becomes:

$$\int_\Omega \left[D_X\left(\frac{\partial^2 w}{\partial x^2}\right)^2 + 2H\left(\frac{\partial^2 w}{\partial x \partial y}\right)^2 + D_Y\left(\frac{\partial^2 w}{\partial y^2}\right)^2\right]dA > 0 \; \forall w(x,y) \neq 0 \tag{5.12}$$

The previously defined integral is certainly ≥ 0 and it is equivalent to zero only if it punctually results:

$$\frac{\partial^2 w}{\partial x^2} = \frac{\partial^2 w}{\partial x \partial y} = \frac{\partial^2 w}{\partial y^2} \; \forall (x,y) \in \Omega \tag{5.13}$$

what implies that:

$$\frac{\partial w}{\partial x} = \frac{\partial w}{\partial y} = const. \; \forall (x,y) \in \Omega \tag{5.14}$$

But as on the boundary it puncutally results:

$$\frac{\partial w}{\partial x} = \frac{\partial w}{\partial y} = 0 \; \forall (x,y) \in \partial\Omega \tag{5.15}$$

thanks to the continuity of the displacement function it would result:

$$\frac{\partial w}{\partial x} = \frac{\partial w}{\partial y} = 0 \; \forall (x,y) \in \Omega \tag{5.16}$$

so obtaining $w(x,y) = const. \forall (x,y) \in \Omega$ and then, thanks again to the continuity on the boundary where the displacement function is punctually null, $w(x,y) = 0 \; \forall (x,y) \in \Omega$. So if the integral of eq. (5.12) is null then the solution reduces to the null displacement function, what implies that the integral is defined strictly positive and the eq. (5.11) is verified. In order

to find the coefficients of eq. (5.4), it is imposed that the functional (5.5) is stationary, so imposing the following MxN conditions:

$$\frac{\partial \Pi}{\partial w_{m,n}} = 0 \; \forall m \in 1...M \; and \; n \in 1...N \tag{5.17}$$

In this case the functional (5.6) can be rewritten as follows:

$$\Pi(w) = \frac{1}{2} \int_{\Omega} \left[D_X w \frac{\partial^4 w}{\partial x^4} + 2Hw \frac{\partial^4 w}{\partial x^2 \partial y^2} + D_Y w \frac{\partial^4 w}{\partial y^4} \right] dA - \int_{\Omega} wp \, dA \tag{5.18}$$

Applying the generalized integration by parts formula, the functional (5.18) can be rewritten as follows:

$$\Pi(w) = \frac{1}{2} \int_{\Omega} \left[D_X \left(\frac{\partial^2 w}{\partial x^2} \right)^2 + 2H \frac{\partial^2 w}{\partial x^2} \frac{\partial^2 w}{\partial y^2} + D_Y \left(\frac{\partial^2 w}{\partial y^2} \right)^2 \right] dA - \int_{\Omega} wp \, dA \tag{5.19}$$

To carry out the computations, it is convenient to use the following coordinate transformations:

$$x = a\xi \; ; \; 0 \leq \xi \leq 1 \tag{5.20}$$

and:

$$y = b\eta \; ; \; 0 \leq \eta \leq 1 \tag{5.21}$$

so that the series is given in non-dimensional form as follows:

$$w(\xi, \eta) = \sum_{m=1}^{M} \sum_{n=1}^{N} \left(1 - cos2\pi m\xi \right) \cdot \left(1 - cos2\pi n\eta \right) w_{m,n} \tag{5.22}$$

and the functional $\Pi(w)$ can be rewritten in the non-dimensional form:

$$\hat{\Pi}(w) = \frac{1}{2} \int_0^1 \int_0^1 \left[\frac{D_X}{a^4} \left(\frac{\partial^2 w}{\partial \xi^2} \right)^2 + 2 \frac{H}{a^2 b^2} \frac{\partial^2 w}{\partial \xi^2} \frac{\partial^2 w}{\partial \eta^2} + \frac{D_Y}{b^4} \left(\frac{\partial^2 w}{\partial \eta^2} \right)^2 - wp \right] d\xi d\eta \tag{5.23}$$

and the stationary point is obtained imposing the MxN equation system:

$$\frac{\partial}{\partial w_{m,n}} \Pi(w) = 0 \; for \, m = 1...M \; ; \; n = 1...N \tag{5.24}$$

So, considering p as uniformly distributed, the generic equation for $m = \overline{m}$ and $n = \overline{n}$ assumes the form:

$$\frac{\partial}{\partial w_{\overline{m},\overline{n}}} \int_0^1 \int_0^1 \left[D_X \left(\frac{\partial^2 w}{\partial \xi^2} \right)^2 + 2 \left(\frac{a}{b} \right)^2 \frac{\partial^2 w}{\partial \xi^2} \frac{\partial^2 w}{\partial \eta^2} + D_Y \left(\frac{a}{b} \right)^4 \left(\frac{\partial^2 w}{\partial \eta^2} \right)^2 \right] d\xi d\eta = 1 \tag{5.25}$$

as it results:

$$\frac{\partial}{\partial w_{\overline{m},\overline{n}}} \int_0^1 \int_0^1 wp\,d\xi d\eta = \int_0^1 \int_0^1 \left(1 - cos2\pi\overline{m}\xi\right) \cdot \left(1 - cos2\pi\overline{n}\eta\right) d\xi d\eta = 1 \tag{5.26}$$

Introducing the previously defined torsional coefficient η_t and the virtual aspect ratio ρ defined as follows:

$$\rho = \frac{a}{b} \sqrt[4]{\frac{D_Y}{D_X}} \tag{5.27}$$

the eq.(5.25) becomes:

$$\frac{1}{\rho^4}\left[\overline{m}^4 w_{\overline{m},\overline{n}} + \sum_{n=1}^{N} 2\overline{m}^4 w_{\overline{m},n}\right] + \overline{n}^4 w_{\overline{m},\overline{n}} + \sum_{m=1}^{M} 2\overline{n}^4 w_{m,\overline{n}} + 2\frac{\eta_t}{\rho^2}\overline{m}^2\overline{n}^2 w_{\overline{m},\overline{n}} = \frac{pb^4}{4\pi^4 D_Y} \tag{5.28}$$

Defining the non-dimensional vertical displacements:

$$\delta = D_Y \frac{w}{pb^4} \; ; \; \delta_{m,n} = D_Y \frac{w_{m,n}}{pb^4} \tag{5.29}$$

the equation system finally becomes:

$$\frac{1}{\rho^4}\left[\overline{m}^4 \delta_{\overline{m},\overline{n}} + \sum_{n=1}^{N} 2\overline{m}^4 \delta_{\overline{m},n}\right] + \overline{n}^4 \delta_{\overline{m},\overline{n}} + \sum_{m=1}^{M} 2\overline{n}^4 \delta_{m,\overline{n}} + 2\frac{\eta_t}{\rho^2}\overline{m}^2\overline{n}^2 \delta_{\overline{m},\overline{n}} = \frac{pb^4}{4\pi^4 D_Y} \tag{5.30}$$

Even if the double cosine trigonometric series converges very slowly, adopting sufficiently high values for M and N, it is possible to obtain a very accurate solution of the equation (5.1) with the boundary conditions (5.2).

5.3 Characterization of the behaviour of clamped stiffened plates

The orthotropic plate bending theory can be applied to the plate of Fig. 5.1 , reinforced by two systems of parallel beams spaced equal distances apart in the x and y directions. The rigidities D_X and D_Y of equation (5.1) can be specialized as follows:

$$D_x = \frac{EI_{ex}}{s_x} \; ; \; D_y = \frac{EI_{ey}}{s_y} \tag{5.31}$$

where E is the Young modulus and s_x (s_y) is the distance between girder (transverses). It is noticed that I_{ex} (I_{ey}) is the moment of inertia, including effective width b_{ex} (b_{ey}) of plating and the attached ordinary stiffeners, of long (short) repeating primary supporting members, respect to the axis whose eccentricity from the reference plane ($z = 0$) e_x (e_y) is to be determined as follows:

$$\frac{b_{ex}}{1 - \nu^2} \int_{P_x} (z - e_x) dz + \int_{A_x} (z - e_x) dz + \left(\frac{b_{ex}}{s_{ex}} - 1 \right) \int_{a_x} (z - e_x) dA = 0 \quad (5.32)$$

and:

$$\frac{b_{ey}}{1 - \nu^2} \int_{P_y} (z - e_y) dz + \int_{A_y} (z - e_y) dz + \left(\frac{b_{ey}}{s_{ey}} - 1 \right) \int_{a_y} (z - e_y) dA = 0 \quad (5.33)$$

According to Shade's works, the torsional coefficient η_t and the virtual aspect ratio ρ can be specialized as follows:

$$\eta_t = \sqrt{\frac{i_{px} i_{py}}{i_x i_y}} \ ; \ \rho = \frac{a}{b} \sqrt[4]{\frac{i_y}{i_x}} \quad (5.34)$$

where i_{px} (i_{py}) is the moment of inertia of effective breadth of plating working with long (short) supporting stiffeners per unit of length. The meaning of the two parameters is quite clear: the torsional coefficient η_t which lies between 0 and 1, exists because only the plating is subject to horizontal shear, while both the plating and the stiffeners are subject to bending stress. Obviously $\eta_t = 1$ and $i_{px} = i_{py} = i_x = i_y = 1$ represent the isotropic plate case. The virtual side ratio ρ is the plate side ratio modified in accordance with the unit stiffnesses in the two directions; as usual it has been admitted that ρ is always equal to or greater than unity. In the next paragraph the quantities represented in the following diagrams are presented.

Deflection at center

The vertical displacement at the plate center ($\eta = \xi = 0.5$) is the maximum and can be so expressed:

$$w_{max} = \sum_{m=1}^{M} \sum_{n=1}^{N} \delta_{m,n} \left(1 - cos\pi m \right) \left(1 - cos\pi n \right) \frac{pb^4}{Ei_y} \quad (5.35)$$

Edge bending stress in plating

The curves of Fig. 5.3 give the bending stress in the plating at the centers

of edges where fixity exists. The stress at the center of such an edge may be treated as the maximum along that edge. The maximum stresses in the plating in the long and short directions respectively are:

$$\sigma_{xp-sup} = \frac{E}{1-\nu^2}\frac{1}{a^2}\frac{\partial^2\delta}{\partial\xi^2}\bigg|_{(0,\frac{1}{2})}r_{xp}\frac{pb^4}{Ei_y} \tag{5.36}$$

$$\sigma_{yp-sup} = \frac{E}{1-\nu^2}\frac{1}{b^2}\frac{\partial^2\delta}{\partial\eta^2}\bigg|_{(\frac{1}{2},0)}r_{yp}\frac{pb^4}{Ei_y} \tag{5.37}$$

as along the edges it results:

$$\frac{\partial^2\delta}{\partial\eta^2}\bigg|_{(0,\frac{1}{2})} = 0 \; ; \; \frac{\partial^2\delta}{\partial\xi^2}\bigg|_{(\frac{1}{2},0)} = 0 \tag{5.38}$$

The equations (5.36) and (5.37) become:

$$\sigma_{xp-sup} = \frac{1}{\rho^2}\frac{4\pi^2}{1-\nu^2}\frac{pb^2r_{xp}}{\sqrt{i_x i_y}}\sum_{m=1}^{M}\sum_{n=1}^{N}\delta_{m,n}m^2\Big(1-cos\pi n\Big) \tag{5.39}$$

$$\sigma_{yp-sup} = \frac{4\pi^2}{1-\nu^2}\frac{pb^2r_{yp}}{i_y}\sum_{m=1}^{M}\sum_{n=1}^{N}\delta_{m,n}n^2\Big(1-cos\pi m\Big) \tag{5.40}$$

Edge bending stress in free flanges

The curves of Fig. 5.4 give the bending stress in the free flanges at the centers of the edges where fixity exists. The stress at the center of such an edge may be treated as the maximum along that edge. The maximum stress for girders and transverses are respectively:

$$\sigma_{xf-sup} = -E\frac{1}{a^2}\frac{\partial^2\delta}{\partial\xi^2}\bigg|_{(0,\frac{1}{2})}r_{xf}\frac{pb^4}{Ei_y} \tag{5.41}$$

$$\sigma_{yf-sup} = -E\frac{1}{b^2}\frac{\partial^2\delta}{\partial\eta^2}\bigg|_{(\frac{1}{2},0)}r_{yf}\frac{pb^4}{Ei_y} \tag{5.42}$$

These equations finally become:

$$\sigma_{xf-sup} = -\frac{4\pi^2}{\rho^2}\frac{pb^2r_{xf}}{\sqrt{i_x i_y}}\sum_{m=1}^{M}\sum_{n=1}^{N}\delta_{m,n}m^2\Big(1-cos\pi n\Big) \tag{5.43}$$

$$\sigma_{yf-sup} = -4\pi^2\frac{pb^2r_{yf}}{i_y}\sum_{m=1}^{M}\sum_{n=1}^{N}\delta_{m,n}n^2\Big(1-cos\pi m\Big) \tag{5.44}$$

It is important to note that when $\rho \to \infty$, k_{yf-sup} is substantially independent on η_t and is equal to $\frac{1}{2}$ that is the beam theory value. Furthermore the

curves show that for low values of η_t the maximum deflections and stresses parallel to the short direction occour at values of ρ between 1.5 and 2.0: this indicates that the long beams add to the load taken by the short beams, instead of helping to support it.

Bending stress in free flanges at center

The curves of Fig. 5.5 give the bending stress in the free flanges at the center of the panel in long and short directions respectively. The stresses :

$$\sigma_{xf-cen} = -E \frac{1}{a^2} \frac{\partial^2 \delta}{\partial \xi^2}\Big|_{(\frac{1}{2},\frac{1}{2})} r_{xf} \frac{pb^4}{Ei_y} \tag{5.45}$$

$$\sigma_{yf-cen} = -E \frac{1}{b^2} \frac{\partial^2 \delta}{\partial \eta^2}\Big|_{(\frac{1}{2},\frac{1}{2})} r_{yf} \frac{pb^4}{Ei_y} \tag{5.46}$$

finally becoming:

$$\sigma_{xf-cen} = -\frac{4\pi^2}{\rho^2} \frac{pb^2 r_{xf}}{\sqrt{i_x i_y}} \sum_{m=1}^{M} \sum_{n=1}^{N} \delta_{m,n} m^2 cos\pi m \Big(1 - cos\pi n\Big) \tag{5.47}$$

$$\sigma_{yf-cen} = -4\pi^2 \frac{pb^2 r_{yf}}{i_y} \sum_{m=1}^{M} \sum_{n=1}^{N} \delta_{m,n} n^2 cos\pi n \Big(1 - cos\pi m\Big) \tag{5.48}$$

It is important to note that when $\rho \rightarrow \infty$, k_{yf-cen} is substantially independent on η_t and is equal to $\frac{1}{24}$ that is the beam theory value. In order to verify the goodness of the method, the following tables show a comparison between the values obtained applying the Rayleigh-Ritz method and the ones taken from Timoshenko et al., 1959, for the isotropic plate ($\eta_t = 1.00$).

ρ	Timoshenko	$k_w(\eta_t = 1.00)$
1.00	0.00126	0.00126
1.20	0.00172	0.00172
1.40	0.00207	0.00207
1.60	0.00230	0.00230
1.80	0.00245	0.00245
2.00	0.00254	0.00253
∞	0.00260	0.00260

Table 5.1: Deflection at center
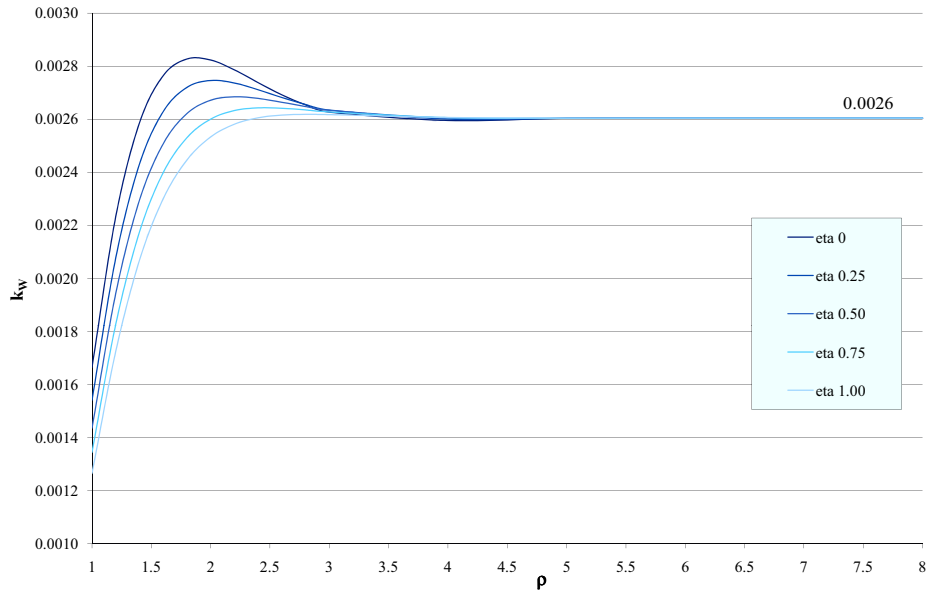
Figure 5.2: Deflection at center
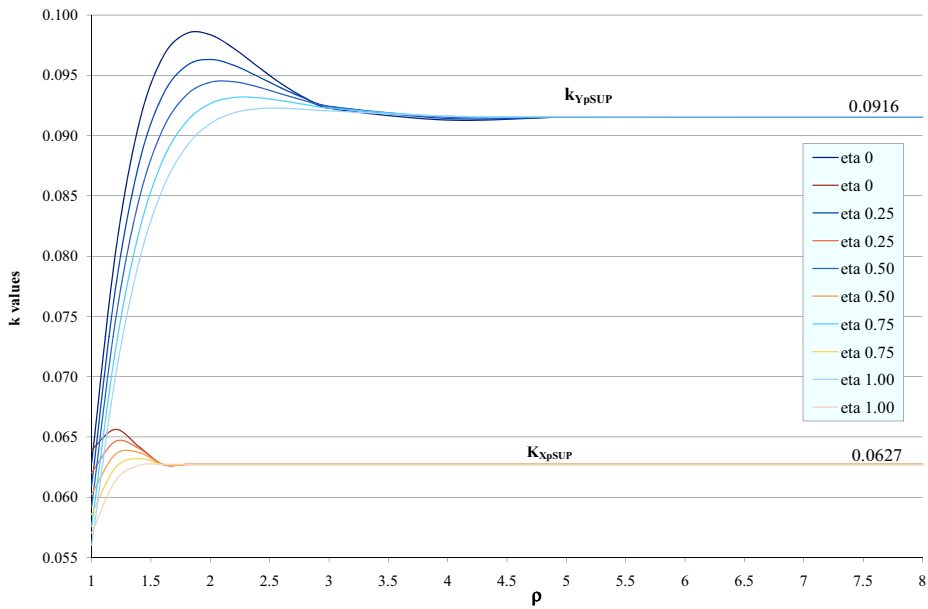
Figure 5.3: Edge bending stress in plating
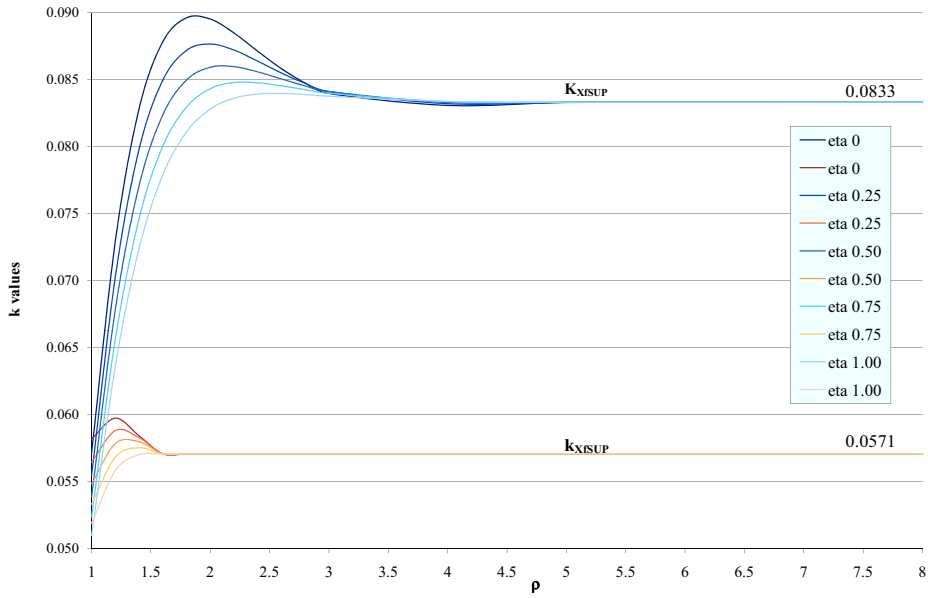
Figure 5.4: Edge bending stress in free flanges
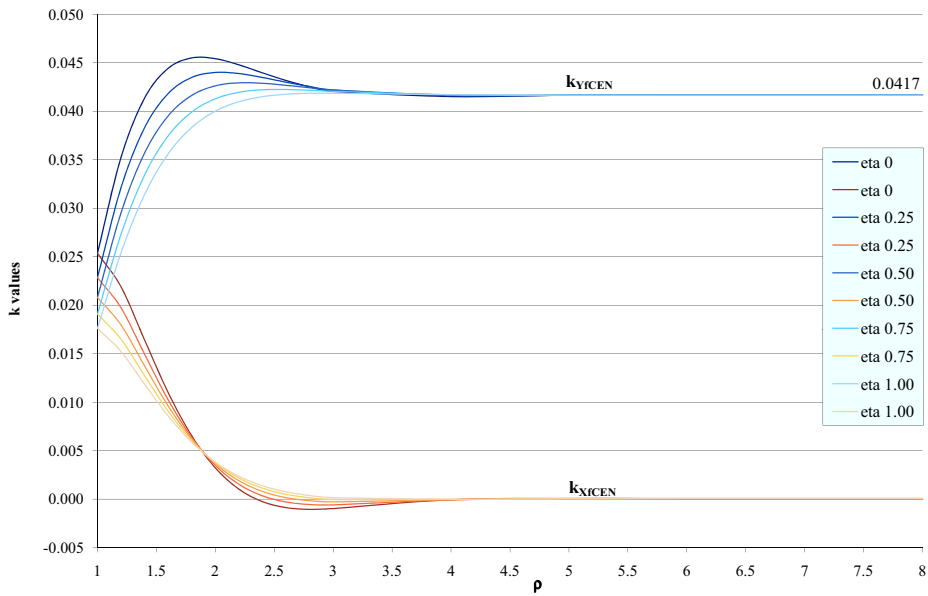
Figure 5.5: Bending stress in free flanges at center

ρ	Timoshenko	$\left(1-\nu^2\right)k_{yp-sup}(\eta_t = 1.00)$
1.00	0.0513	0.0510
1.20	0.0639	0.0636
1.40	0.0726	0.0724
1.60	0.0780	0.0779
1.80	0.0812	0.0811
2.00	0.0829	0.0828
∞	0.0833	0.0833

Table 5.2: Edge bending moment in short direction

ρ	Timoshenko	$\left(1-\nu^2\right)k_{xp-sup}(\eta_t = 1.00)$
1.00	0.0513	0.0510
1.20	0.0554	0.0558
1.40	0.0568	0.0570
1.60	0.0571	0.0571
1.80	0.0571	0.0571
2.00	0.0571	0.0571
∞	0.0571	0.0571

Table 5.3: Edge bending moment in long direction

5.4   Convergence of the method

In this paragraph the influence of the number of harmonics on k values is shown. As the convergence behaviour depends on rho and η_t, in the examined case it was assumed $\rho = 5$ and $\eta_t = 0.50$. The indexes $M = N$ have been varied from 5 up to 100, in order to obtain a number of harmonics comprised between 25 and 10000. If the number of harmonics is > 4900, i.e. M=N > 70, a good convergence in the assessment of k values, and then of the proposed curves, is obtained for practical purposes, as it can be appreciated from the following figures, where the convergence behaviour of k_w, K_{xf-sup} and K_{yf-sup} is shown.
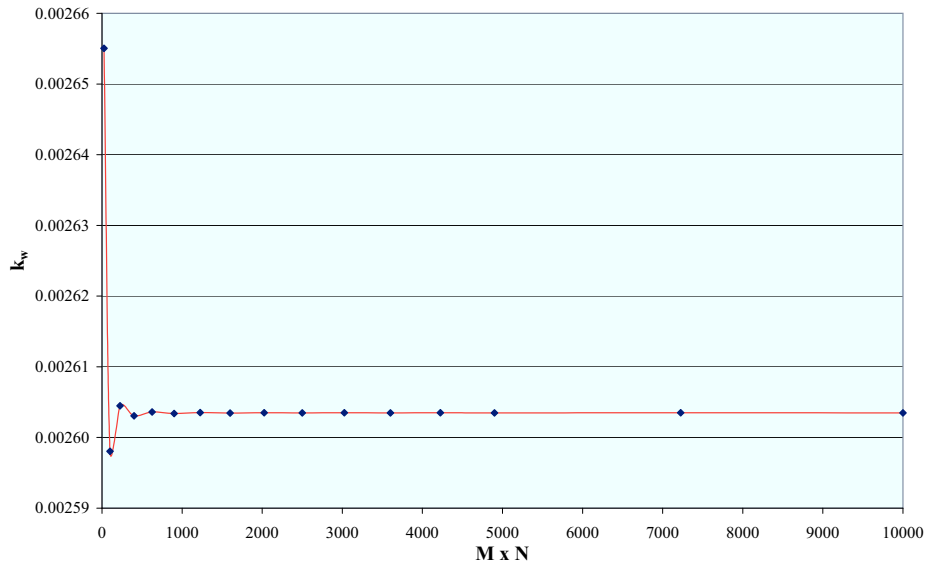
Figure 5.6: K_w convergence
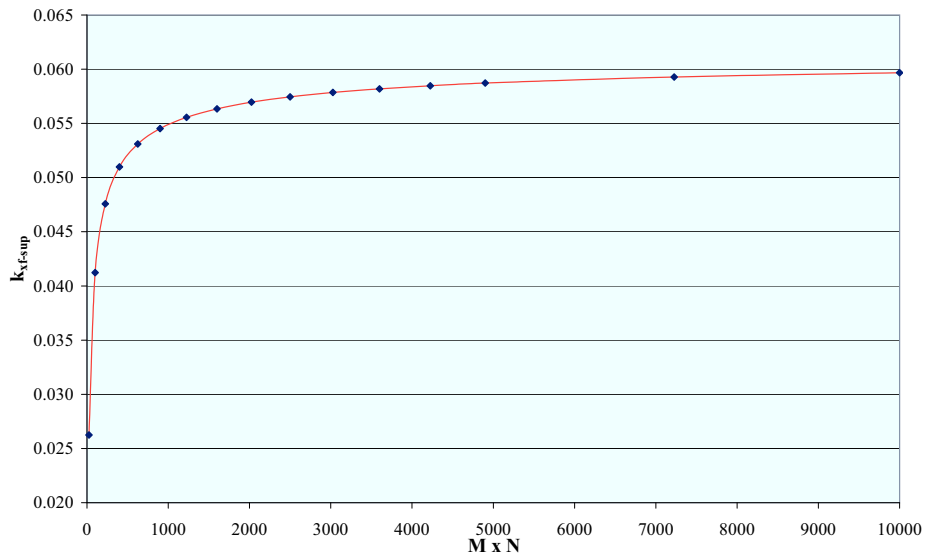
Figure 5.7: K_{xf-sup} convergence

5.5   The case of discontinuous loads

The partial differential equation cup(5.1) has been written with reference to a distributed normal pressure load which is a continuous function in the plate domain ℵ. Now let us suppose that $p(x,y) \in L^2(\Omega)$, so that the set of

86
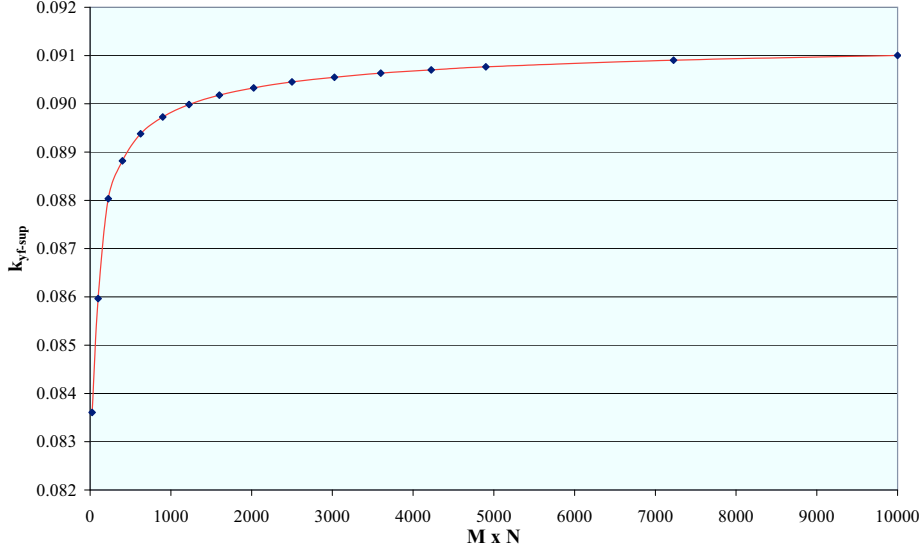
Figure 5.8: K_{yf-sup} convergence

discontinuity points has zero measure according to Lebesgue. Let's define by $\aleph_0 \subseteq \aleph$ the point set where $p(x,y)$ is discontinuous and by $\aleph_1 \subset \aleph$: $m(\aleph_1) = 0$ the point set where $p(x,y)$ is discontinuous. The two subsets define a partition of $\aleph$:

$$\aleph_0 \cup \aleph_1 = \aleph \; ; \; \aleph_0 \cap \aleph_1 = \oslash \tag{5.49}$$

Rigorously, as the eq. (5.1) is valid point by point only where $p(x,y$ is continuous, the functional (5.19) has to be extended only to the $\aleph_0$ domain. But, as $p(x,y$ is continuous almost everywhere in $\aleph$, the functional $\Pi(w)$ can be extended to the entire $\aleph$ domain. It is noticed that, as $w \in L^2(\Omega)$, according to the Schwartz-Holder inequality $pw \in L^1(\Omega)$. Moreover, as an integral extended to a set of zero measure is equal to zero according to Lebesgue, the following equalities hold:

$$\Pi(w)|_{\aleph_0} = \Pi(w)|_{\aleph_0 \cup \aleph_1} = \Pi(w)|_{\aleph} \tag{5.50}$$

Then, it is possible to apply the equation (5.1) not only when the load function is continuous in $\aleph$, but also when it is continuous almost everywhere in $\aleph$, in both cases extending the functional (5.19) to the entire domain according to the identity (5.50). The extension to load functions continuous

almost everywhere according to Lebesgue is particularly useful when it is necessary to schematize loads continuous at intervals such as the wheeled loads for garage decks. In this case, in fact, the effective load distribution can be modelled as an equivalent pressure, transversally constant but longitudinally discontinuous:

$$p_{eq.}(\xi, \eta) = p_i \ \xi \in [\alpha_i, \beta_i] \ \forall \ \eta \in [0, 1] \tag{5.51}$$

Chapter 6

Numerical applications

Some numerical applications of the proposed theories are presented, to test the codes developed in MATLAB, and analyze some ships with large openings on deck. The aim of the first application is to compare the vertical and horizontal tangential stress fields, obtained applying the theories presented in Ch. 1 and 2, with the results obtained by a FE analysis, carried out by ANSYS of a section already analyzed by Hughes [12]. The second application is relative to the non-uniform torsion analysis of a bulk-carrier; the theory discussed in Chapter 3 is applied and the relevant results are compared with the ones obtained by the classical Vlasov's theory. The deformability of transverse bulkheads, schematized as orthotropic plates, is discussed and taken into due consideration in the analysis. The subject of the third group of applications is the exact solution of the non-uniform torsion problem: preliminarily, in order to verify the goodness of the applied FE procedure, a numerical sample is discussed, to compare the obtained results with some known published data; then a containership is analyzed to highlight some non-linearities in the warping stress field, not accounted by the classical theories. Finally, an application of the orthotropic plate bending theory to garage decks is presented, to evaluate the role of girders and transverses when the longitudinal distribution of the equivalent pressure due to the vehicle loads is discontinuous at intervals. A stress and a strain energy analysis is carried out for a ro-ro deck and a procedure to obtain the scatlings of primary supporting members as function of a mean load parameter, is presented.

6.1 Shear stress fields for the Hughes' section

In order to estimate the influence of the shear deflection, an application has been carried out, based on the simplified structure considered by Hughes [12]. Two numerical procedures can be developed: the first one, adopted by Hughes, is a numerical translation of the mixed Dirichlet-Neumann problem, and by the assumption of $\varphi = 0$ on the neutral axis it allows to operate on two systems with a reduced number of equations, but its application to the equations (1.63) that include nodal values lying to both parts $A_1(x)$ and $A_2(x)$ of $A(x)$ necessarily implies a step by step procedure (it is interesting to note that the reduction of the bidimensional Dirichlet-Neumann problem (1.44) to a monodimensional one, allows to reduce the second (1.44) to $\dfrac{\partial \varphi}{\partial n} = 0$, and so to make the problem direct, from a theoretical point of view). The second one, a numerical translation of the Neumann problem, can be applied in a direct form on the whole semi-structure, and removes the essential indeterminacy of the Neumann problem, by the assumption (1.51) which makes the warping a pure deformation displacement and allows to substitute the relevant equation for anyone of the (1.63) system (the first one in this application).

A validation of this last procedure has been carried out, by a comparison with the results obtained by the flow theory and presented by Hughes. In the following the section scheme and geometry data are presented. For each branch, numbered from 1 to 6, the extremity nodes, the thickness and length are shown. The system (1.63), written without any attention to the nodes'

Branch	I node	II node	t(mm)	ℓ (m)
1	1	2	32	10
2	2	5	32	20
3	2	3	32	10
4	3	4	32	20
5	4	5	68	10
6	5	6	60	10

Table 6.1: Section geometry data
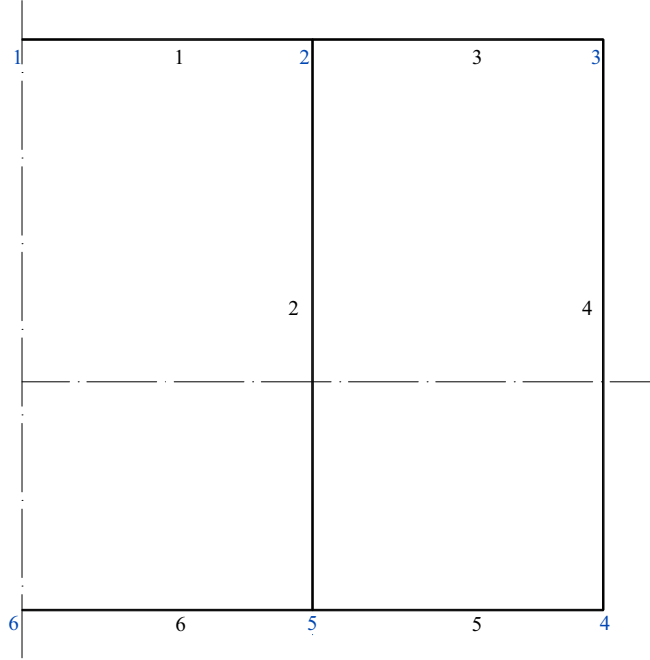
Figure 6.1: Section scheme

numbering, because of the small rank of the coefficient matrix, and simplified by dividing by $t_1 = \cdots = t_4$ reduces to the following matrix equation:

$$
\mathbf{A} \cdot
\begin{bmatrix}
\varphi_1 \\
\varphi_2 \\
\varphi_3 \\
\varphi_4 \\
\varphi_5 \\
\varphi_6
\end{bmatrix}
=
\begin{bmatrix}
-4000 \\
104.11 \\
44.11 \\
-29.1 \\
-104.11 \\
-75
\end{bmatrix}
\tag{6.1}
$$

with:

$$
\mathbf{A} =
\begin{bmatrix}
10 & 40 & 30 & 41.26 & 60 & 18.75 \\
-0.1 & 0.25 & -0.1 & 0 & -0.05 & 0 \\
0 & -0.1 & 0.15 & -0.05 & 0 & 0 \\
0 & 0 & -0.05 & 0.26 & -0.21 & 0 \\
0 & -0.05 & 0 & -0.21 & 0.45 & -0.19 \\
0 & 0 & 0 & 0 & -0.19 & 0.19
\end{bmatrix}
\tag{6.2}
$$

91

that gives the same distribution law of the normalized tangential stresses $\overline{\tau}_{xs,i}^{n} = \dfrac{I}{Q(x)}\overline{\tau}_{xs,i}$ obtained by Hughes:

$$
\overline{\tau}_{xs,i}^{n} = \begin{cases} 12s & 1^{st}branch \\ -137.42 - 12s + 0.5s^2 & 2^{nd}branch \\ 17.42 - 12s & 3^{rd}branch \\ -102.60 - 12s + 0.5s^2 & 4^{th}branch \\ -67.10 + 8s & 5^{th}branch \\ -80.00 + 8s & 6^{th}branch \end{cases} \tag{6.3}
$$

Now, in order to estimate the differences between the Vlasov's and Saint-Venant's theories for the shear stress determination, a numerical comparison with the vertical shear tangential stresses obtained by a FE analysis is carried out, in order to verify the goodness of the two theories. In the following table and figure for each branch the vertical shear normalized tangential stresses, in m^2, are presented: in the relevant figure the red curves are relative to the Vlasov's values, the black ones to the Saint-Venant's values, the blue ones to the values obtained by the FE analysis carried out by ANSYS.

Similarly, the normalized tangential stresses due to the horizontal shear $\overline{\tau}_{xs,i}^{n} = \dfrac{I_\zeta}{Q_H(x)}\overline{\tau}_{xs,i}$ are evaluated applying both the theories. In the relevant figure the red curves refer to Vlasov's values, while the dashead areas to the Saint-Venant's values. Concerning the vertical position of the shear center, it has been verified that some light differences appear between the two theories thansk to the effect of the free lateral contraction of the beam cross-section:

$$
\zeta_Q = 6.15\,m\,(SV)\,;\zeta_Q = 6.28\,m\,(V) \tag{6.4}
$$

It seems that this new theory, developed starting from the Saint-Venant bending-shear displacement field, furnishes, respect to the classical Vlasov one, results closer to the ones obtained by the FE analysis, especially for the branches at deck and bottom; some discrepancies may be observed only in correspondence of the intersections between the longitudinal bulkhead and the bottom, due to local effects not taken into account either by the Vlasov's or by the Saint-Venant's like theory.
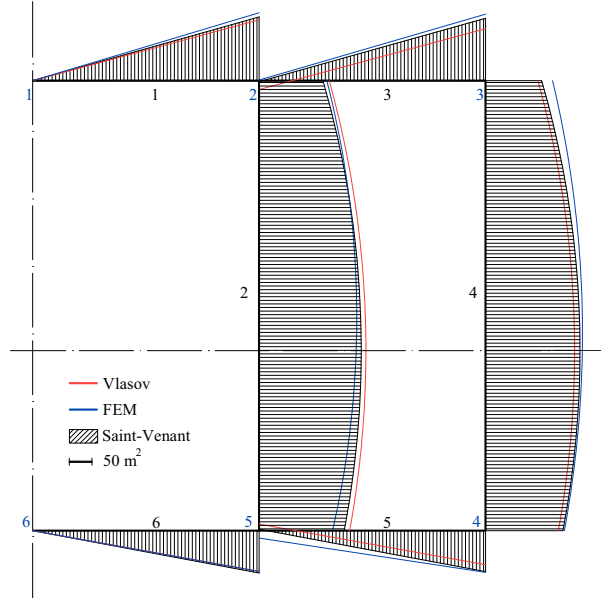
Figure 6.2: Vertical shear normalized tangential stresses
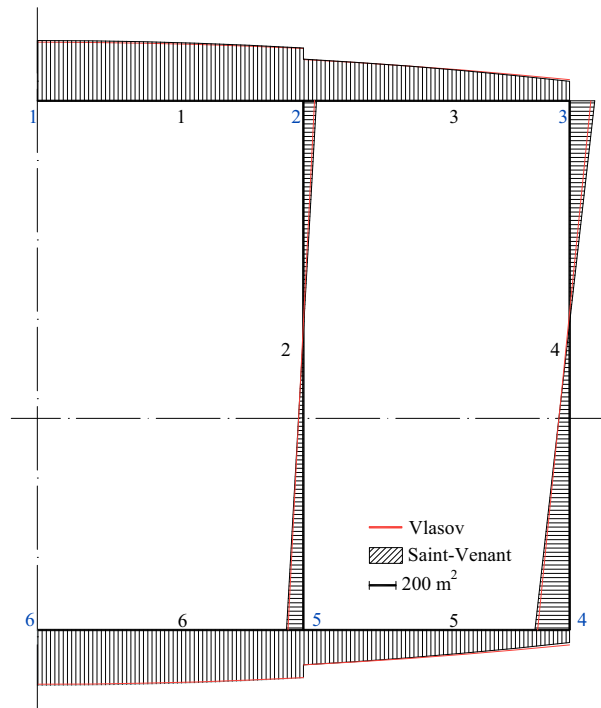
Figure 6.3: Horizontal shear normalized tangential stresses

Branch 1	FEM	Vlasov	Saint-Venant
First node	0	0	0
Half branch	-66.64	-60.00	-62.67
Second node	-133.94	-120.00	-125.33
Branch 2	FEM	Vlasov	Saint-Venant
First node	-132.77	-137.42	-125.20
Half branch	-191.27	-207.42	-198.30
Second node	-143.94	-177.42	-166.97
Branch 3	FEM	Vlasov	Saint-Venant
First node	-1.13	17.42	2.39
Half branch	-68.47	-42.58	-60.28
Second node	-131.31	-102.58	-122.95
Branch 4	FEM	Vlasov	Saint-Venant
First node	-131.32	-102.58	-110.06
Half branch	-189.25	-172.58	-183.17
Second node	-154.44	-142.58	-151.84
Branch 5	FEM	Vlasov	Saint-Venant
First node	-82.19	-67.10	-80.76
Half branch	-51.88	-27.10	-38.99
Second node	-14.63	12.90	2.79
Branch 6	FEM	Vlasov	Saint-Venant
First node	-80.54	-80.00	-83.56
Half branch	-40.94	-40.00	-41.78
Second node	0.00	0.00	0.00

Table 6.2: Vertical shear normalized tangential stresses

Branch 1	Vlasov	Saint-Venant
First node	443.36	455.57
Half branch	430.86	441.52
Second node	393.36	399.37
Branch 2	Vlasov	Saint-Venant
First node	83.42	97.96
Half branch	-16.57	-14.42
Second node	-116.57	-126.81
Branch 3	Vlasov	Saint-Venant
First node	309.94	315.21
Half branch	247.44	244.97
Second node	159.94	146.63
Branch 4	Vlasov	Saint-Venant
First node	159.94	188.95
Half branch	-40.06	-35.82
Second node	-240.06	-260.59
Branch 5	Vlasov	Saint-Venant
First node	-112.97	-94.65
Half branch	-200.47	-192.99
Second node	-262.97	-263.23
Branch 6	Vlasov	Saint-Venant
First node	-360.21	-361.33
Half branch	-397.71	-403.47
Second node	-410.21	-417.52

Table 6.3: Horizontal shear normalized tangential stresses

6.2 Non-uniform torsion analysis for a bulk-carrier

To test the significance of the theory proposed in Chapter 3, an application has been carried out for a bulk-carrier, in order to estimate the effect of the longitudinal distribution of the applied wave torque loads on the bimoment and unit twist angle distributions. The results obtained applying the classical Vlasov's theory, the refined one and the one corrected taking into account the bulkhead deformability, with regards to the unit twist angle and bimoment longitudinal distribution, are discussed. The bulk-carrier main dimensions and geometrical characteristics of the cross-section are listed in the following table: it is noticed that the shear center vertical position is very low due to the shape of the cross-section. Youngs modulus, shear modulus and Poissons ratio are: $E = 2.08 \cdot 10^8 \ kN/m^2$, $G = 0.80 \cdot 10^8 \ kN/m^2$, $\nu = 0.3$. All the properties of the cross-section have been determined by a dedicated program developed in MATLAB, based on the strip-theory of thin-walled girders. Concerning the global energy coefficient C_B and C_{TB},

Length between perpendiculars	=	172.00 m
Scantling length	=	170.48 m
Breadth	=	30.00 m
Depth	=	14.70 m
Scantling draught	=	9.90 m
Displacement	=	43,600 t
Block coefficient	=	0.84
Navigation coefficient	=	1.00
Cross section area	=	2.40 m^2
Vertical position of neutral axis above B.L.	=	5.56 m
Vertical position of twist centre	=	-12.13 m
Vertical moment of inertia	=	77.45 m^4
Horizontal moment of inertia	=	293.01 m^4
Torsional modulus	=	5.40 m^4
Warping modulus	=	15,603 m^6

Table 6.4: Bulk-carrier main dimensions

as the bulkhead is corrugated, it is possible to assume directly $D_y = H = 0$. From the data listed in the previous table, it is possible to calculate $C_B =$

Closed section long. extension	a	$=$	7.90 m
Bulkhead spacing	l_0	$=$	27.20 m
Net hatch length	l_1	$=$	19.30 m
One half of bulkhead breadth	b	$=$	15.00 m
Bottom vertical position	z_B	$=$	-5.56 m
Deck vertical position	z_D	$=$	9.14 m
Bulkhead height	h_B	$=$	14.70 m
Moment of inertia-half corrug.	I_{eZ}	$=$	0.00391 m^4
Half corrugation breath	s_Z	$=$	1.43 m
Upper stool moment of inertia	I_{TB}	$=$	0.0401 m^4

Table 6.5: Bulkhead main dimensions

0.191 m^5 and $C_{TB} = 5.773 \ m^5$, so obtaining:

$$I_t^* = \left(1 + 0.409 + 0.211\right) I_t = 1.62 I_t = 8.75 m^4 \qquad (6.5)$$

It is noticed that the bulkhead contribution in this case is negligible, as there are no horizontal stiffeners. Anyway, as the contribution due to the closed hull segment is very important, a consistent global increase of the hull torsional rigidity is obtained. In the following tables and figures the aft and fore abscissas of the examined holds are listed and the geometry data are presented: for each branch the first and the second node, the thickness t in mm and the length ℓ are shown. Then the longitudinal distributions of the unit twist angle and the bimoment are also shown assuming for the wave torque the load condition 1 where the ship direction forms an angle of 60 deg with the prevailing sea direction. The effect of bulkhead on the

Item	Aft	Fore
Hold 2	23.64	50.84
Hold 3	-3.56	23.64
Hold 4	-30.76	-3.56

Table 6.6: Holds longitudinal extensions
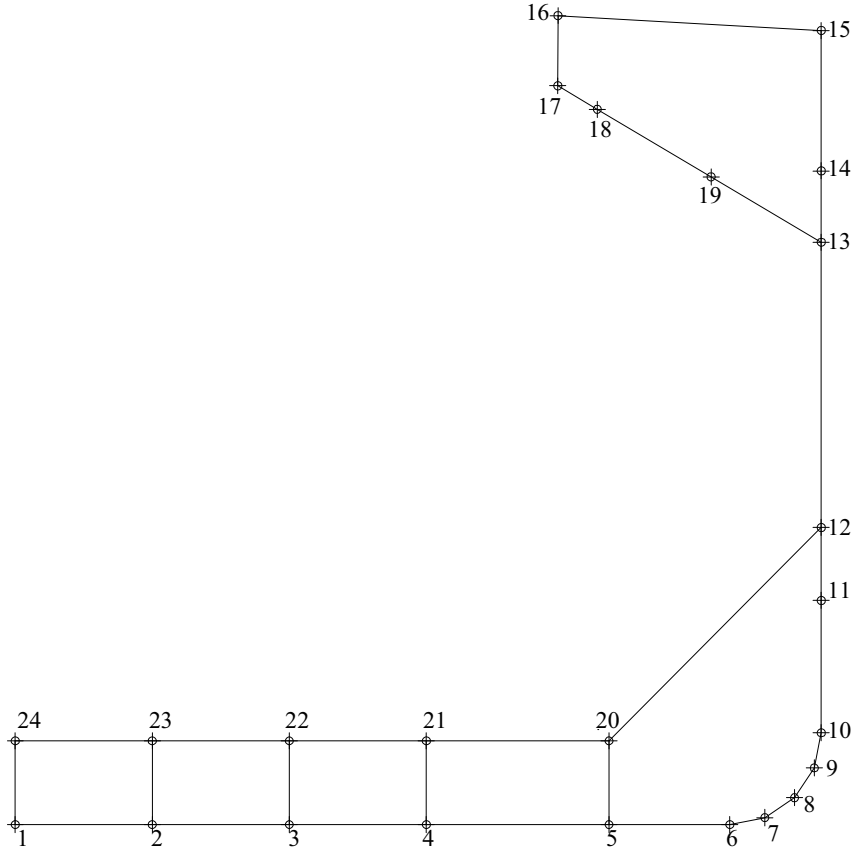
Figure 6.4: Bulk-carrier section scheme

longitudinal distribution of the unit twist angle is, in this case, negligible, while some appreciable differences arise for the bimoment: in the relevant diagram dashed curves refer to the classical Vlasov's theory, while the continuous ones to the refined theory. Particularly, concerning the bimoment peak values, in table 6.8 the maximum values in Nm^2 are shown verifying that the classical theory often overestimates them as regards the refined one. Some differences arise taking into account the bulkhead deformability expecially for the hold 2. Finally the warping stress distribution is shown for a bimoment $B = -3.00 \cdot 10^9 Nm^2$.

B	I	II	t	ℓ	B	I	II	t	ℓ
1	1	2	16	2.55	16	16	17	26	1.30
2	2	3	15	2.55	17	17	18	26	0.85
3	3	4	15	2.55	18	18	19	20	2.46
4	4	5	15	3.40	19	13	19	16	2.38
5	5	6	15	2.25	20	12	20	19	5.59
6	6	7	15	0.66	21	20	21	24	3.40
7	7	8	15	0.66	22	21	22	24	2.55
8	8	9	15	0.66	23	22	23	24	2.55
9	9	10	15	0.66	24	23	24	24	2.55
10	10	11	14.5	2.45	25	1	24	6.5 (x2)	1.55
11	11	12	16.5	1.35	26	2	23	11	1.55
12	12	13	16.5	5.28	27	3	22	11	1.55
13	13	14	16.5	1.32	28	4	21	11	1.55
14	14	15	26	2.60	29	5	20	14	1.55
15	15	16	26	4.90					

Table 6.7: Bulk-carrier geometry data

Hold	x (m)	Refined	Classical	Bulkhead deformability
2	23.64	-1.04E+09	-5.72E+08	-5.69E+08
2	50.84	-2.07E+08	2.61E+07	2.50E+07
3	-3.56	-2.68E+09	-2.38E+09	-2.35E+09
3	23.64	1.36E+09	1.81E+09	1.78E+09
4	-30.76	-3.02E+09	-3.16E+09	-3.12E+09
4	-3.56	2.86E+09	3.09E+09	3.05E+09

Table 6.8: Bimoment peak values
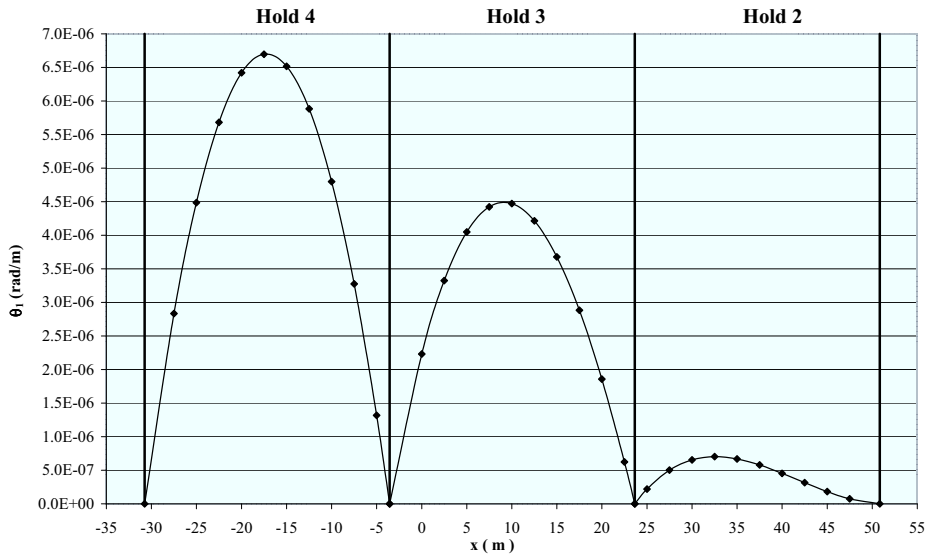
Figure 6.5: Unit twist angle longitudinal distribution
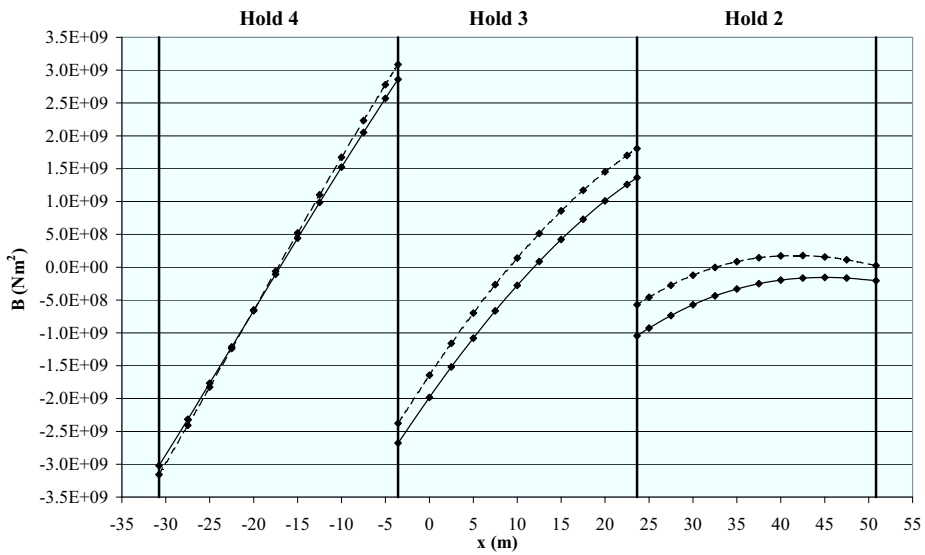
Figure 6.6: Bimoment longitudinal distribution

100

20 N/mm^2
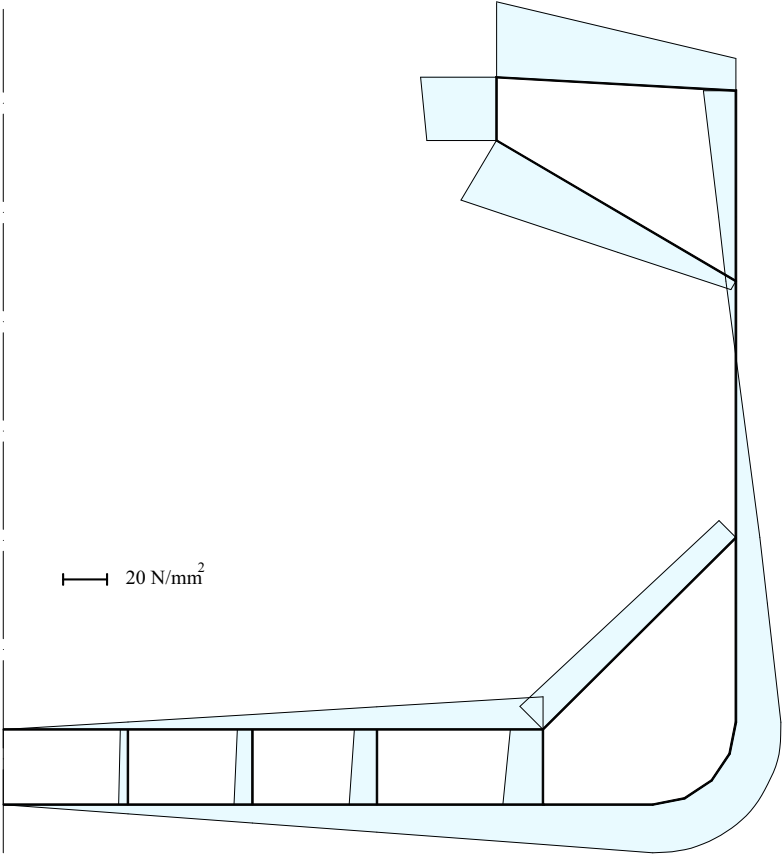
Figure 6.7: Warping stresses distribution

6.3 The exact solution of restrained torsion for a double T section

As said, in Chapter 4 a new theory based on the development into trigonometric series of the displacement field has been extended to beams with multiconnected cross-section, such as ship structures, and a suitable numerical code, based on the PDE Toolbox of MATLAB, has been developed. In order to verify the goodness of the developed numerical code, an application has been carried out for a beam already analyzed by C.J. Burgoyne and H. Brown [6], falling indisputably within the thin-wall domain. The aims of this application are:

- to verify the goodness of the applied FE method by a numerical comparison with the results presented in [6];

- to verify the convergence of the solution when the number of harmonics increases;

- to make a comparison on the unit-twist angle and bimoment longitudinal distribution with the classical approximate theories for thin-walled elastic beams.

In the following figure the section scheme is shown, while the other data useful in the analysis are:

- Poisson modulus ν=0.3;

- Beam length $L = 6.4$ m;

- Polar moment of inertia $I_p = 1.165082\text{E-}4\ m^4$.

In table 6.9 a numerical comparison with the results presented in [6] for the first eight harmonics is presented, verifying a very good agreement between the two codes; in the analysis a fine mesh with 24576 elements has been adopted. In tab. 6.10, instead, the number of triangles defining the mesh has been varied considering two different cases with 96 and 1536 triangles: it has been verified for the first eight harmonics that, increasing the harmonics index, the influence of the elements number on the results becomes almost
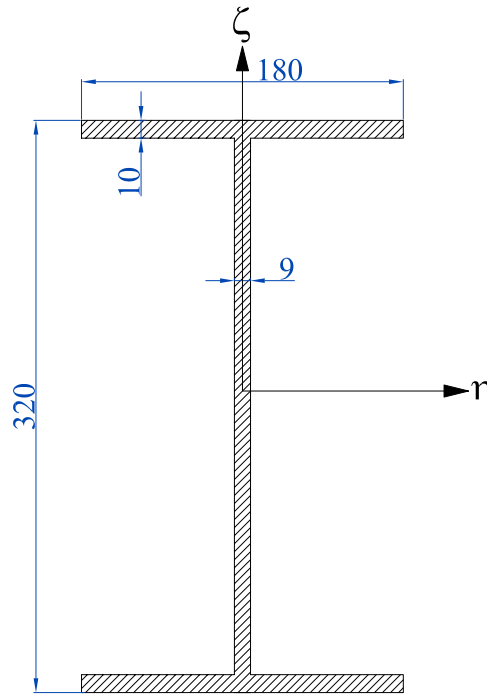
Figure 6.8: Double T section scheme

totally neglegible, while it is considerable for the first ones.   In the follow-
ing figures, increasing the harmonics number, the convergence behaviour of
the unit twist angle function, evaluated at x = 0.1 m and x = 3.2 m, is
also shown as this parameter is the most representative one in the study of
the non-uniform torsion. All the presented results are relative to a mesh
with 24576 elements; the applied torque has been assumed unitary. In this
case it is possible to verify that 100 harmonics are substantially sufficient
to obtain a consistent result.   It seems also useful a comparison with the
classical Vlasov's theory for thin-walled elastic beams. Concerning the unit
twist angle longitudinal distribution, in the classical theory it can be evalu-
ated by the following differential equation, obtained by a global congruence
condition:

$$GI_t\vartheta_1 - EI_w\frac{d^2\vartheta_1}{dx^2} = M_t \tag{6.6}$$

to which the following boundary conditions must be added:

$$\vartheta_1(0) = \vartheta_1(L) = 0 \tag{6.7}$$
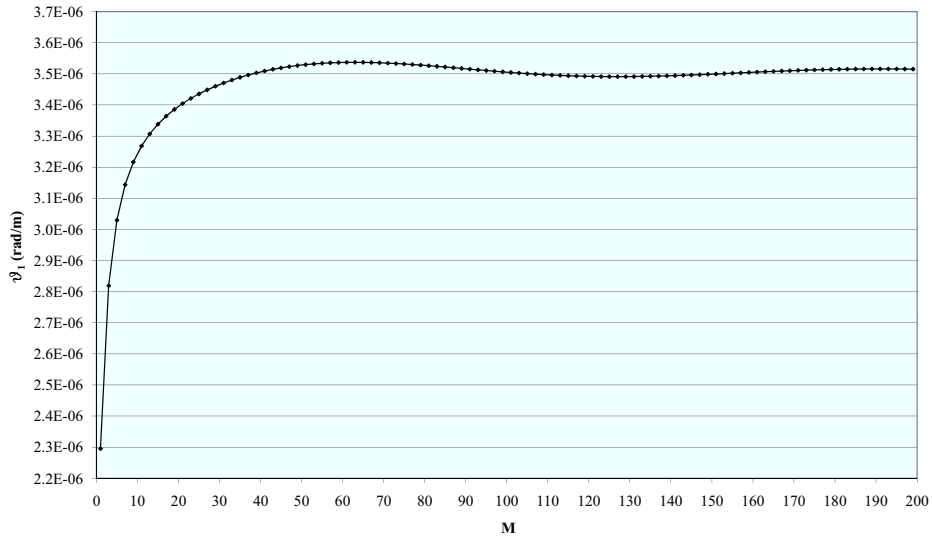
Figure 6.9: Unit twist angle convergence at x = 0.1 m
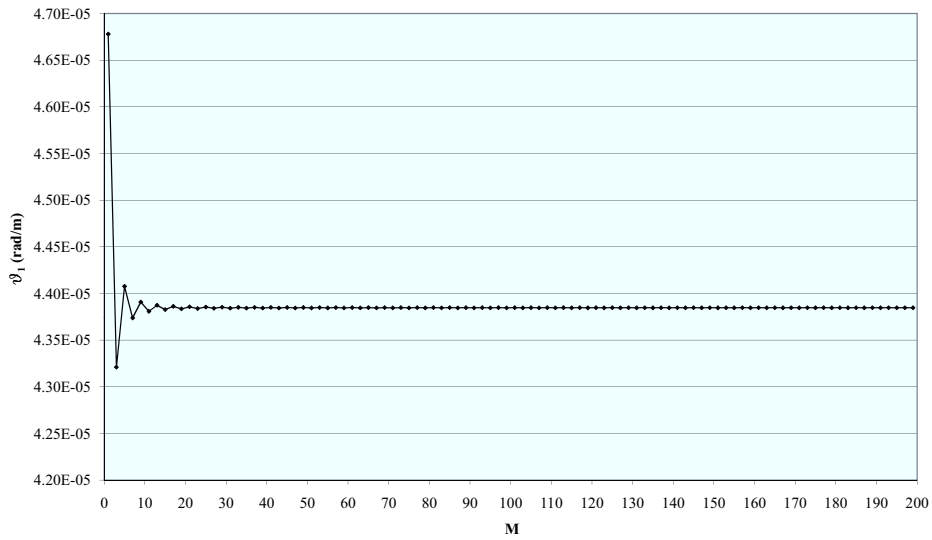
Figure 6.10: Unit twist angle convergence at x = 3.2 m

Index	Burgoyne (x_B)	Present (x_P)	Percentage difference
m	$I_p + H_m$	$I_p + H_m$	$\frac{x_B - x_P}{x_P} \cdot 100$
1	3.38E-07	3.40E-07	0.577
2	7.72E-07	7.74E-07	0.229
3	1.48E-06	1.49E-06	0.100
4	2.46E-06	2.46E-06	0.041
5	3.67E-06	3.67E-06	0.016
6	5.10E-06	5.10E-06	-0.001
7	6.72E-06	6.72E-06	0.003
8	8.49E-06	8.49E-06	-0.002

Table 6.9: Numerical comparison with published data

Index	x_{96}	x_{1536}	Percentage diff.	Percentage diff.
m	$I_p + H_m$	$I_p + H_m$	$\frac{x_{96} - x_P}{x_P} \cdot 100$	$\frac{x_{1536} - x_P}{x_P} \cdot 100$
1	5.80E-07	3.55E-07	70.331	4.435
2	1.01E-06	7.89E-07	31.025	1.948
3	1.73E-06	1.50E-06	16.276	1.015
4	2.70E-06	2.48E-06	9.942	0.616
5	3.92E-06	3.69E-06	6.763	0.416
6	5.36E-06	5.12E-06	4.975	0.305
7	6.98E-06	6.73E-06	3.885	0.239
8	8.76E-06	8.50E-06	3.181	0.197

Table 6.10: Influence of the mesh

In eq. (6.6) I_t is the DSV torsional modulus, while I_w is the beam warping coefficient. Starting from the position:

$$\beta = \frac{GI_t}{EI_w} \tag{6.8}$$

the general solution of eq. (6.6) can be so expressed:

$$\vartheta_1(x) = \frac{M_t}{GI_t}\left[1 - cosh\left(\sqrt{\beta}x\right) - \frac{1 - cosh(\sqrt{\beta}L)}{sinh(\sqrt{\beta}L)}sinh\left(\sqrt{\beta}x\right)\right] \tag{6.9}$$

η	ζ	$\sigma_{x-classical}$	$\sigma_{x-exact}$	$\dfrac{\sigma_{x-classical} - \sigma_{x-exact}}{\sigma_{x-exact}}$
m	m	N/mm^2	N/mm^2	%
0.09	0.155	0.09959	0.10213	-2.487
0.07	0.155	0.07762	0.07714	0.622
0.05	0.155	0.05542	0.05439	1.894
0.03	0.155	0.03322	0.03242	2.468
0.01	0.155	0.01103	0.01082	1.941
0	0.155	0	0	—

Table 6.11: Warping stresses distribution over the double T section flange

For monoconnected thin-walled beams the following approximate expression can be adopted for the beam torsional coefficient:

$$I_t = \frac{1}{3} \sum_i^N \ell_i t_i^3 = 1.9533E - 07 m^4 \tag{6.10}$$

having denoted by ℓ_i and t_i the length and the thickness of each branch constituting the beam cross-section. As regards the warping coefficient for thin-walled double T beams subjected to non-uniform torsion, the following approximate expression can be adopted (see [5]):

$$I_w = \frac{1}{24} \ell_{i-WEB} \ell_{i-FLANGE}^3 t_{i-FLANGE} = 2.3352E - 07 m^4 \tag{6.11}$$

In the following figures the unit twist angle and bimoment longitudinal distributions are shown for a unitary applied torque. In this case no appreciable differences between the two theories have been noticed. Finally the warping stresses in some chosen points of the cross-section in correspondence of the left beam end have been evaluated verifying, also in this case, that a good convergence is achieved into a low harmonics number (see also fig. 6.13) and a good agreement with the classical theory is also obtained.
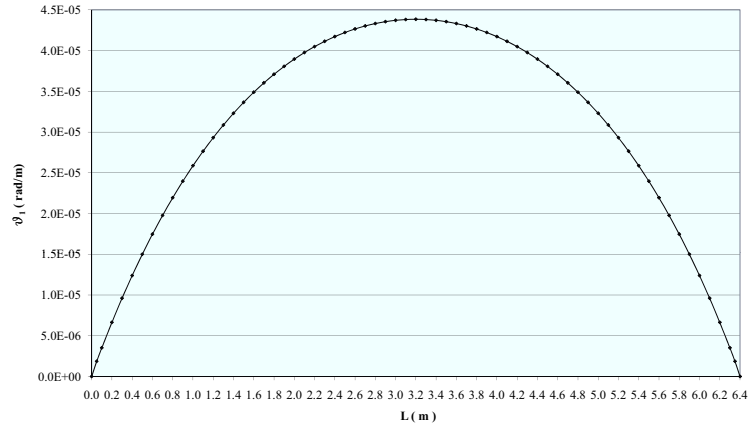
Figure 6.11: Unit twist angle longitudinal distribution
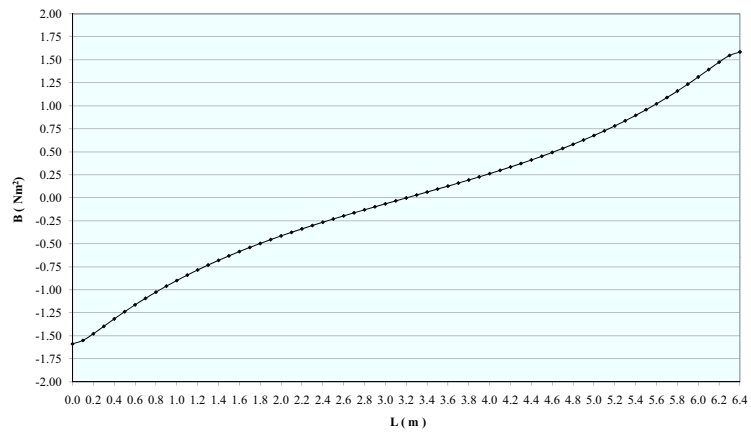
Figure 6.12: Bimoment longitudinal distribution
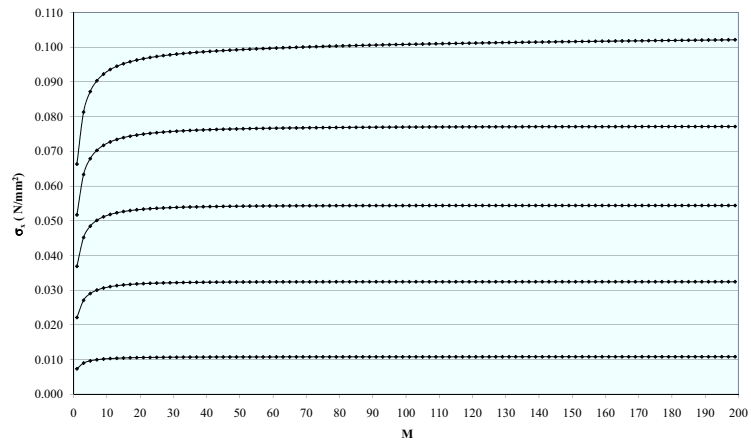
Figure 6.13: Warping stresses convergence for the double T section

107

6.4   The exact solution of restrained torsion for a containership

In the following application a simplified containership section is analyzed, in order to verify the feasibility of the theory presented in Chapter 4 for the evaluation of the warping stress field. The section main data are the following ones:

- Poisson modulus $\nu = 0.3$;

- Hold length $L = 40\ m$;

- Cross section area $A = 2.50\ m^2$;

- Vertical position of G above baseline $z_G= 5.81\ m$;

- Vertical position of twist center $\zeta_Q = $ -11.9 m;

- Vertical moment of inerta $I_\eta = 102.65\ m^4$;

- Horizontal moment of inerta $I_\zeta = 325.07\ m^4$;

- Product of inerta $I_{\eta\zeta} = 0$;

- Polar moment of inerta $I_p = 427.72\ m^4$;

- Torsional coefficient $I_t = 9.57\ m^4$;

- Warping coefficient $I_w = 13917\ m^6$.

In the following the section scheme is presented, while in table 6.12 for each branch the first node, the second node, the length and the thickness are shown. In table 6.13, assuming a constant applied torque equal to $10^5 kNm$, the warping stresses, evaluated applying the exact theory and the refined one by Hajdin and Kollbruner, are determined in correspondence of the left beam end section. See also fig. 6.15 for the warping stress distribution over the cross-section, where the dashed and continuous lines refer to the classical and exact theories, respectively.   From Fig. 6.15 it is clear that the warping stress distribution over each branch isn't linear, as some stress concentrations arise, especially in correspondence of the intersections

Branches	I node	II node	t (mm)	l (m)
1	1	2	20	4.0
2	2	3	20	4.0
3	3	4	20	2.4
4	4	5	20	4.6
5	5	6	15	4.4
6	6	7	15	15.6
7	7	8	15	2.0
8	8	9	15	15.6
9	9	10	15	2.6
10	10	11	15	2.6
11	11	12	18	2.4
12	12	13	18	4.0
13	13	14	18	4.0
14	1	14	15	1.8
15	2	13	15	1.8
16	3	12	15	1.8
17	4	11	15	1.8
18	6	9	15	2.0

Table 6.12: Containership section geometry data

between the branches. Concerning the hull girder yielding check, for ships having large openings on the strength deck, it is well known that the normal stresses induced by torque, vertical and horizontal bending moments have to be superimposed, by means of appropriate combination factors. The maximum warping stress values are reached in correspondence of the bottom-side and deck-inner side intersections, where the stresses due to vertical and horizontal bending moments become maximum, too. From the analysis, the following results have been obtained at the above mentioned intersections:

- Bottom - side : $\sigma_{x-e} = 25.05\,N/mm^2 = 1.5\sigma_{x-c}$

- Deck - inner side: $\sigma_{x-e} = 53.11\,N/mm^2 = 2.0\sigma_{x-c}$

Nodes	$\sigma_{x-exact}$	$\sigma_{x-classical}$	$\dfrac{\sigma_{x-classical} - \sigma_{x-exact}}{\sigma_{x-exact}}$
Items	N/mm^2	N/mm^2	%
1	0	0	—
2	4.7	4.44	-5.53
3	10.24	8.9	-13.09
4	14.26	11.61	-18.58
5	25.05	17.01	-32.10
6	10.48	9.44	-9.92
7	-17.08	-19.63	14.93
8	-53.11	-26.44	-50.22
9	13.47	6.75	-49.89
10	-9.73	3.92	-140.29
11	5.28	8.85	67.61
12	2.16	6.83	216.20
13	0.77	3.42	344.16
14	0	0	—

Table 6.13: Containership warping stresses at nodes

Denoting by σ_B the combined vertical and horizontal bending moment stress, the total primary one, obtained adopting for the warping part the classical and the exact theories, respectively, can be so expressed:

- Classical theory : $\sigma_1 = \sigma_B + \sigma_{x-c}$

- Exact theory: $\sigma_1^* = \sigma_B + \sigma_{x-e}$

Thanks to the positions $\sigma_{x-e} = \beta_c \sigma_{x-c}$ and $\sigma_{x-c} = \alpha_c \sigma_1$, the following percentage variation, as regards σ_1, is obtained:

$$\Delta = \frac{\sigma_1^* - \sigma_1}{\sigma_1} \cdot 100 = \alpha_c(\beta_c - 1) \cdot 100 \qquad (6.12)$$

so that for any $\beta_c > 1$ σ_1 is underestimated as regards σ_1^* , which is potentially higher than the admissible stress. For example, if $\alpha_c = 0.20$, assuming at bottom-side $\beta_c = 1.5$ and at deck-inner side $\beta_c = 2.0$, the relative percentage variations, as regards σ_1, are $\Delta = 10\%$ and $\Delta = 20\%$.
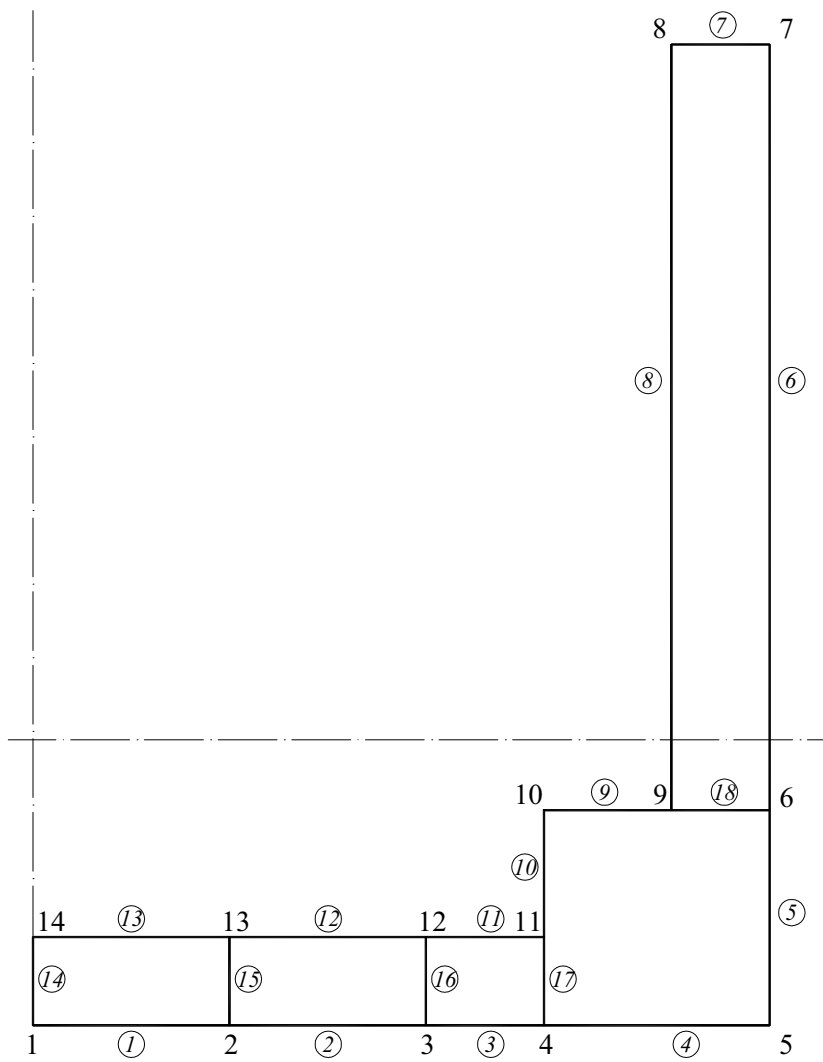
Figure 6.14: Containership section scheme

$\longmapsto$20 N/mm^2
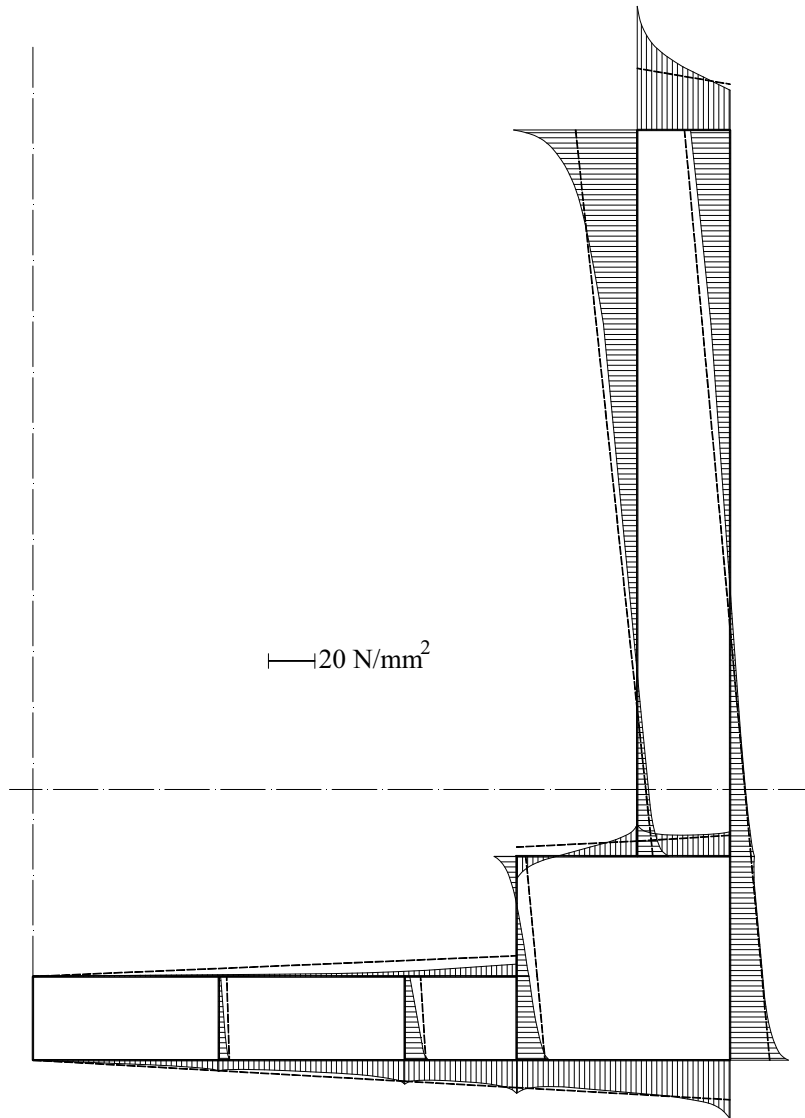
Figure 6.15: Containership warping stresses distribution

6.5 An application of the orthotropic plate theory to garage decks

In this section an application has been carried out for the evaluation of the highest stresses acting on the primary supporting members of a Ro-ro PANAMAX ship used to carry heavy vehicles, schematizing the entire deck as a clamped orthotropic plate; particularly, it has been investigated the influence of the longitudinal distribution of wheeled loads on the normal stresses in girders and transverses, in order to highlight the plate effect, which re-distributes the load peaks on transverses, unlike the isolated beam scheme. The ship main dimensions are: $L_{BP} = 195.00$ m; $B = 32.25$ m; $D = 25.92$ m; $\Delta = 44200$ t; transverses and girders, have, respectively, 970x11+320x30 and 970x12+280x30 T sections, while longitudinals are 240x10 offset bulb plates, in high-strength steel with $\sigma_y = 355$ N/mm^2. According to the symbols and notations defined in Chapter 5, the data assumed in the analysis are:$L_X = 160m$; $\ell = L_Y = 24m$; $s_x = 4m$; $s_y = 2.463m$; $s = 0.667m$; $t_{plating} = 14mm$; $I_{ex} = 967698cm^4$; $I_{ey} = 911559cm^4$; $I_{px} = 178784cm^4$; $I_{py} = 244515cm^4$; $r_{xf} = 83.66cm$; $r_{yf} = 75.30cm$; $\rho = 7.41$; $\eta_t = 0.22$. In the following figures the deck scheme and the reference vehicle are shown. For primary supporting members sub-
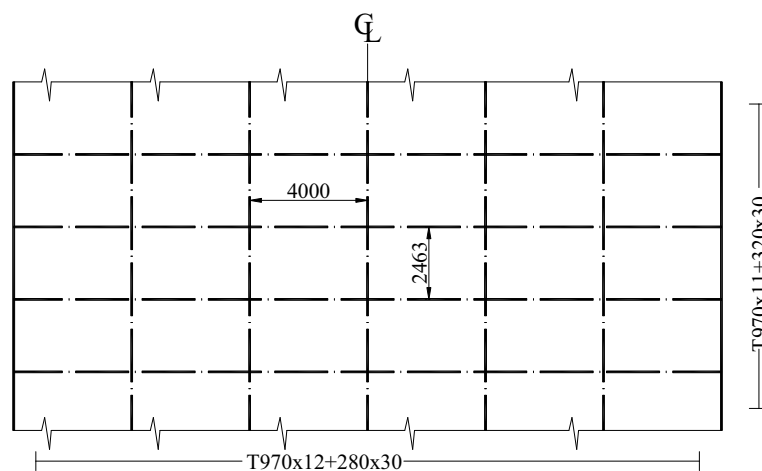
Figure 6.16: Ro-ro Panamax deck scheme

jected to wheeled loads, yielding checks have to be carried out considering a maximum pressure load, equivalent to the maximum vertical, static and dynamic, applied forces; the static part in kN/m^2 can be evaluated according to the following formula, suggested by R.I.NA., 2009:

$$p_{eq.stat} = \frac{n_V Q_A}{\ell s_y}\left(3 - \frac{X_1 + X_2}{s_y}\right)g \qquad (6.13)$$

having denoted by:

- $n_V=$ the number of vehicles located on the primary supporting member;

- $Q_A =$ the maximum axle load in t;

- $X_1 =$ the minimum distance, in m, between two consecutive axles;

- $X_2 =$ the minimum distance, in m, between the axles of two consecutive vehicles;

- $\ell =$ the span, in m, of the primary supporting members (in this case equal to the deck breadth);

- $s_y =$ the spacing, in m, between transverses.

The maximum total equivalent pressure is the sum of the static term and the dynamic one and can be so expressed:

$$p_{eq.max} = p_{eq.stat}\left(1 + a_Z\right) \qquad (6.14)$$
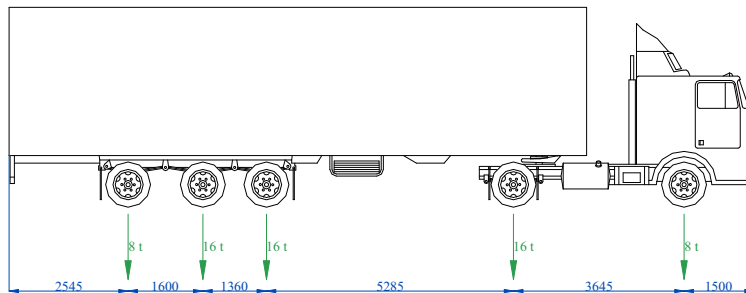
Figure 6.17: Truck axle loads

having denoted by a_Z the ship vertical acceleration. The formula suggested by RINA Rules is valid only if an axle is located directly on a supporting member, but if this condition is not verified, the previous relation can't be directly applied. So, it is convenient to generalize the eq. (6.13) by the following one:

$$p_{eq.stat} = \frac{n_V}{\ell s_y} \sum_{i=1}^{n_A} Q_{A,i} \left(1 - \frac{X_i}{s_y}\right) g \qquad (6.15)$$

where n_A is the number of axles between s_y and s_y and X_i is the distance of the $i - th$ axle load from the considered supporting member. From eq. (6.15), the actual equivalent pressure p_i, including inertial force, is obtained similarly to eq. (6.14). In such a way it is possible to model the load distribution on the deck on the basis of axle loads and geometric characteristics of vehicles. As in this case the deck isn't loaded by a uniform pressure load, but by a load function discontinuous at intervals, the eq. (5.26) has to be replaced by the following one:

$$\frac{\partial}{\partial w_{\overline{mn}}} \int_0^1 \int_0^1 pw\,d\xi d\eta = p_{eq.max} \sum_{i=1}^{n_T} \kappa_i \left(\beta_i - \alpha_i - \frac{sin2\pi\overline{m}\beta_i - sin2\pi\overline{m}\alpha_i}{2\pi\overline{m}}\right)$$
$$(6.16)$$

having denoted by n_T the number of intervals where p is continuous, coinciding in this case with the number of transverses, $p_{eq.max}$ the maximum equivalent pressure, as given by eq. (6.14) and κ_i a load parameter defined as follows:

$$\kappa_i = \frac{p_i}{p_{eq.max}} = \frac{p[\alpha_i, \beta_i]}{p_{eq.max}} \qquad (6.17)$$

In the case under examination, with $n_V = 8$ and $a_Z = 0.411g$, the maximum total pressure is $p_{eq.max} = 48647N/m^2$. The longitudinal distribution of the equivalent pressure is shown in the following diagram. The maximum stresses on girders and transverses are, respectively:

$$\sigma_{xf-sup} = 154N/mm^2 \; ; \; \sigma_{yf-sup} = 176N/mm^2 \qquad (6.18)$$

In the following diagram the ratio k_1 between the stress on the $i - th$ transverse and the maximum one is shown: by the comparison with the longitudinal distribution of the equivalent pressure, it is immediately possible to verify that there is a redistribution of the loads. Particularly, the longitudinal

distribution of the stresses acting on transverses is much less discontinuous than the applied external loads: this implies that girders permit to unload the most loaded transverses and overload the least loaded ones. Concerning
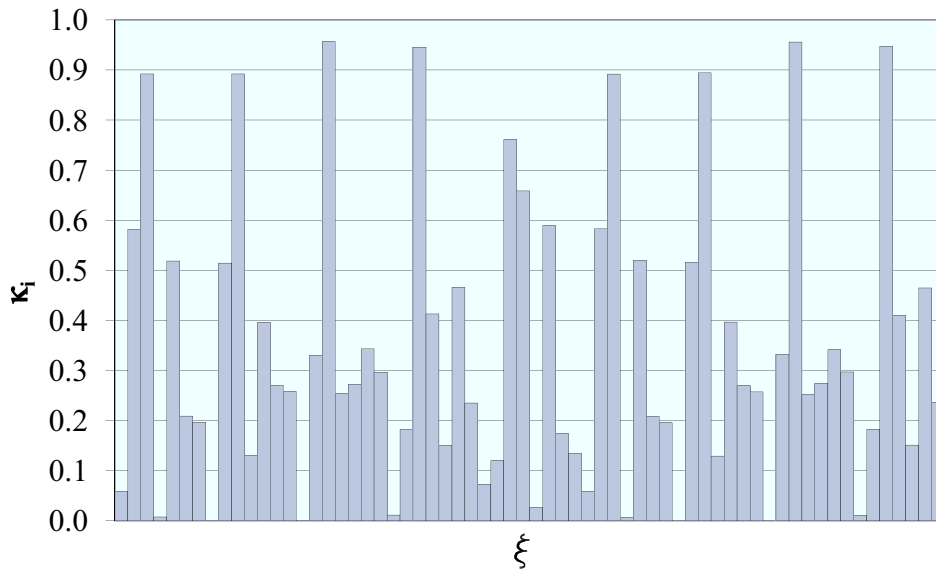
Figure 6.18: Equivalent pressure longitudinal distribution
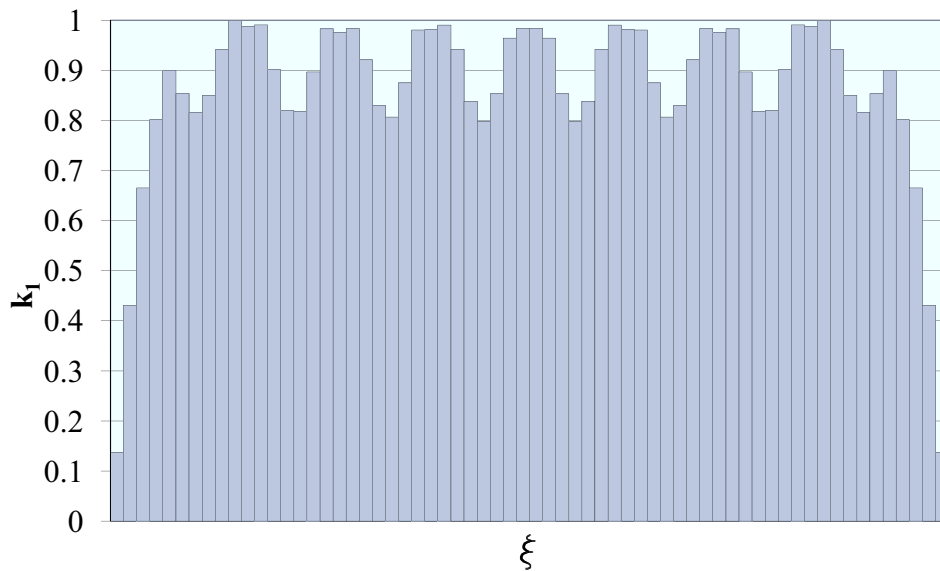
Figure 6.19: Longitudinal distribution of stresses on transverses

116

the strain energy evaluation, the total external work can be so expressed:

$$L_e = \frac{1}{2} \int_\Omega pw dA \tag{6.19}$$

so obtaining:

$$L_e = \frac{1}{2} \frac{p_{eq.max}^2 L_Y^5 L_X}{Ei_y} \sum_{i=1}^{n_T} \kappa_i \sum_{n=1}^{N} \sum_{m=1}^{M} \delta_{m,n} \left(\beta_i - \alpha_i - \frac{sin2\pi m\beta_i - sin2\pi m\alpha_i}{2\pi m} \right) \tag{6.20}$$

Similarly, it is possible to evaluate the strain energy absorbed by girders:

$$L_{girder} = \frac{1}{2} \int_\Omega D_X \left(\frac{\partial^2 w}{\partial x^2} \right)^2 dA \tag{6.21}$$

whence:

$$L_{girder} = \frac{2\pi^4}{\rho^4} \frac{p_{eq.max}^2 L_Y^5 L_X}{Ei_y} \sum_{\overline{m}=1}^{M} \sum_{\overline{n}=1}^{N} \overline{m}^4 \delta_{\overline{m},\overline{n}} \left(\delta_{\overline{m},\overline{n}} + 2 \sum_{n=1}^{N} \delta_{\overline{m},n} \right) \tag{6.22}$$

Concerning the transverses, the following equality holds:

$$L_{transv} = \frac{1}{2} \int_\Omega D_Y \left(\frac{\partial^2 w}{\partial y^2} \right)^2 dA \tag{6.23}$$

whence:

$$L_{transv} = 2\pi^4 \frac{p_{eq.max}^2 L_Y^5 L_X}{Ei_y} \sum_{\overline{m}=1}^{M} \sum_{\overline{n}=1}^{N} \overline{n}^4 \delta_{\overline{m},\overline{n}} \left(\delta_{\overline{m},\overline{n}} + 2 \sum_{m=1}^{M} \delta_{m,\overline{n}} \right) \tag{6.24}$$

Finally the third term, relative to the distortion, can be written as follows:

$$L_{dist} = \frac{1}{2} \int_\Omega 2H \frac{\partial^2 w}{\partial x^2} \frac{\partial^2 w}{\partial y^2} dA \tag{6.25}$$

whence:

$$L_{dist} = 4\pi^4 \frac{\eta_t}{\rho^2} \frac{p_{eq.max}^2 L_Y^5 L_X}{Ei_y} \sum_{m=1}^{M} \sum_{n=1}^{N} m^2 n^2 \delta_{m,n} \tag{6.26}$$

In the case under examination the values of the strain energy components, in Nm, are:

$$L_e = 306225; \ L_{girder} = 18624; \ L_{transv} = 280462; \ L_{dist} = 7139 \tag{6.27}$$

while the corresponding percentage values as regards the total work done by the external forces are:

$$L_{girder} = 6.0\,\%; \ L_{transv} = 91.6\,\%; \ L_{dist} = 2.4\,\% \tag{6.28}$$

Taking into account that there are 5 girders of length 160 m and 64 transverses of length 24 m, the main strain energy per unit of length absorbed by girders and transverses can be so expressed:

$$l_{girder} = \frac{18624}{5 \cdot 160} = 23 \frac{Nm}{m} \,;\, l_{transvr} = \frac{280462}{64 \cdot 24} = 183 \frac{Nm}{m} \qquad (6.29)$$

Finally, if the deck were loaded by a uniform pressure $p = p_{eq.max} = 48647N/m^2$ the maximum stresses on girders and transverses would be:

$$\sigma_{xf-sup-U} = 446N/mm^2 \,;\, \sigma_{yf-sup-U} = 475N/mm^2 \qquad (6.30)$$

The relevant ratios between the maximum actual stresses and the ones obtained considering a uniformly distributed pressure equivalent to the maximum values are:

$$\psi_x = \frac{\sigma_{xf-sup}}{\sigma_{xf-sup-U}} = 0.35 \,;\, \psi_y = \frac{\sigma_{yf-sup}}{\sigma_{yf-sup-U}} = 0.37 \qquad (6.31)$$

Denoting,now, by n_T the number of transverses along the deck length (in this case equal to 64), it is possible to define a new term, namely the mean load parameter χ:

$$\chi = \frac{\sum\limits_{i}^{n_T} \kappa_i}{n_T} \qquad (6.32)$$

that, in the case under examination, is equal to 0.35, so very close to the values assumed by ψ_x and ψ_y. Starting from this position, it seems possible to introduce a simplified procedure that permits to evaluate the maximum actual stresses acting on girders and transverses, starting from a uniformly distributed pressure equal to $p_{eq.max}$, subsequently multiplying the relevant stresses by χ, so obtaining:

$$\sigma_{xf-sup} = \chi\sigma_{xf-sup-U} \,;\, \sigma_{yf-sup} = \chi\sigma_{yf-sup-U} \qquad (6.33)$$

The following expressions can be adopted to determine the mean load parameter χ, , as function of different vehicles' typologies and the distance between transverses s_y:

- Trailers: $\chi = 0.212 + 0.076s_y$;

- Transporters: $\chi = 0.102 + 0.192s_y$;

- Cars: $\chi = 0.601 + 0.093s_y$;

- Buses: $\chi = 0.001 + 0.122s_y$.

The previous analysis has shown that the effective wheeled load distribution, expressed by means of the mean load parameter χ has great influence on the loading of girders and transverses. Particularly, it has been observed that transverses absorb the great part of the load, while girders contribute to a re-distribution of stresses, unloading the most loaded transverses and loading the least loaded ones, so that it seems appopriate to assume that the entire deck is uniformly loaded by a pressure equal to χp_{eq-max}. Now, as for ro-ro decks ρ is much greater than 1, it is possible to directly assume the values $k_{yf-sup} = 0.833$ and $k_{xf-sup} = 0.0571$. Denoting by $\sigma_{all.-tr.}$ and $\sigma_{all.-gird.}$ the allowable stresses for transverses and girders respectively, it is possible to evaluate the minimum section modulus required for transverses by the following relation:

$$W_{ey-min} = \chi \frac{0.0833 p_{eq.max} L_Y^2 s_y}{\sigma_{all.-tr.}} \qquad (6.34)$$

with $p_{eq.max}$ in N/m^2, L_Y and s_y in m, $\sigma_{all.-tr.}$ in N/mm^2 and W_{ey-min} in cm^3. The modulus is inclusive of plating effective breadth b_{ex}. The condition valid for girders is:

$$W_{ex-min} = \chi^2 \frac{0.0033 p_{eq.max}^2 L_Y^4 s_x s_y}{I_{ey} \sigma_{all.-long.}^2} r_{xf} \qquad (6.35)$$

with s_x in m, I_{ey} in cm^4, r_{xf} in cm, W_{ex-min} in cm^3. For the symbols not defined here, see Chapter 5. In conclusion, in this application it has been highlighted that transverse beams absorb the most part of the external work done by the pressure load, as it could be expected. Besides, it has been found that there is an appreciable re-distribution of the load, so that almost the same maximum stresses are obtained considering simply the mean pressure acting uniformly on the deck; then those stresses can be evaluated directly by the orthotropic plate charts. From that, the suggestion for a simple procedure for the preliminary dimensioning of ro-ro deck primary supporting members is given. Other extensions of this theory have been carried out to define a procedure that permits to evaluate, in a preliminary project phase,

the total deck structural weight as function of the vehicles' typologies, the deck breadth, the spacing between ordinary stiffeners and transverses and the maximum height of primary supporting members.

Conclusions

At the end of the work, it's in the writer's opinion that some useful suggestions have been furnished for a more accurate analysis of tangential and warping stresses in ship structures due to shear and non-uniform torsion. Starting from the classical Vlasov's theory for thin-walled beams, some theoretical developments have been reached for the bending-shear response of a ship structure loaded by a longitudinally variable shear. It has been found that a new warping stress field, not accounted by the classical theories, arise. It can be predicted that this stress field can be appreciable for all those loading conditions characterized by great values of the unit vertical load such as the alternate holds loading one for bulk-carriers. The influence of the warping stress field has been evaluated for a bulk-carrier and it has been found that the relevant results are in a good accordance with the ones obtained by a FE analysis, carried out by ANSYS.

Subsequently, a new theory for thin-walled beams has been developed, starting from the bending-shear Saint-Venant displacement field, verifying that the contraction of the ship cross-section, assumed null in the classical theories, produces a redistribution of tangential stresses and a light variation of the shear center vertical position.

Concerning the non-uniform torsion problem, a new procedure, that permits to take into account the longitudinal variability of the applied static and wave torque, has been developed starting from the refined displacement field by Kollbruner and Hajdin. Furthermore, a technique to consider the influence of bulkhead deformability on the bimoment and unit twist angle longitudinal distribution, has been presented.

Besides, a new theory for the non-uniform torsion that permits, despite the

classical one, to fully respect the indefinite equilibrium equation along the beam axis, has been developed specifically aimed to analyze beams with multiconnected cross-section, such as ship structures, with the boundary conditions represented by the transverse bulkheads at the extremity of a single hold. A containership has been analyzed verifying that the warping stress field is non-linear along the branches and some stress concentrations arise, especially at the intersections bottom-bilge and deck-inner side.

As for the non-uniform torsion problem the bulkheads have been schematized as clamped orthotropic plates, the Huber partial differential equation with all edges clamped has been fully solved and the viability of the orthotropic plate theory has also been highlighted by the application to the stress analysis in primary supporting members of some ro-ro garage decks, with an equivalent pressure longitudinally continuous at intervals. Some numerical applications have been carried out, in order to verify the viability of the proposed theories by a numerical comparison with the results obtained by a FE analysis.

It is in the writer's hope that this work can give some useful contributions for the analysis of primary stress in ship structures and new suggestions to researchers for further developments.

Publications list

Publications in Conference Proceedings:

1. A. Campanile, M. Mandarino, V. Piscopo, M. Turtoro, *A numerical method for the shear stress determination*, Proceedings of the 2nd Conference on Marine Research and Transportation ICMRT 07, Ischia 28-30 June 2007, ISBN 88-901174-3-5, pp. 9;

2. A. Campanile, M. Mandarino, V. Piscopo, *Considerations on dimensioning of garage decks*, Proceedings of the 2nd Conference on Marine Research and Transportation ICMRT 07, Ischia 28-30 June 2007, ISBN 88-901174-3-5, pp. 10;

3. A. Campanile, M. Mandarino, V. Piscopo, *Application of the orthotropic plate theory to garage deck dimensioning*, Proceedings of the 6th International Conference on High-Performance Marine Vehicles HIPER 08, Napoli 18-19 September 2008 - ISBN 88-901174-9-4, pp. 15;

4. V. Piscopo, *On the Saint-Venant bending-shear stress in thin-walled beams*, Proceedings of the 6th International Conference on High-Performance Marine Vehicles HIPER 08, Napoli 18-19 September 2008 - ISBN 88-901174-9-4, pp. 14;

5. A. Campanile, M. Mandarino, V. Piscopo, *Design charts for clamped orthotropic plates*, Proceedings of the 18th Symposium on Theory and Practice of Shipbuilding SORTA 08 - Pula 16-18 October 2008 - ISBN 978-953-6313-95-2 (FSB) pp. 8;

6. A. Campanile, M. Mandarino, V. Piscopo, *The warping shear stress*, Proceedings of the 18th Symposium on Theory and Practice of Ship-

building SORTA 08 - Pula 16-18 October 2008 - ISBN 978-953-6313-95-2 (FSB) pp. 8;

7. A. Campanile, M. Mandarino, V. Piscopo, *A procedure for estimating the structural weight of ro-ro decks*, Proceedings of the 13th International Congress of International Maritime Association of Mediterranean IMAM 09, ISBN 978-975-561-355-0, Istanbul 12-15 October 2009, pp.8;

8. A. Campanile, M. Mandarino, V. Piscopo, *On the non uniform torsion in thin-walled beams* On the non uniform torsion in thin-walled beams, Proceedings of the 13th International Congress of International Maritime Association of Mediterranean IMAM 09, ISBN 978-975-561-355-0, Istanbul 12-15 October 2009, pp.8;

9. A. Campanile, E. Fasano, M. Mandarino, V. Piscopo, *Statistical properties of tanker net section modulus*, accepted for the publication in Proceedings of the 16th International Conference of Ship and Shipping Research NAV 2009, Messina 25-27 November, 2009, pp.10;

Publications on journals:

1. A. Campanile, M. Mandarino, V. Piscopo, A. Pranzitelli, *On the exact solution of non-uniform torsion for beams with axialsymmetric cross-section*, Worl Academy of Science, Engineering and Technology Volume 55 July 2009, ISSN 2070-3724 pp. 36-45;

2. A. Campanile, M. Mandarino, V. Piscopo, *On the exact solution of non-uniform torsion for beams with asymmetric cross-section*, Worl Academy of Science, Engineering and Technology Volume 55 July 2009, ISSN 2070-3724 pp. 46-53;

3. A. Campanile, M. Mandarino, V. Piscopo, *On the influence of the warping shear stress on the hull girder strength*, accepted for the publication on Journal of Ship Research (lettera of acceptance dated 8th September, 2009), pp.14.

Bibliography

[1] V.Z. Vlasov, *Thin-walled elastic beams*, Israel Program for Scientific Translations, Jerusalem 1961.

[2] M. Capurso, *Sul calcolo delle travi di parete sottile in presenza di forze e distorsioni*, La Ricerca Scientifica, Roma, 1964.

[3] A. Pittaluga, *Thin-walled beams theory and ship design*, Technical Bulletin R.I.NA. n. 63, 1978.

[4] Von Kárman T., Christensen N.B., *Methods of analysis for torsion with variable twist*, Journal of the Aeronautical Sciences, vol.11, n.2, 1944.

[5] C.F. Kollbrunner, N. Hajdin, *Dünnwandige Stäbe, Band 1*, Springer-Verlag, 1972.

[6] C.J. Burgoyne, E.H. Brown, *Non uniforom elastic torsion*, International Journal of Mechanical Sciences, Vol. 36, No. 1, pp. 23-38, 1994.

[7] C.J. Burgoyne, E.H. Brown, *Non uniforom elastic torsion and flexure of members with asymmetric cross-section*, International Journal of Mechanical Sciences, Vol. 36, No. 1, pp. 39-48, 1994.

[8] T. Coppola, E. Fasano, M. Mandarino, A. Turtoro *The restrained warping applied to catamarans*, Fast '97 Papers pp. 115-124, 1997.

[9] E. Abrahamsen, *Torsion of ships*, I.S.S.C. Rpt., 1961.

[10] Ir. G. De Wilde, *Structural problems in ships with large hatch openings*, International Shipbuilding Progress, pp. 7-33, Jan-Feb, 1967.

[11] K. Haslum, A. Tonnensen, *An analysis of torsion in ship hulls*, European Shipbuilding No. 5/6, pp. 67-90, 1972.

[12] O. Hughes, *Ship structural design: a Rationally-Based, Computer-Aided, Optimization Approach*, SNAME Edition, 1988.

[13] RINA Rules, 2009.

[14] I. Senjanović, S. Tomašević, S. Rudan, T. Senjanović, *Role of transverse bulkheads in hull stiffness of large container ships*, Engineering Structures, Vol. 30, Issue 9, September 2008, pp. 2492-2509.

[15] A. E. H. Love, *A treatise on the mathematical theory of elasticity*, Dover Books.

[16] A. D. Polyanin, *Linear partial differential equations for Engineers and Scientists*, Chapman & All/CRC, 2002.

[17] R. Fiorenza, *Appunti delle lezioni di Analisi Funzionale*, Gli Strumenti di Coinor, 2005.

[18] K.T. Tang, *Mathematical Method for Engineers and Scientists 3*, Springer, 2006.

[19] H.A. Shade *Design Curves for Cross-Stiffened Plating under Uniform Bending Load* , Trans. SNAME, 49, 1941.

[20] S. Timoshenko, S. Woinowsky-Krieger, *Theory of Plates and Shells* , Mc-Graw-Hill Book Company, 1959.

[21] A. Campanile, M.Mandarino, V. Piscopo, M. Turtoro, *A numerical method for the shear stress determination* , ICMRT 07 2nd International Conference on Marine Research and Transportation, Ischia $28^{th} - 30^{th}$ June, 2007.

[22] Timoshenko S., Woinowsky-Krieger S., *Theory of plates and shells*, Mc-Graw Hill Book Company, 1959.

[23] Young D., *Analysis of clamped rectangular plates*, Journal of Applied Mechanics, Volume 7, No. 4, December 1940.